Molecular Pharmacology of an Insect GABA Receptor

A dissertation submitted to the University of Cambridge for the degree of Doctor of Philosophy

Ian Vincent McGonigle (BA)

King's College

Cambridge

2010

Preface

The work presented here in this dissertation was carried out in the Department of Biochemistry at the University of Cambridge between October 2007 and September 2010. All of the work was carried out by the author except where otherwise stated in the text.

This dissertation has not been submitted, in whole or part, for a degree or diploma at any other university.

Acknowledgements

There are so many people to whom I owe a great deal of gratitude. To begin with I must thank the Medical Research Council UK for funding my studentship. Without financial support this could never have happened. However it is Sarah Lummis, my PhD supervisor, who has *really* made this possible. From when I first visited Cambridge to interview until my dissertation was written - some three and a half years later - Sarah has been a tremendous support. More than anybody else I owe her a huge thank you; thank you for everything Sarah.

On a daily basis my project was supported and guided by Andy Thompson. Andy is an exceptional scientist and his electrophys expertise, his good company and his enthusiasm have made my PhD a truly enjoyable experience; thanks Andy. In moments of molecular biology crisis Kerry Price has always been there with her enthusiasm, knowledge and advice; thanks Kerry. No better person to be sitting beside! Jamie Ashby, with his knowledge of structural biology and computer modelling has also been a pleasure to work with. In the lab, Mariza and Linda deserve mention and thanks. They were always there to answer my questions about practical things and their knowledge and experience were greatly valued. The many students and visitors who have passed through 'Skylab' have enhanced the experience of my PhD. Particular mention goes to Kat, David and Sita, who have all been great colleagues. Nick from computer support also deserves thanks. How many times did I have some nightmare of a problem with my computer that he could fix in only a few minutes? Chris and Tom from the photography team also deserve mention for their help with poster and dissertation printing; thanks guys.

With Sarah's kind support and encouragement I was fortunate enough to have made a trip to Argentina, where in Cecilia Bouzat's lab I learned single-channel electrophysiology. Cecilia was a fantastic hostess. From the moment she picked me up at the Bahía Blanca bus station, bleary-eyed after an overnight bus ride from Buenos Aires, until the moment she saw me fly off to Iguazú, she was wonderful; thank you so much for welcoming me into your lab and into your home. Muchas gracias. In the lab Jeré was a fantastic teacher and great company; thanks for everything Jeré. To Marie-José and Diego, thank you both for entertaining me at the

weekends and showing me such wonderful places as Monte Hermoso and Villa Ventana. I really enjoyed those days with you. I loved Argentina, so thank you all for making this possible.

My time in Cambridge has been hugely shaped by my time spent at King's College. King's has been my home for the past three years and my experiences there will remain unforgettable. Bert Vaux, the graduate tutor at King's has been a fantastic support and deserves particular mention; thanks Bert for getting me to Thailand for the Fireball world sailing championships, thank you for all of your help along the way and thanks for your friendship, great company and conversation.

I have made so many good friends at King's. Ross, Luke, Dom and Tom, you guys are heroes of the highest order. To Ruben, Ben, Cornelius, Tom and Dom, playing in the band with you was awesome; I owe you all so much for the enjoyment you have given me. To the rest of my good friends at King's (you know who you are!), thanks guys. To John, André and Shayne at the bar, you guys have been great. Because of your good company and chat I always felt right at home in King's.

To Sandra, you have been truly amazing! Thank you for introducing me to such wonderful things as Serbian coffee, sleeping till noon and to a generally relaxed attitude to life! You are the best!

Hats off to Savino's, Bella Napoli and Manna Mexico. Without such wonderful lunches and coffee I would never have had the energy to get this dissertation written. Furthermore, late night writing couldn't have been done without Gardie's and the 'Van-of-Death' providing much needed fuel, so thanks to you guys too.

In terms of travel, weekend trips home to Dublin wouldn't have been possible without Ryanair, so thanks to Michael O'Leary for making Irish flights cheaper than British trains!!!

Final words of thanks go to my parents, Al and Ben, for teaching me the importance of education and supporting me all the way.

Thank you all…..

Contents

List of Tables and Figures

Chapter 4. Molecular characterisation of agonists that bind to RDL receptors

Chapter 5. Investigating the GABA binding site of RDL receptors

Chapter 6. Characterisation of *Ginkgo biloba* extracts on RDL receptors

Chapter 7. Single-channel analysis of heteromeric 5-HT_3 receptors

Abbreviations

3-APP	3-aminopropylphosphonic acid
4-AB	4-amino-1-butanol
5-AV	5-aminopentanoic acid
5-HT	5-hydroxy-tryptamine
aa	Amino acid
Å	angstrom (1×10^{-10} M)
ACh	Acetylcholine
AChBP	Acetylcholine binding protein
APS	Ammonium persulfate
BB	Bilobalide
cAMP	Cyclic adenosine monophosphate
cDNA	Complementary deoxyribonucleic acid
CNS	Central nervous system
cRNA	Complementary ribonucleic acid
ddH_2O	Double distilled water
DEPC	Diethylpyrocarbonate
DMEM	Dulbecco's modified eagle's medium
DNA	Deoxyribonucleic acid
EBOB	4-n-[3H]propyl-4'-ethynylbicycloorthobenzoate
EC_{50}	Concentration of agonist at which half I_{MAX} is achieved
ECD	Extracellular domain
E.coli	*Escherichia coli*
EDTA	Ethylenediaminetetraacetic acid
ELIC	*Erwinia chrysanthemi* ligand gated ion channel
EPSP	Excitatory post-synaptic potential
GA	Ginkgolide A
GABA	γ-amino-butyric-acid
$GABA_AR$	γ-amino-butyric-acid type A receptor
$GABA_BR$	γ-amino-butyric-acid type B receptor
$GABA_CR$	γ-amino-butyric-acid type C receptor
GB	Ginkgolide B
GC	Ginkgolide C

GHB	γ-hydroxy-butyric-acid
GLIC	*Gloeobacter violaceus* ligand gated ion channel
GlyR	Glycine receptor
GRD	Glycine-like receptor of *Drosophila*
HEK293	Human Embryonic Kidney 293 cells
I_{MAX}	Maximal current
IPSP	Inhibitory post-synaptic potential
LB	Luria-Bertani
LCCH3	Ligand-gated chloride channel homologue 3
LGIC	Ligand-gated ion channel
M (1-4)	Transmembrane spanning domain (1-4)
MD	Molecular dynamic
MOD-1	*C.elegans* Cys-loop receptor Modulation Of locomotion Defective 1
mRNA	Messenger ribonucleic acid
n_H	Hill coefficient
NR	No functional response detected
o/n	Overnight
PABA	Para-amino benzoic acid
pcDNA3.1	Mammalian expression vector
PEG	Polyethyleneglycol
pGEMHE	*Xenopus* oocyte expression vector
PTX	Picrotoxin
RDL	Resistant to Dieldrin
RT	Room temperature
SEM	Standard error of the mean
SCAM	Substituted cysteine accessibility mutagenesis
ssDNA	Single-stranded DNA
TACA	4-amino-2-butenoic acid
TBPS	t-butylbicyclophosphorothionate
TEVC	Two electrode voltage clamping
THIP	4,5,6,7-tetrahydroisoxazolo[5,4-c]pyridin-3-ol
TMD	Transmembrane domain
UV	Ultra-violet
WT	Wild-type
ZAC	Zinc-activated channel

Amino acids

A (Ala)	alanine	M (Met)	methionine
C (Cys)	cysteine	N (Asn)	asparagine
D (Asp)	aspartate	P (Pro)	proline
E (Glu)	glutamate	Q (Gln)	glutamine
F (Phe)	phenylalanine	R (Arg)	arginine
G (Gly)	glycine	S (Ser)	serine
H (His)	histidine	T (Thr)	threonine
K (Lys)	lysine	V (Val)	valine
I (Ile)	isoleucine	W (Trp)	tryptophan
L (Leu)	leucine	Y (Tyr)	tyrosine

Summary

Cys-loop receptors are ligand-gated ion channels that are involved in fast synaptic neurotransmission in the central and peripheral nervous system. The Cys-loop receptor RDL ('resistant to dieldrin') is a GABA-gated chloride channel from *Drosophila melanogaster* and is a major target site for insecticides. The aim of this dissertation was to characterise RDL receptors with particular focus on the agonist binding site.

To assess the potency of a range of GABA analogues on RDL receptors, I expressed receptors in *Xenopus* oocytes and used voltage-clamp electrophysiology to detect receptor responses. I carried out computational modelling of these analogues to determine the dipole separation distances and atomic charges. Computational calculations and functional experiments revealed that agonists require a charged ammonium and an anionic centre, with the most potent agonists having a dipole separation distance of ~5 Å. I made a homology model of the extracellular domain of RDL and docked the active analogues into the putative binding site. I then conducted mutagenesis studies to test the accuracy of this model. Functional data from mutagenesis studies broadly support the location of GABA within this model. This model may be useful for further structure–activity studies and rational drug design.

Natural compounds from the traditional Chinese medicine '*Ginkgo biloba*' (ginkgolide A, ginkgolide B and bilobalide) have potent insecticidal properties and are similar in structure to picrotoxin. I tested the effect of these compounds on RDL receptor function using voltage-clamp electrophysiology. All compounds were found to inhibit RDL receptor function. I probed the binding site of these compounds using site-directed mutagenesis and electrophysiology. Mutations to the 2'A and 6'T channel-lining (M2) residues greatly reduced the potency of these compounds. I then made a homology model of the transmembrane domain of RDL and docked these compounds into the channel. Compounds docked into the channel pore close to the 2' and 6' channel-lining residues and H-bonding interactions were detected at these locations.

Ginkgolides are therefore antagonists of RDL receptors, binding in the channel close to the 2' and 6' residues and this may be the mechanism underlying their potent insecticidal properties.

The 5-HT_3 receptor is a member of the Cys-loop receptor family and shows homology to RDL receptors. To explore different techniques for studying Cys-loop receptor function I assessed the functionality of two brain derived transcripts of the 5-HT3B subunit (Br1 and Br2) using single-channel electrophysiology and a fluorometric assay. Receptors containing Br1 were found to have a conductance identical to the 5-HT3B subunit whilst Br2 receptors were found not to be expressed. This finding has implications for 5-HT_3 brain signalling, in which Br1 may play an important role.

In conclusion, work here has described how agonists bind to and activate RDL GABA receptors and I have identified a candidate mechanism for the potent insecticidal properties of *Ginkgo biloba* extracts. I have also confirmed that 5-HT_3 receptor brain transcript Br1 forms functional channels with similar properties to the 5-HT3B subunit.

Chapter 1

Introduction

1.1 Neurotransmission

Neurons convey information to one another through the use of both electrical and chemical signals. Neurons pass an electrical signal down the length of their axons by means of voltage-gated ion channels which open in response to local changes in membrane potential. The passing of this signal along the axon is known as an action potential. Action potentials can trigger the release of vesicles containing neurotransmitters from the pre-synaptic membrane. Neurotransmitters propagate the signal that was generated as an electrical action potential as a chemical signal by binding to their post-synaptic receptors and eliciting the opening of ion channels. These ligand-gated ion channels can contribute to either excitatory post-synaptic potentials (EPSPs) or inhibitory post-synaptic potentials (IPSPs). Ligand-gated ion channels allow the conversion of the chemical signal transmitted by neurotransmitters to a change of post-synaptic potential on a millisecond timescale, thus facilitating fast synaptic transmission.

1.2 The ligand-gated ion channel superfamily

The "ligand-gated ion channel" (LGIC) family of membrane proteins refers to a group of structurally related receptors that consist of a ligand-binding domain, and an intrinsic ion-channel domain. Fast synaptic neurotransmission is mediated by these LGICs, which open in response to the binding of neurotransmitter molecules. The three major classes of LGICs are ATP gated ion channels (P2X receptors), the family of glutamate gated-ion channels (NMDA, AMPA and kainate receptors) and the Cys-loop family of LGICs (Hogg *et al.*, 2005). Intracellular second messenger activated receptors such as NAADP (nicotinic acid adenine dinucleotide phosphate), ryanodine and IP_3 activated receptors - which are involved in the release of intracellular calcium stores - are also ligand-gated ion channels in this superfamily (Taylor and Laude, 2002). These types of LGICs are distinct from – and should not be

confused with – other ion channels which can be activated by distinct ligand-activated receptors; for example, the $GABA_B$ receptors are G-protein coupled receptors which can (indirectly, through a small G-protein) activate potassium channels (See Ong and Kerr (2000) for a review). Whilst $GABA_B$ and $GABA_A$ receptors are the two major classes of vertebrate GABA receptors, from here onwards we will focus on the Cys-loop receptor family of LGICs, with special focus on $GABA_A$ receptors, which are pentameric intrinsic ion channel receptors.

1.3 Cys-loop receptors

Members of the Cys-loop receptor family share amino acid sequence homology. Receptors include the nicotinic acetylcholine receptor (nAChR), the γ-amino-butyric-acid type A receptor ($GABA_AR$), the glycine receptor (GlyR) the serotonin type 3 receptor ($5\text{-}HT_3R$) (Barnard, 1992) and the more recently discovered zinc-activated channel (ZAC) (Davies *et al.*, 2003; Hogg *et al.*, 2005). Cys-loop receptor subunits are approximately 420-600 amino acids in size with a mass of 50-70 kDa and different members of the family share approximately 30% sequence identity.

Cys-loop receptors can be distinguished by their different sensitivity to agonists and their intrinsic ionic selectivity. Both nAChR and $5\text{-}HT_3$ receptors select cations, which usually results in EPSPs favouring the generation of an action potential in the post-synaptic neuron. The $GABA_AR$ and GlyR usually mediate post-synaptic inhibition of neurotransmission by generating IPSPs via the influx of anions into the post-synaptic neuron. The direction of ion flux through channels is dependent on the local electrochemical gradient and there are cases where anion channels can in fact be excitatory; in the developing neocortex for example, the activation of $GABA_A$ channels results in chloride efflux, leading to the generation of EPSPs (Staley *et al.*, 1995). For the most part, however, $GABA_A$ receptor activation results in a hyperpolarisation of the post-synaptic neuron which disfavours the opening of voltage-gated ion channels and the

generation of an action potential. Glycine receptors dominate motor neuron inhibition, whilst GABA is the major inhibitory neurotransmitter in the brain.

Cys-loop receptors have also been identified in insects. For example, recent studies in the fruit fly (*Drosophila melanogaster*) (Bocquet *et al.*, 2009) honey bee (*Apis mellifera*) and red flour beetle (*Tribolium castaneum*) (Jones and Sattelle, 2007; 2006: Littleton and Ganetzky, 2000) have identified Cys-loop receptors, including nAChRs (Sattelle *et al.*, 2005), anion and cation GABA-gated channels (Buckingham *et al.*, 2005) and glutamate- and histamine-gated anion channels (Gisselmann *et al.*, 2002; Stein *et al.*, 2003; Zheng *et al.*, 2002).

Cys-loop receptors have also been identified in other species of animal; in the small crab (*Cancer borealis*), GABA- and glutamate-gated anion channels have been identified (Duan and Cooke, 2000; Swensen *et al.*, 2000). Additionally, the nematode *Caenorhabditis elegans* possesses a wide range of Cys-loop receptors, with 90 ligand-gated ion channel genes identified to date (Bargmann, 1998). These include the receptors EXP-1, a GABA-gated cation channel that mediates enteric muscle contraction (Beg and Jorgensen, 2003) and MOD-1, a serotonin-gated anion channel (Ranganathan *et al.*, 2000). A review of the Cys-loop receptors of *Caenorhabditis elegans* has been published recently by Jones and Sattelle (2008). More recently, Cys-loop receptor orthologues have been identified in the bacteria *Gloebacter violaceus* and *Erwinia chrysanthemi*, including a proton-gated anion-channel (GLIC) and a putative anion-channel (ELIC), for which an agonist has yet to be identified (Bocquet *et al.*, 2009: Hilf and Dutzler, 2009; 2008). These findings confirm the prevalence of Cys-loop receptors in prokaryotes.

1.4 GABA

GABA has long been known to exist in plants and bacteria, where it serves a metabolic role in the Krebs cycle; it is synthesized by decarboxylation of glutamate by the enzyme glutamic acid decarboxylase. In the 1950s GABA was discovered to be a free amino acid in the brain (Roberts and Frankel, 1950) (Fig. 1.1) and GABA was accepted as a neurotransmitter following the observation that GABA application inhibits *Ascaris* body muscles by opening

chloride channels (Del Castillo *et al.*, 1963). It is now known that these actions of GABA are mediated by a GABA-gated chloride channel, the $GABA_A$ receptor (Schofield *et al.*, 1987). In vertebrate neurons the activation of $GABA_A$ receptors usually permits the diffusion of chloride ions into the cell, hyperpolarising the membrane and decreasing the excitability of the cell.

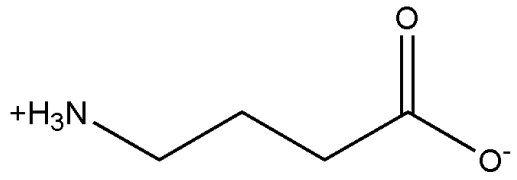

Figure 1.1 Chemical structure of GABA (γ-amino-butyric acid). GABA is a carboxylic acid with a pK_a of 4.03. At typical physiological pH, the amino group is protonated and the carboxylate carries a negative charge (Huxtable *et al*, 1987).

1.5 $GABA_A$ receptor structure

$GABA_A$ receptors are ionotropic ligand-gated ion channels consisting of five subunits which can be assembled with varying stoichiometries. To date, 19 mammalian $GABA_AR$ subunits have been isolated by cDNA cloning; 6α, 4β, 3γ, 1δ, 1ε and 3ρ subunits. For distinction, receptors consisting of only ρ subunits are referred to as $GABA_CRs$, although these receptors are technically a sub-class of $GABA_ARs$ (Barnard *et al.*, 1998). The α1 subunit is the most abundant isoform in the adult mammalian brain (Luque *et al.*, 1994) whilst α2 and α3 subunits are found predominantly in the spinal cord (Persohn *et al.*, 1991). β subunits co-express with α and γ subunits, with the γ subunit conferring benzodiazepine sensitivity. δ subunits and γ subunits co-express with α and β subunits and the predominant isoform in the mammalian brain includes $2\alpha_1$ and $2\beta_2/2\beta_3$ subunits, along with either δ or γ subunits (Somogyi *et al.*, 1996). ρ subunits are localised within retinal bipolar cells, with only low densities found in the brain (Cutting *et al.*, 1992; Cutting *et al.*, 1991; Enz and Cutting, 1999). Each subunit consists of a large extracellular, ligand-binding, domain, a transmembrane domain containing four membrane-crossing α-helices (M1–M4) and a large M3–M4 intracellular loop (See Fig. 1.2). The

second transmembrane spanning regions (M2) are arranged centrally, forming the water-filled, channel pore. Loops within the extracellular domain are involved in ligand binding and are named A to F (Fig. 1.2 & Fig. 1.3). Receptors consist of a pseudo-symmetrical arrangement of subunits within the neuronal membrane (Fig. 1.4).

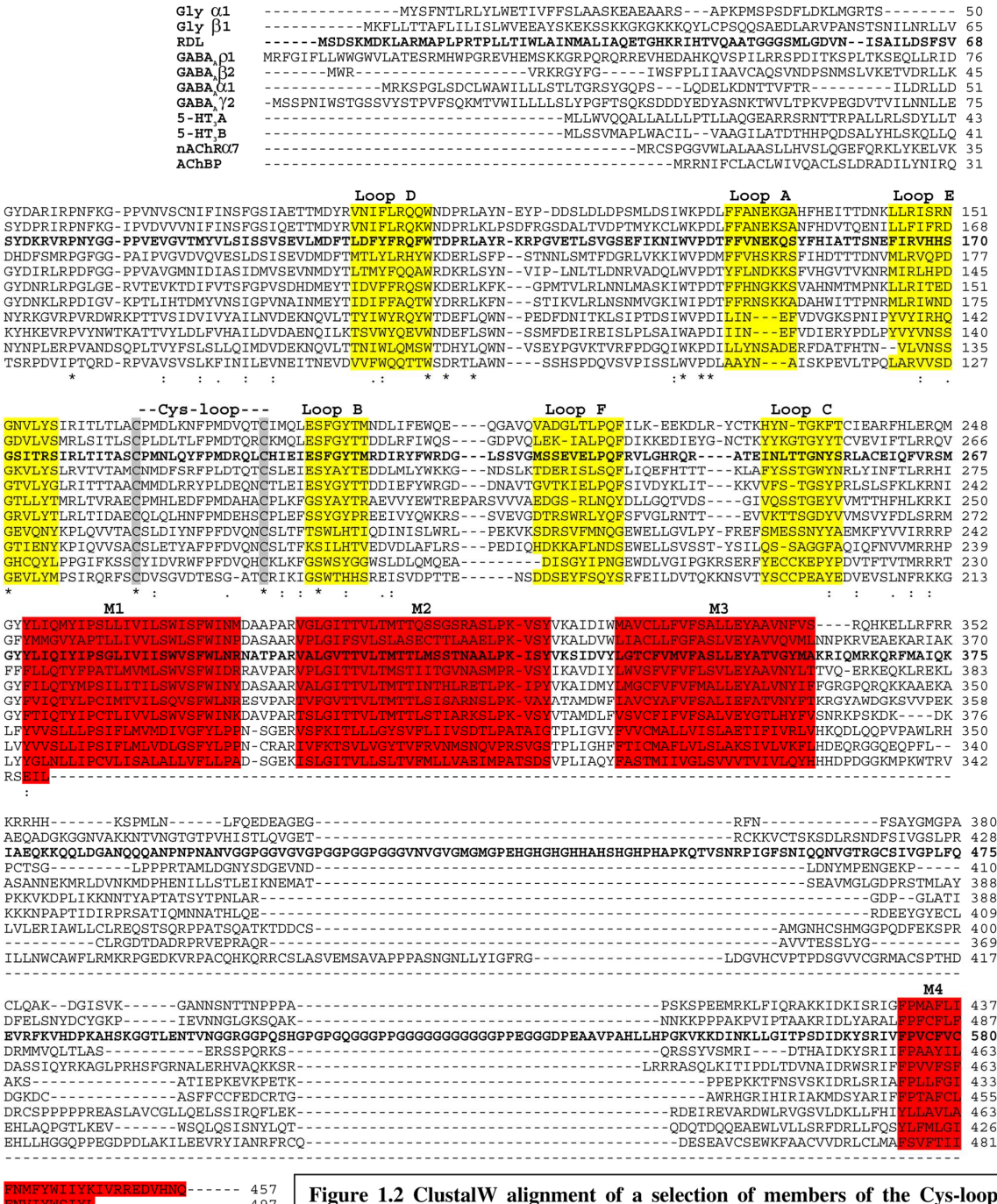

Figure 1.2 ClustalW alignment of a selection of members of the Cys-loop receptor family. Extracellular loops A-F and transmembrane regions M1-M4 are highlighted and labelled, as is the signature Cys-loop. Residues are annotated as being identical (*), conserved (:) and semi-conserved (.). Homologous protein acetylcholine binding protein (AChBP), has been included to display its similarity to the extracellular domains of Cys-loop receptors.

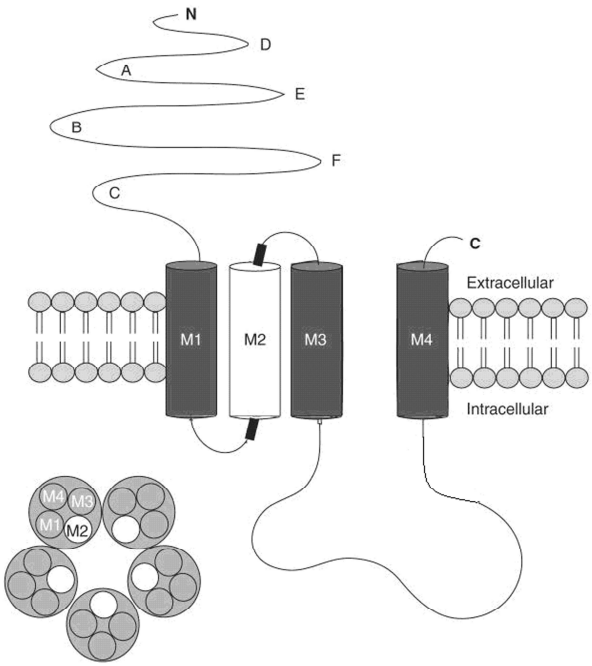

Figure 1.3 Schematic of a Cys-loop receptor. Loops within the extracellular domain are labelled by using common nomenclature A-to-F. Four transmembrane spanning regions are labelled M1, M2, M3 and M4. A large intracellular loop extends between transmembrane regions M3 and M4. Subunits form a pentameric arrangement to yield a complete receptor. Taken from Thompson and Lummis, 2007, with copyright permission granted from *Expert Opinion on Therapeutic Targets*.

Acetylcholine binding protein (AChBP), is a soluble acetylcholine scavenging protein which is secreted by glial cells in the fresh water snail *Lymnaea stagnalis* (Smit *et al.*, 2001). This protein is homologous to the nicotinic acetylcholine receptor and other Cys-loop receptors (See in Fig. 1.2). The crystal structure of this protein at 2.7 Å resolution has thus yielded insight into the structure of the extracellular domain of Cys-loop receptors (Brejc *et al.*, 2001). Additionally, the structure of the extracellular domain of the nAChR α1 subunit has been solved to 1.9 Å (Dellisanti *et al.*, 2007). These advances have led to the prediction that the extracellular domains of homologous Cys-loop receptors would be predominantly β-sheet in structure. Electron micrograph images of the full length AChR from the electric organ of the *Torpedo* ray at 4 Å resolution have revealed the structure of the full receptor (Miyazawa *et al.*, 2003) showing the transmembrane regions to be α-helical (Fig. 1.4).

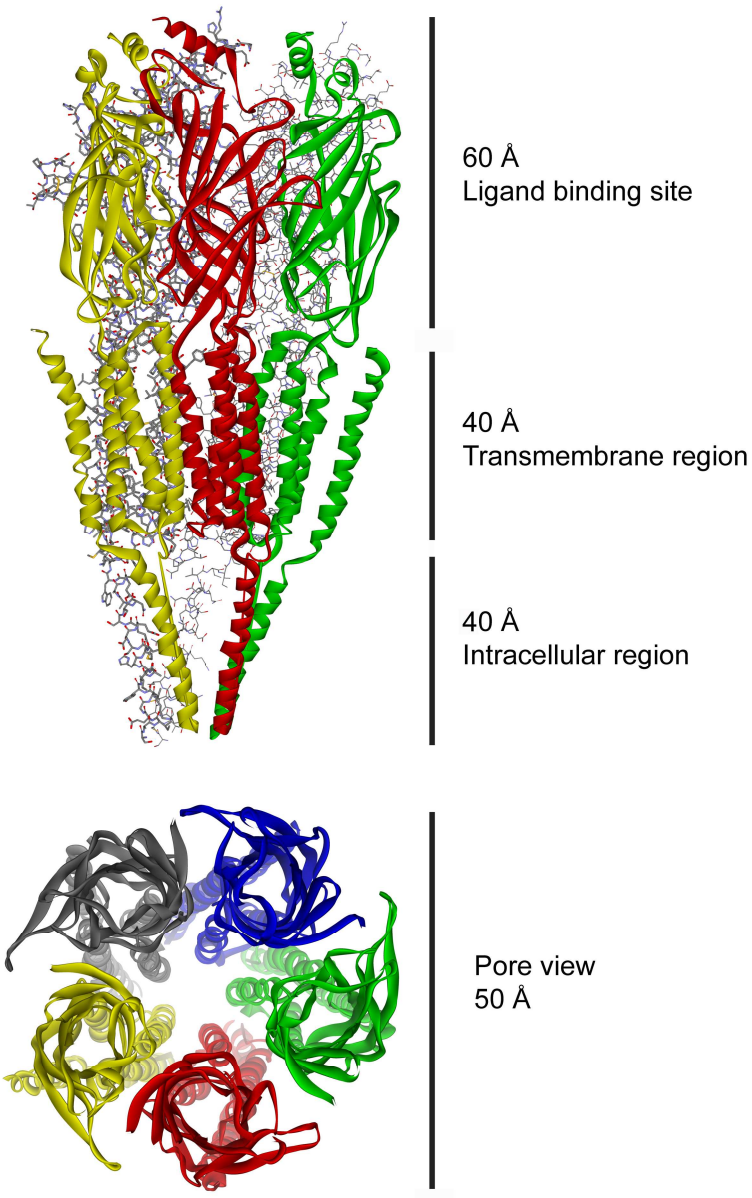

Figure 1.4 Structure of a Cys-loop receptor. Above: Ribbon structure of the refined structure of the acetylcholine receptor from the electric organ of the Torpedo ray at 4 Å resolution (pdb ID: 2bg9) (Miyazawa *et al.*, 2003). Two of the five subunits are displayed in atomic stick format to enhance perspective. Individual subunits are labelled red, yellow and green for distinction. The extracellular domain is largely β-sheet and the transmembrane and intracellular domains are α-helical. **Below:** Pore view of the receptor from the extracellular perspective. Five subunits (labelled grey, blue, green, red and yellow for distinction) form a pentameric arrangement to yield a complete receptor.

1.6 Receptor activation

1.6.1 Gating

Gating refers to the mechanism of transduction which links agonist binding at the extracellular domain to the opening of the channel gate some 50 Å away. To facilitate comparison between the channel-lining residues of the second transmembrane domain (M2) of different Cys-loop receptor channels, a prime number notation is used starting with the highly conserved positively-charged residues at the cytoplasmic end of M2, defined as 0′, increasing to another ring of charged residues at the extracellular end denoted as 20′ (Miller, 1989). The gate is deemed to be located at the "hydrophobic girdle" between M2 residues 9' and 14' (Bali and Akabas, 2007; Miyazawa *et al.*, 2003; Panicker *et al.*, 2002). The free energy derived from the binding of agonist to its binding site in the extracellular domain induces a conformational change which is transmitted to the gate and causes opening of the ion channel. Whilst most of the studies of channel gating have been done on AChRs, I will discuss studies from a range of receptors to illustrate the similarities across receptor types. Such studies can provide clues as to the mechanisms which underlie Cys-loop receptor function in general terms.

Linear free-energy relationship analysis of mutant nAChRs has shown that a local conformational change in the binding site is propagated as a conformational wave to the channel (Grosman *et al.*, 2000). An *in-silico* study of loop C, which forms part of the ligand binding site, in the human α7 nicotinic acetylcholine receptor (nAChR) described initial coupling between ligand binding and channel gating (Cheng *et al.*, 2006); these targeted molecular dynamic (MD) simulations suggest that gating movements of the α7 receptor may involve relatively small structural changes within loop C of the ligand-binding domain. A more recent structural study of AChBP, co-crystallised with agonists and antagonists bound, shows a 'capping' motion of loop C closing the binding site cavity, thereby trapping bound agonist molecules. Residues at the apex of loop C moved inwards as much as 7 Å with agonists bound. However, antagonists caused loop C to move outwards as

much as 4 Å providing a mechanism underlying their inhibitory effects (Hansen *et al.*, 2005). These findings agree with the previous modelling of Cheng *et al* for nAChRs, but the magnitude of loop C movement presented by Hansen would suggest that loop C undergoes larger movements during agonist binding than previously suggested.

Environment-sensitive fluorescent probes have been used to identify residues involved in the gating mechanism. When the agonist is applied, changes in fluorescence can be monitored and related to conformational changes involved in gating. A recent study of the GlyR by Lynch and Pless (2009) showed that most fluorescently labelled residues in loops C and F yielded fluorescence changes identical in magnitude for glycine and strychnine (a GlyR antagonist) but distinct maximal fluorescence responses for labels on loops D and E. A similar study of $GABA_A$Rs has shown that homologous residues within loop E of both β and α subunits display a similar fluorescence change during gating (Muroi *et al.*, 2006), suggesting a similar structural transition occurs in both subunits. A follow on study by the same authors showed that residues in loop D (α_1L127C and β_2L125C) also produce an increase in fluorescence in response to GABA binding (Muroi *et al.*, 2009). This presents the hypothesis of a 'global transition' with similar movements in different subunits occurring during channel gating.

Agonist binding causes changes at the extracellular domain which are thought to induce a structural transition which causes a widening of the channel pore, formed by the five M2 helices. Indeed, images of the nAChR trapped in the open state showed that the M2 rods were tilted outwards from their resting configuration (Unwin, 1995). The kinks in the α-helices facing the channel pore (M2-region) had rotated to face the side, increasing the pore diameter by about 4 Å. With the solution of the crystal structures of related prokaryotic Cys-loop receptors - ligand gated ion channels from a bacterium (ELIC) (Hilf and Dutzler, 2008) and from a cyanobacterium (GLIC) (Hilf and Dutzler, 2009), a similar channel in a putatively open conformation - the pore structure in putatively both open and closed states has been revealed. Examining the

differences in pore structure between these two receptors suggests that the M2 helices relax and tilt around their M2 longitudinal axis with a widening of the channel at the extracellular end (Fig. 1.5). Studies of nAChRs support this hypothetical transition: a fluorophore attached to nicotinic acetylcholine receptor β M2 region (a Cys side chain introduced at the β 19' position in the M2 region) has been used to detect productive binding of agonist in the nAChR. During agonist application, fluorescence increased by approximately 10%, and the emission peak shifted to lower wavelengths, indicating a more hydrophobic environment for the fluorophore (Dahan *et al.*, 2004). A more recent study of the muscle AChR suggests that small structural rearrangements may underlie channel opening. Ionisable amino acids were engineered into M1 and M3 and the effects on channel gating were monitored. The effect of proton transfer was determined using single-channel electrophysiology and it was determined that the M2 helices move by no more than 1.5 Å (Cymes and Grossman, 2008). This prediction is supported by computational approaches which predict that a 1.5 Å widening of the pore is sufficient to increase the channel conductance to values that are close to those observed experimentally (Corry, 2006).

In 5-HT_3 receptors an essential proline residue has been identified which has been shown to undergo a *trans-cis* isomerisation during gating which is necessary for channel opening. This study was carried out using unnatural amino-acid mutagenesis where the proline 8* residue was replaced with proline analogues favouring the *trans* conformer. The trend observed showed that the *trans* conformer prevented channel gating (Lummis *et al.*, 2005a). This suggests a possible "switching mechanism" for channel gating revolving around the isomerisation of the proline 8* residue. This proline residue is not however present in GABA or glycine receptors, thusly confounding the possibility of a unified model for channel gating for all LGICs.

There is some disagreement in the literature regarding the magnitude of the structural transitions underlying receptor activation, however there is a common agreement amongst many studies; a structural rearrangement amongst

extracellular binding site loops leads to a structural transition which causes a widening of the channel pore leading to ion flux. While specific residues may take on different roles in different receptors, it seems that this overview is appropriate for many, if not all, of the Cys-loop receptors.

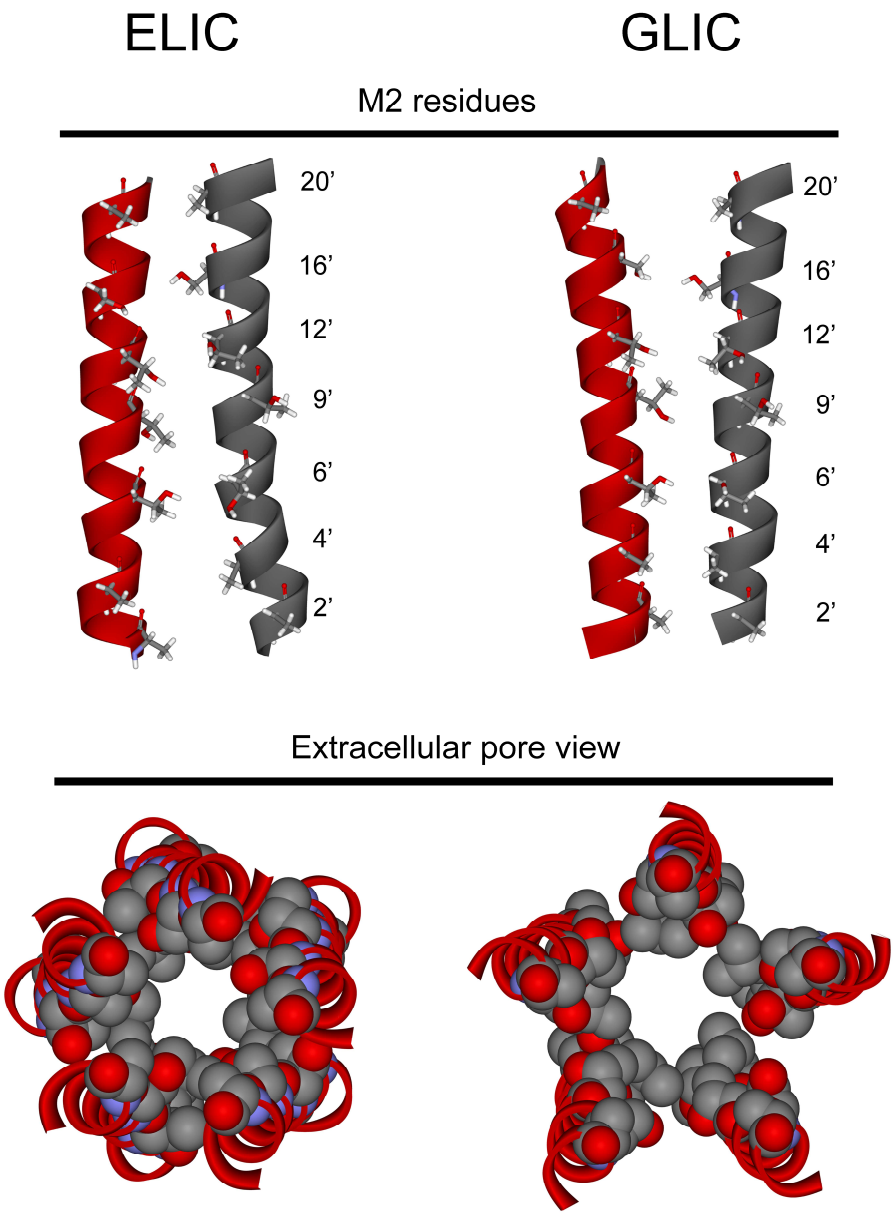

Figure 1.5 Examination of the pore structure of GLIC and ELIC, prokaryotic Cys-loop receptors, in putative open and closed states, respectively. Above: Two adjacent M2 regions of the pore with channel-lining residues labeled and side chains in stick representation. A difference in the M2 helical axis is obvious with a tilting away from the pore at the extracellular end of GLIC. **Below:** View of the channel pore from the extracellular position. M2 residues are in the space filling representation to demonstrate the pore cavities dimensions. A wider pore is observed in GLIC suggesting that the tilting of the helices results in a widening of the channel pore.

1.6.2 Interface residues

Studies of the regions which bridge the extracellular and transmembrane domains have led to the identification of several critical "interface residues." Structures from the extracellular domain which constitute this interface include the β1-β2 loop, the Cys-loop, the β8-β9 loop and the end of the β10 loop. The pre-M1 region, the M2-M3 linker and the C-terminal of M4 are also involved in this interface (Fig. 1.6) (Bartos *et al.*, 2009a).

Studies of chimeric receptors composed of AChBP tethered to the pore domain of the 5-HT_3AR has led to an understanding of some of these coupling regions. Whilst the chimera is expressed at the cell surface, binding of ACh is unable to trigger channel opening, however with the substitution of three regions (β1-2 loop, Cys-loop and β8-9 loop) in AChBP, ACh binds with lower affinity but is capable of triggering channel opening (Bartos *et al.*, 2009a). It has also been demonstrated that the ECD of α7 AChRs can be successfully coupled to the 5-HT_3AR, as the ECD of α7 has similar interface residues (Bouzat *et al.*, 2008) (Fig. 1.6). This construct has proven to be a good model for studying the role of interface regions, leading to the hypothesis that activation depends on a "complex network of loops," where specific interactions between interface residues can not always be successfully substituted with loops from other receptors (Bouzat *et al.*, 2008).

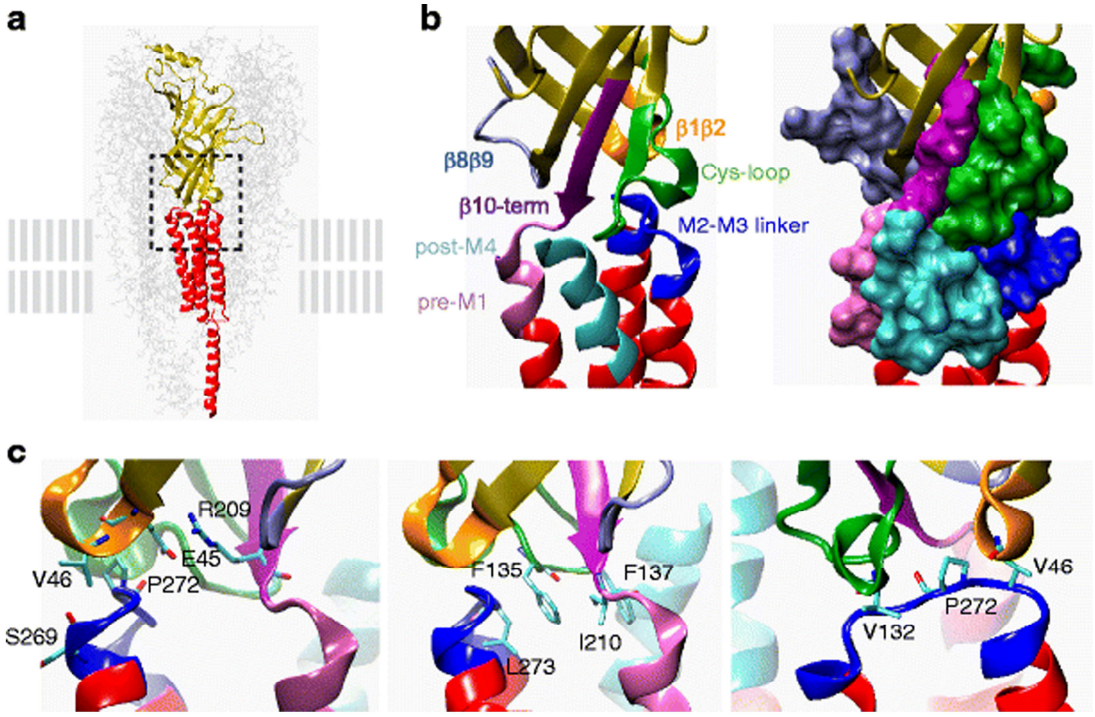

		β1β2	Cys-loop	β8β9	β10 + pre-M1	M2M3	post-M4
nAChα1	torpedo	DEVNQI	CEIIVTHFPFDQQNC	MESGEW	IMQRIPLYFVVN	SSAVPLIGKY	FAGR--LIELSQ
nAChα1	human	DEVNQI	CEIIVTHFPFDEQNC	MESGEW	VMQRLPLYFIVN	SSAVPLIGKY	FAGR--LIELNQ
nAChα7	human	DEKNQV	CYIDVRWFPFDVQHC	IPNGEW	TMRRRTLYYGLN	SDSVPLIAQY	LMSAPNFVEAVS
5HT3A	human	DEKNQV	CSLDIYNFPFDVQNC	MNQGEW	VIRRRPLFYVVS	AIGTPLIGVY	VMLWSIWQYA--
GABAα1	human	SDHDME	CPMHLEDFPMDAHAC	EDGSRL	HLKRKIGYFVIQ	A-YATAMDWF	WATYLNREPQLK
GABAβ2	human	SEVNMD	CMMDLRRYPLDEQNC	VTKIEL	KLKRNIGYFILQ	P-YVKAIDMY	WLYYVN------
Glyα1	human	AETTMD	CPMDLKNFPMDVQTC	ADGLTL	HLERQMGYYLIQ	S-YVKAIDIW	WIIYKIVRREDV

Figure 1.6 The interface between extracellular and transmembrane domains. **Above:** a structure of the *Torpedo* nAChR with one of its subunits highlighted with the extracellular domain in *yellow* and the transmembrane and intracellular domains in *red*. The interface is shown in the *dashed square*. **b** View of the structures at the interface. *Left*: The different segments are coloured as follows: *orange* (β1-2 loop), *ice blue* (β8-9 loop), *green* (Cys-loop), *purple* (β10-terminal), *pink* (pre-M1), *blue* (M2-M3 linker), and *cyan* (post-M4). *Right*: Surface representation of the interface loops. **c** Different views of the interface with key residues labelled. Ile210 in *Torpedo* nAChR corresponds to Leu210 in the human receptor. **Below:** Subunit sequences at the receptor interface. Taken from Bartos *et al.*, 2009a. with copyright permission from *Mol. Neurobiol*.

Similar work on $GABA_A$ receptors has shown that receptor activation depends on electrostatic interactions between charged residues in the β1-2 loop and the Cys-loop (Asp57 and Asp149) as well as Lys279 in the M2-M3 linker (Kash *et al.*, 2003). An equivalent residue in the $5\text{-}HT_3AR$ (Lys81 in the β1-2 loop) lies close to the extracellular end of M2 (26'A and 27'I) and mutational analysis has

shown that this residue is involved in channel opening (Reeves *et al.*, 2005). In the $GABA_CR$, residue Glu92, situated in the β1-2 loop has been shown to form a salt-bridge with pre-M1 residue Arg258 (Price *et al.*, 2007; Wang *et al.*, 2007). In the same study it was shown that this specific interaction is absent in the $5HT_3AR$ (Price *et al.*, 2007).

An interaction between residues in the pre-M1 and the M2-M3 linker has been identified in the human muscle nAChR. It was suggested that agonist binding disrupts a salt-bridge between pre-M1 Arg209 and Glu45 in the β1-2 loop, which in turn triggers a wave of interactions which propagate towards the channel (Lee and Sine, 2005). This hypothesis is supported by a related study which showed that Arg209 and Glu45 move early during the gating process (Purohit and Auerbach, 2007). Recent studies investigating the sequence of movements of residues during gating has led to the construction of a Φ map, which suggests that agonist binding triggers motions which causes a movement of the Cys-loop and β1-2 loop, followed by the M2-M3 linker, several M2 residues and finally the gate at the channel pore (9'-14' region) (Bafna *et al.*, 2008; Chakrapani *et al.*, 2004; Grutter *et al.*, 2005; Zouridakis *et al.*, 2009)

The coupling of agonist binding to channel opening some 50 Å away involves several conserved regions, particularly the pre-M1 region, loop C and loop β1-β2. Though specific residues and interactions seem to vary across receptor types, there seems to be an overall degree of similarity across the Cys-loop family, suggesting a conserved mechanism of receptor gating.

1.6.3 Kinetic schemes

Kinetic schemes have been posited which fit the observed single-channel behavior of Cys-loop receptors. Most of these schemes have been for the nAChR and GlyR, which are amenable to single-channel analysis (Auerbach, 2010; Lape *et al.*, 2008; Sine and Engel, 2006). Sine describes a "primed" state which precedes channel opening at the nAChR (Mukhtasimova *et al.*, 2009) (Figure 1.7). The channels' closed to open transition is agonist-independent and

is preceded by two primed closed states; the singly primed state has an intermediate duration and triggers brief openings, whereas the doubly primed state has a brief duration and triggers long-lived openings. The priming step is thus a spontaneous transition that occurs after agonist binding. Similarly, Colquhoun describes a "flip" state of the GlyR, "a structural change which takes place while the channel is still shut." This suggests that there is a structural change which occurs after agonist has bound but before the channel has opened. Both of these schemes suggest that a structural transition occurs which precedes channel opening and that initial binding of a ligand can influence the binding of subsequent ligands to adjacent binding sites. A similar conformational change for the high-conductance isoform of the 5-HT_3AR has been reported (Corradi *et al.*, 2009), suggesting that this may be a conserved mechanism across the Cys-loop receptor family.

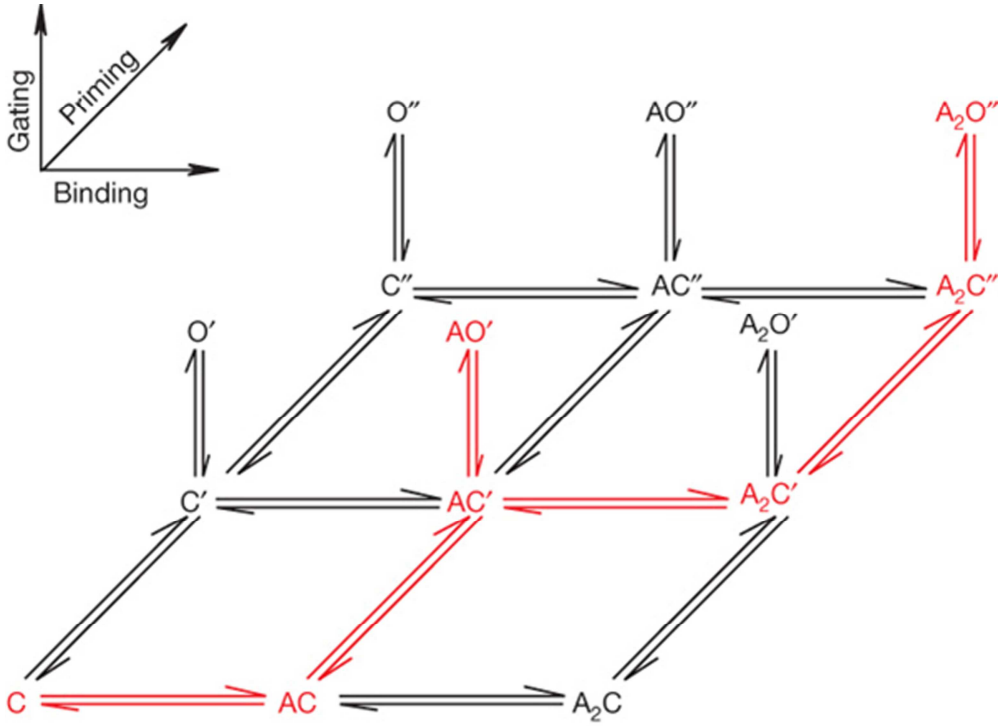

Figure 1.7 Kinetic scheme for Cys-loop receptor activation. Agonist binding, priming and channel gating steps are shown. C, C' and C" symbolize closed states, whereas O' and O" symbolize open states. A symbolises an agonist molecule. In the absence of agonist, the C' and C" states are negligible, indicating that the first step in the activation process generates AC, from which there are three possible paths towards A_2C". Taken from Mukhtasimova *et al.*, 2009, with copyright permission from *Nature*.

A structural study of AChBP described how agonists stabilise loop C in a fully contracted state, whereas peptide inhibitors stabilise loop C in a fully extended conformation (Ulens *et al.*, 2009). This study utilised the strategy of co-crystallisation of AChBP with bound agonists and antagonists. These data, demonstrating a structural rearrangement of loop C following agonist binding, support the theoretical "flip" or "primed" states described by Colquhoun and Sine. Indeed, by providing a structural explanation of such transition states, Ulens has shown how such mechanisms may be part of Cys-loop receptor gating.

Gating of the Cys-loop receptors seems to involve small structural changes at the ligand binding site which cause a change in the stability of the closed state of the M2 helices. The opening of the gate is dependant on this structural change. Whilst the basic mechanism for gating is generally understood, all of the intricate molecular determinants have yet to be characterised. There has thus yet to be posited a unified model of gating dynamics for all members of the Cys-loop family.

1.7 Ligand binding site

The agonist binding site is located in the extracellular region at the interface between adjacent subunits. There is thus a theoretical maximum of five agonist binding sites per receptor. The binding site is comprised of six discontinuous loops (A-F). The ligand binds between Loops A, B and C, on the principal subunit, and loops D, E and F on the complementary subunit (Akabas, 2004) (Figure 1.8).

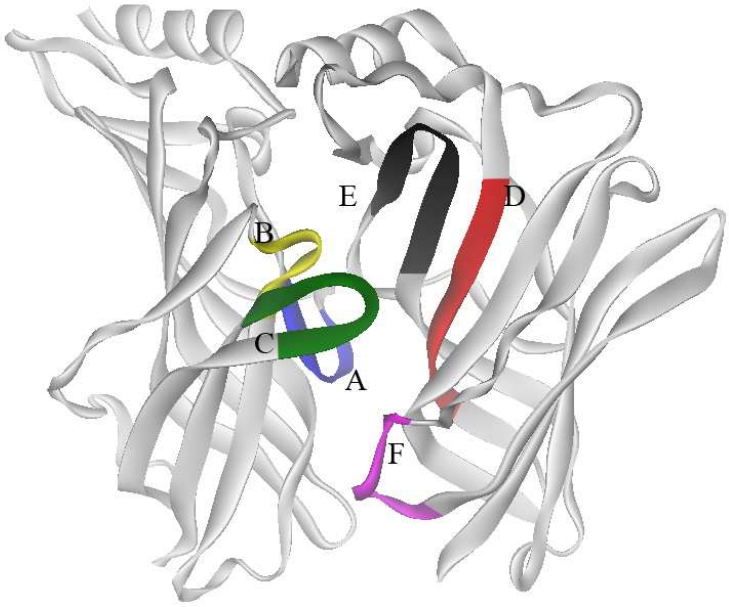

Figure 1.8 Extracellular domain of a Cys-loop receptor. The ligand-binding site is comprised of residues from loops A, B and C from the principal subunit and D, E and F from the complementary subunit.

Functional experiments show that many Cys-loop receptors have a Hill coefficient greater than one - suggesting cooperativity - indicative of more than one agonist binding site per receptor. Single-channel experiments for the 5-HT_3AR have led to the hypothesis that three occupied ligand binding sites lead to maximal receptor activation (Corradi *et al.*, 2009). A similar study in the 5-HT_3AR showed that receptors with three binding sites at non-consecutive subunit interfaces exhibit maximal mean channel open time and receptors with binding sites at three consecutive or two non-consecutive interfaces exhibit intermediate open time. However, receptors with binding sites at two consecutive or one interface exhibit a brief open time (Rayes *et al.*, 2009). The increased receptor activity associated with the occupation of non-consecutive binding sites suggests that the structural rearrangement inherent in channel opening involves movements within the extracellular domains which affect adjacent binding sites. This hypothesis of 'structural transitions' is supported by voltage-clamp fluorometry studies of the GlyR (Pless and Lynch, 2009a; 2009b; 2009c) which show that an agonist specific structural change occurs in the loops of the extracellular domain that is correlated with agonist efficacy.

Many residues involved in binding GABA in the $GABA_A$ receptor have been identified within the extracellular binding site loops. In particular, hydroxylated residues, aromatic residues and charged residues have been identified as being important in ligand binding. Several aromatic residues which form an "aromatic box," a hydrophobic surface favourable for ligand stabilisation, have been identified: α_1Phe64, β_2Tyr62, β_2Tyr97 and β_2Tyr205. Hydroxylated residues α_1Ser68, β_2Thr160, β_2Thr202, β_2Ser204 and β_2Ser209 are critical for ligand binding. Charged residues are also involved in GABA binding: α_1Arg120, α_1Asp183, α_1Arg66 and β_2Arg207. These residues probably stabilise the carboxylate moiety of the ligand (Amin and Weiss, 1993; Boileau *et al.*, 2002; Newell and Czajkowski, 2003; Wagner *et al.*, 2004; Westh-Hansen *et al.*, 1997; Westh-Hansen *et al.*, 1999). A different repertoire of residues which are involved in GABA binding have been identified in the $GABA_C$ receptor: Tyr102, Arg104, Tyr106, Phe138, Val140, Arg158, Tyr198, Phe240, Thr244 and Tyr247 (Amin and Weiss, 1994; Harrison and Lummis, 2006; Lummis *et al.*, 2005b; Zhang *et al.*, 2008). Similarly to the $GABA_A$ receptor, these findings suggest an important role for aromatic, hydroxylated and charged residues in the $GABA_C$ receptor binding site. A review of GABA binding sites has described these data recently (See Lummis, 2009). In $GABA_A$ receptors GABA binds in a partially folded conformation, whilst in $GABA_C$ receptors it is in an extended conformation (Jones *et al.*, 1998; Woodward *et al.*, 1993). Although conformations of GABA within the binding sites of different GABA receptors varies somewhat, an overall similarity of location seems to be conserved.

1.8 Insect GABA receptors

Insect GABA receptors are one of the major targets of insecticides (Raymond-Delpech *et al.*, 2005) and Fipronil, an antagonist of insect GABA receptors, is one of the most important insect control chemicals to date (Sammelson *et al.*, 2004). Other insecticides such as α-endosulfan and lindane target GABA receptors as a means of inducing a lethal convulsant state within their pestilent targets (Chen *et al.*, 2006).

Several transcripts have been identified in *D.melanogaster* which may form GABA-gated anion channels. Whilst transcripts CG6927, CG7589, CG11340, and CG12344 have not yet been functionally assessed (Buckingham *et al.*, 2005), transcripts RDL, GRD and LCCH3 have been heterologously expressed and assessed functionally. These three oligomeric invertebrate GABA receptor subunits have a similar degree of sequence homology with the characterised vertebrate $GABA_A$ receptor subunits as they do with each other (30-38%)(Hosie and Sattelle, 1996a)(Figure 1.9). These insect GABA receptor subunits form heteromeric receptors with varying properties when expressed heterologously (Gisselmann *et al.*, 2004; Hosie *et al.*, 1997) (Table 1.1). It has been shown that GRD and LCCH3 coassemble to form GABA-gated cation channels when cRNA is co-injected into *Xenopus laevis* oocytes (Gisselmann *et al.*, 2004). This suggests that RDL may play an important role in the formation of heteromeric GABA receptors. Furthermore, RDL orthologues have been identified in many other insect species; examples include the house fly (Eguchi *et al.*, 2006), red flour beetle (Jones and Sattelle, 2008), honeybee (Dupuis *et al.*, 2010), German cockroach (Kaku and Matsumura, 1994), and mosquito (Du *et al.*, 2005). Furthermore, RDL receptors from the mosquito, cockroach and small brown planthopper have been functionally assessed (Shotkoski *et al*., 1994; Shotkoski *et al.*, 1996; Eguchi *et al.*, 2006; Narusuye *et al.*, 2007).

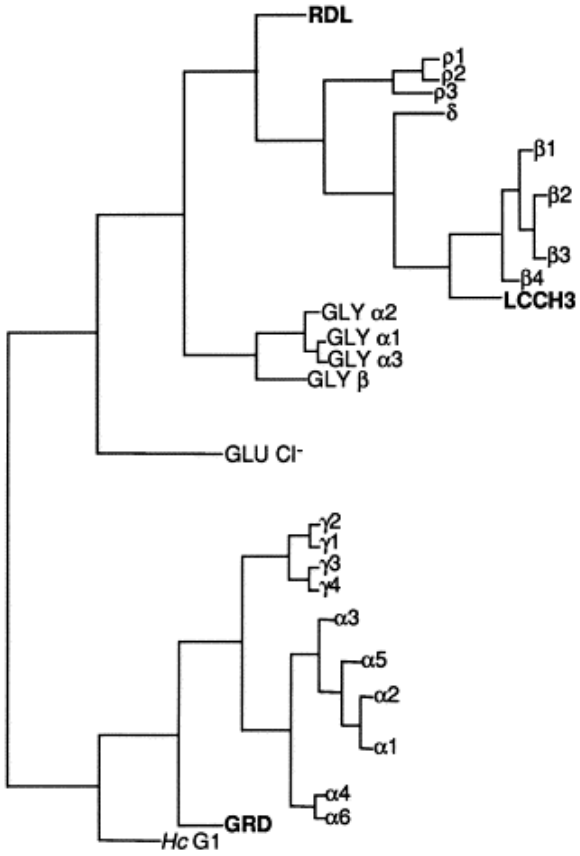

Figure 1.9 A dendrogram illustrating the relative similarity of known insect GABA receptor subunits and other ligand-gated anion-channels. Vertebrate GABA receptor subunits are marked α,β, etc., GLY refers to GlyR subunits while Glu Cl^- and Hc G1 refer to glutamate-gated chloride-channels and a putative GABAR or GlyR subunit from *Haemonchus contortus*. The RDL subunit is most closely related to vertebrate $GABA_A$ ρ subunits. Taken from Hosie *et al.*, 1997, with copyright permission from *Trends in Neurosciences*.

Table 1.1 Pharmacology of insect GABA receptor subunits when co-expressed and expressed alone.

Subunit combination	Heterologous expression	Pharmacology	Reference
RDL homomer	Oocytes, Sf-21; S2	Picrotoxinin-sensitive; Bicuculline-insensitive	(Hosie *et al.*, 1996; Millar *et al.*, 1994; Buckingham *et al.*, 1994; Lee *et al.*, 1993; ffrench-Constant *et al.*, 1993a)
RDL + LCCH3	Oocytes, Sf-21	Picrotoxinin-insensitive; Bicuculline-sensitive	(Zhang *et al.*, 1995b)
RDL + GRD	Not reported	Not reported	N/A
GRD + LCCH3	Oocytes (cation channel)	Picrotoxinin-sensitive; Bicuculline-insensitive	(Gisselmann *et al.*, 2004)

Native insect GABA receptors are insensitive to the $GABA_A$ competitive antagonist bicuculline and sensitive to $GABA_A$ receptor agonists 3-aminopropanesulfonic acid (3-APS), isoguvacine, muscimol and the $GABA_A$ and Glycine non-competitive antagonist picrotoxin (Buckingham *et al.*, 1994). This pharmacology distinguishes them from both vertebrate $GABA_C$ receptors, where 3-APS is an antagonist, and $GABA_A$ receptors which are sensitive to bicuculline and show sensitivity to many allosteric modulators (Sieghart, 1995; Hosie and Sattelle, 1996b). Insect GABA receptors are also sensitive to a range of non-competitive antagonists including Fipronil, TBPS and EBOB (Buckingham *et al.*, 1994). The replacement of alanine 302 with serine or glycine in all subunits encoded by the *rdl* gene renders RDL-containing receptors 100-fold less sensitive to PTX than wild-type (ffrench-Constant *et al.*, 1993a). RDL forms picrotoxin insensitive receptors when expressed with LCCH3 (Zhang *et al.*, 1995b), suggesting that LCCH3 is the predominant subunit in these heteromers. However, when LCCH3 is coexpressed with GRD, picrotoxin sensitivity is restored on the cationic GABA-gated channel (Gisselmann *et al.*, 2004). RDL is the best studied of these subunits as it can be expressed readily in *Xenopus* oocytes where it forms functional homomers with pharmacology similar to that of native insect neurons (Zhang *et al.*, 1994). As such, RDL receptors are considered to be pharmacologically representative of insect GABA-gated ion channels in general.

1.9 RDL receptors

The RDL subunit was originally identified in mutant *D.melanogaster* strains showing resistance to the insecticide dieldrin, hence the name "RDL" (ffrench-Constant *et al.*, 1991; ffrench-Constant *et al.*, 1993b). Dieldrin blocks the channel of RDL receptors and an Ala to Ser mutation was identified in the pore lining M2 region (Ala302), which conferred resistance. RDL receptor subunits in *D. melanogaster* can occur as a variety of different splice variants resulting in varying agonist sensitivities (Buckingham *et al.*, 2005; Hosie *et al.*, 2001; Hosie *et al.*, 2001). The regions which are modified lie in exons 3 and 6 (Fig.

1.10). These alternative transcripts are named a, b (exon 3), c and d (exon 6). The RDLac variant is considered the canonical isoform and this is the isoform used in this study.

Figure 1.10 Regions of *rdl* (the gene for the RDL subunit) which are alternatively spliced. Exons 3 and 6 undergo alternative splicing resulting in altered agonist sensitivity (Buckingham *et al.*, 2005). Exons 3 and 6 correspond to extracellular loops D and F respectively. Reproduced with permission, from McGonigle *et al.*, 2009, *Biochemical Society Transaction*, (Pt 6):1404-6. © the Biochemical Society (http://www.biochemsoctrans.org).

RDL receptors were first expressed heterologously in *Xenopus* oocytes by ffrench-Constant *et al.* (1993a) and then in an insect cell line (S2 cells) by Millar *et al.* (1994). More recent studies have focussed on the role of alternative splicing in this receptor subunit; indeed, studies on the three cloned splice variants of *rdl* have revealed differences in agonist potency with GABA EC_{50}s of 9-30, 56-60 and 100-150 µM for the ac, ad and bd splice variants, respectively (Buckingham *et al.*, 2005; Hosie and Sattelle, 1996a), suggesting that the variant residues are involved in receptor activation. Since these spliced regions lie in the extracellular domain, close to the binding site of all Cys-loop receptors, alterations in this region could reduce agonist affinity and/or gating efficacy.

Heterologously expressed RDL receptors have similar characteristics to GABA receptors of cultured *Drosophila* neurons (Zhang *et al.*, 1994), and RDL

subunits are widely distributed throughout the adult and embryonic *Drosophila* CNS (Aronstein and ffrench-Constant, 1995; Harrison *et al.*, 1996; Hosie *et al.*, 1997); thus it is reasonable to assume that these receptors play a major role in inhibitory neurotransmission in the insect CNS. Indeed it has been shown using RNA knock down that RDL receptors are essential to olfactory learning and the associated conditioned stimulus pathway in *Drosophila* (Liu *et al.*, 2009; Liu and Davis, 2009). A more recent study has shown, using gene knockdown, that RDL has a role in learning in *Drosophila* and in particular RDL negatively modulates olfactory associative learning (Liu *et al.*, 2007). This highlights the functional importance of RDL in insect neuronal signalling. This study also provided high quality immunocytochemical staining images of RDL distribution throughout the fly brain, showing RDL expression to be distributed widely, with RDL receptors detected on neuronal dendrites and axons but not cell bodies. Nonetheless, RDL receptors were detected widely throughout the antennal lobes and mushroom bodies.

It has been shown that RDL subunits can also coassemble with glutamate receptor subunits to form functional GABA-gated anion channels (Ludmerer *et al.*, 2002). Since RDL can form heteromeric receptors with both Glutamate receptors as well as other insect GABA receptor-subunits (Gisselmann *et al.*, 2004) (Table 1.1), it probably plays a role in the insect CNS, potentially generating a diverse set of GABA receptors. Studies of single-channel properties of RDL containing GABA receptors from cultured *Drosophila* neurons are similar to those of RDL homomers (Zhang *et al.*, 1995b); the single-channel conductance for inward currents was 21 pS for RDL homomers, versus 28 pS for GABA receptors on cultured neurons (Zhang *et al.*, 1994).
The distribution of putative RDL-like GABA receptors has been demonstrated in the brain of the adult house cricket *Acheta domesticus*, using specific antisera (Strambi *et al.*, 1998) (Fig. 1.11). The mapping of RDL subunits using RDL-specific anti-sera confirms the widespread distribution of RDL containing GABA receptors in the insect nervous system, similarly to that shown in *Drosophila* (Liu *et al.*, 2009).

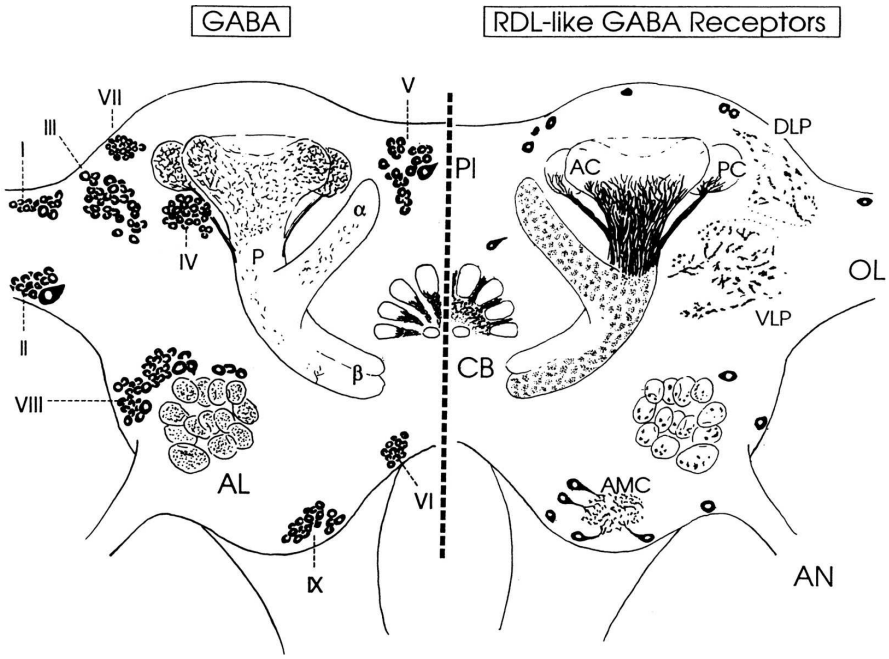

Figure 1.11 Distribution of RDL receptors in the adult house cricket *Acheta domesticus.* Diagram summarising, in frontal view, the distribution of RDL-like GABA receptors (*right*) and of the GABA-like immunoreactivity (*left*). Except for the mushroom bodies, immunoreactivity in the neuropils has been omitted for clarity. Nine groups (I-X) of GABAergic neurons were indicated as well as neurons immunoreactive to the RDL-GABA receptor subunit antiserum. (AC) Anterior calyx of mushroom body; (PC) posterior calyx of mushroom body; (P) peduncle of mushroom body; (α) α lobe of mushroom body; (β) β lobe of mushroom body; (AL) antennal lobe; (CB) central body; (OL) optic lobe; (PI) pars intercerebralis; (AN) antennal nerve; (AMC) antennal motor center; (DLP) dorsolateral protocerebrum; (VLP) ventrolateral protocerebrum. Taken from Strambi *et al.*, 1998, with copyright permission granted from *Cold Spring Harbour Laboratory Press*.

RDL subunits are homologous to $GABA_A$, glycine, $5\text{-}HT_3$ and nACh receptors (Dougherty, 2008) (See Fig. 1.2). Extrapolation from vertebrate receptor data suggests that all of these proteins are pentameric, consisting of five subunits arranged pseudo-symmetrically around a central ion pore (Miyazawa *et al.*, 2003; Sine and Engel, 2006). RDL however has a larger M3-M4 intracellular loop than its vertebrate orthologues, containing some 86 more residues (See Fig. 1.2). There is as yet no structural information available for RDL receptors, however we have recently published a homology model of the RDL extracellular domain based on AChBP, which shows a range of agonists

docked into the agonist binding site and predicts a range of ligand-receptor interactions (McGonigle and Lummis, 2010) (See Fig. 1.12).

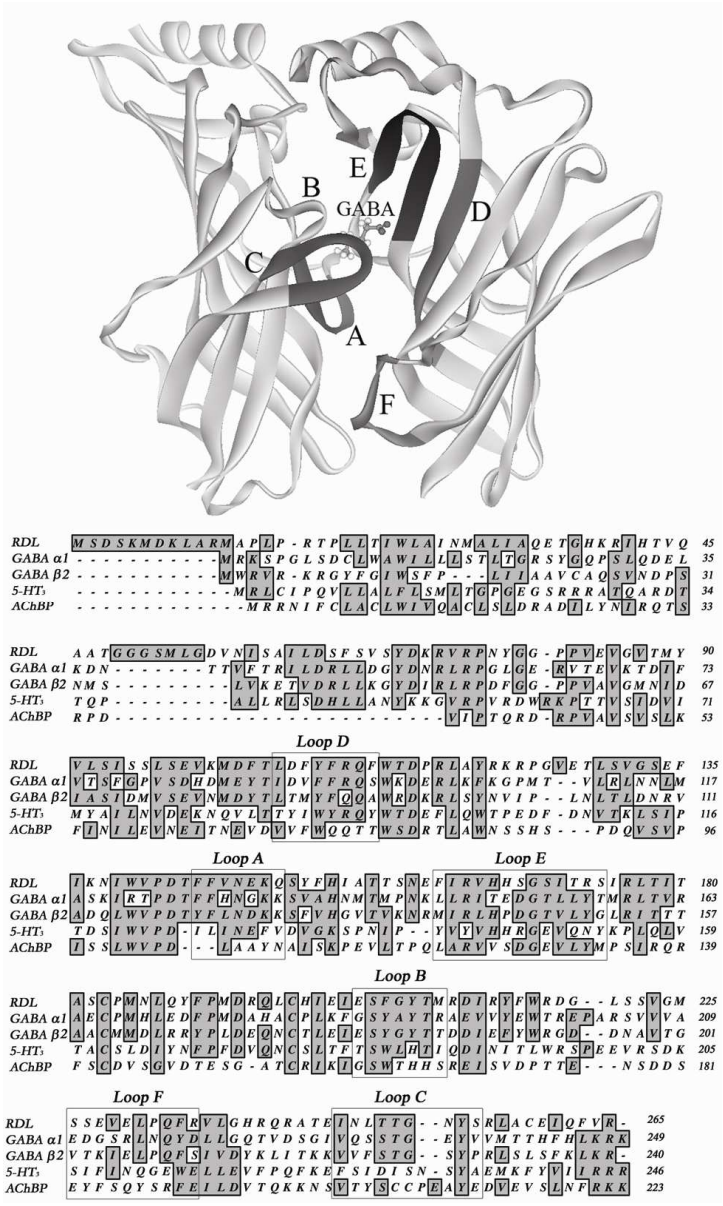

Figure 1.12. Model of the extracellular domain of RDL. Above RDL extracellular domain dimer. A 3D homology model of the extracellular domain of an RDL GABA receptor based on the crystal structure of AChBP (pdb: 1i9b) at 2.7 Å resolution. Extracellular loops A-F contribute to the agonist binding site. A GABA molecule is docked close to loops A, B and C. **Below:** Sequence alignment of RDL and related Cys-loop receptors. Aromatic residues that contribute to the binding pocket in the RDL receptor have mostly aromatic residues in the equivalent locations in other Cys-loop receptors. Taken from McGonigle *et al.*, 2010, with copyright permission from *ACS Biochemistry*.

RDL receptors are widely accepted as a good model for the behaviour of insect GABA receptors (Buckingham *et al.*, 2005). They mimic closely the

pharmacology of native insect GABA receptors (Buckingham *et al.*, 1994) and RDL receptors are located widely in the insect CNS (Sattelle *et al.*, 2000; Strambi *et al.*, 1998). Insect GABA receptors are also the major site for insecticide action (Buckingham *et al.*, 2005; Casida, 1993; Casida, 2009) and RDL receptors expressed in *Xenopus* oocytes represent an effective insecticide/drug screening platform. RDL receptors are thus a model system for studying insect GABA receptors and Cys-loop receptors in general. By characterising RDL receptors we will gain a greater insight into the mechanisms underlying agonist binding as well as receptor function. Achieving a clear understanding of the determinants of the agonist binding site in RDL receptors will be a great aid in the rational design of RDL-specific antagonists, potentially paving the path to a new wave of selective insecticides as well as a greater understanding of insect GABA receptors.

2.0 Thesis Aims

In this thesis I use biophysical, pharmacological, and computational methods as well as site directed mutagenesis to assess the structure and function of RDL receptors.

In chapter 3 I determine the biophysical properties of wild-type RDL receptors using electrophysiological methods, assessing pH sensitivity, ionic selectivity and expression rates of receptors. In chapter 4 I report a structure-activity study of the agonist binding site, testing the potency of a range of GABA analogues and performing molecular modelling and docking simulations at the binding site. In chapter 5 I utilise site-directed mutagenesis and functional studies to assess the accuracy of my model of the binding site model. In chapter 6 I assess the potency of *Ginkgo biloba* extracts on RDL receptor function and use mutagenesis and molecular modelling to assess the nature of the binding interaction. In chapter 7 I assess the functionality of two brain-derived transcripts of the 5-HT_3B subunit (Br1 and Br2) using electrophysiological and fluorometric methods.

The overall aim of this thesis is to achieve a greater understanding of how Cys-loop receptors function at a molecular level.

Chapter 2

Materials & Methods

2.1 Suppliers and addresses

Ambion UK [Applied Biosystems], Lingley House, 120 Birchwood Boulevard, Warrington, WA3 7QH, UK

Bruxton Corporation, 6416 34th Ave, NW Seattle, WA 98107-2607, USA

Dow Corning Corporation, Corporate Centre, PO Box 994, MIDLAND MI, 48686-0994, USA

Garner Glass, 91711- 4921 Claremont, CA, USA

Gibco [Invitrogen Ltd], 3 Fountain Drive, Inchinnan Business Park, Paisley, PA4 9RF, UK

GraphPad Software, 2236 Avenida de la Playa, La Jolla, CA 92037, USA

Greiner, Brunel Way, Stroudwater Business Park, Stonehouse, GL10 3 SX, UK

Harvard Apparatus Ltd, PO BOX 126, Edenbridge, Kent TN8 6WF, UK

Labtech, 1 Acorn house, The Broyle, Ringmer, East Sussex, BN8 5NN, UK

Molecular Devices UK, Winnersh Triangle, 660-665 Eskdale Road, Wokingham, Berkshire, RG41 5TS, UK

Molecular Devices US, 1311 Orleans Drive, Sunnyvale, CA 94089-1136, USA

National Instruments, 11500 N Mopac Expwy, Austin, TX 78759-3504, USA

NEB (New England Biolabs), 240 County Road, Ipswich, MA 01938-2723, USA

Qiagen, QIAGEN House, Fleming Way, Crawley, West Sussex, RH10 9NQ, UK

Sigma-Aldrich Company Ltd., The Old Brickyard, New Road, Gillingham, Dorset, SP8 4XT, UK

Stratagene [Agilent Technologies, UK], South Queensferry, West Lothian, EH30 9TG, UK

Sutter Instrument Company, One Digital Drive, Novato, CA 94949, USA

2.2 Subcloning of rdl into pGEMHE

RDL subunit cDNA (GenBank accession number P25123) was gifted by N.Millar. The *rdl* gene (ac splice variant) was subcloned from pcDNA3.1 (Gibco: Invitrogen) into pGEMHE, the *Xenopus* oocyte expression vector, using the restriction sites *Afl*II and *Xba*I; the pGEMHE vector contains 3'- and 5'-untranslated regions of a *Xenopus* β-globin gene, which has been shown to facilitate very high expression of a number of exogenous proteins in *Xenopus* oocytes (Liman *et al.*, 1992). Positive clones containing the *rdl* gene insert were detected by carrying out restriction digests.

2.3 Preparation of mRNA

20 µg wild-type DNA in pGEMHE was linearised by digestion with *Nhe*1 HF (NEB) in 50 µL volume. 2 µL of proteinase K (1 mg/mL) was added to the reaction mixture and the sample was incubated at 37°C for 1 h in order to degrade any protein in the cDNA sample. DEPC treated water was added to give a final volume of 300 µL. DNA was purified with one phenol/chloroform extraction followed by one chloroform extraction. DNA was precipitated by the addition of 0.1 volumes 3M sodium acetate and 3 volumes 100% ice-cold ethanol. The mixture was left at -20°C for at least 1 h. DNA was pelleted by centrifugation for 15 min at 13,000 g at 4°C. The pellet was washed with 70% ethanol, air dried and resuspended in 10 µL DEPC water. Linearised DNA was diluted to 1 mg/mL and 1 µL was used for an *in vitro* transcription reaction using T7 mMESSAGE mMACHINE kit (Ambion). cRNA concentration was determined by measuring the A_{280} of a diluted aliquot of mMESSAGE product (2 µL diluted in 500 µL ddH_2O) using a benchtop spectrophotometer, taking the original template cDNA into account. An aliquot of cRNA was then diluted to 50 ng/µL for oocyte injection.

2.4 Oocyte preparation

Harvested *Xenopus laevis* oocytes were washed in four changes of ND96 saline (96 mM NaCl, 2 mM KCl, 1 mM $MgCl_2$, 5 mM HEPES, pH 7.4), de-folliculated in ND96 saline with 1 mg/mL collagenase for approximately 2 h, washed again in four changes of saline, and then transferred to injection media (ND96 saline containing 2.5 mM Na-pyruvate, 0.66 mM theophyllen and 52 µM of gentamycin). Healthy stage V-VI oocytes were selected and injected with 5 ng mRNA and injected oocytes were stored in ND96 saline at 17ºC in 94 mm cell culture dishes (Greiner). Electrophysiological recordings were taken from oocytes ~24 h post-injection.

2.5 Electrophysiological recordings

Oocytes from the African clawed frog *Xenopus laevis* are a favoured heterologous expression system amongst electrophysiologists working on ion channels. Two-electrode voltage clamping (TEVC) of the oocyte allows any changes in current that result from an ion channel opening event to be recorded digitally and quantified. This technique allows the response following agonist application to be monitored, yielding quantitative results within real time.

Conventional TEVC of *Xenopus* oocytes was performed using standard electrophysiological protocols. A GeneClamp 500B amplifier was connected to a PC running CLAMPEX v6.0.3 software via a DigiDate1200 Series Interface (all Axon Instruments, Molecular Devices UK). Glass microelectrodes were pulled from GC150TF-10 glass capillaries (Harvard apparatus) using a P-87 micropipette puller (Sutter) to a resistance of 1-2 MΩ and back filled with 3 M KCl. 3 M KCl agar bridges connected ground electrodes to the bath (Fig. 2.1). Oocytes were held at a potential of -60 mV unless stated otherwise and perfused continuously with ND96 saline (recording saline) at a rate of 10-15 mL/min.

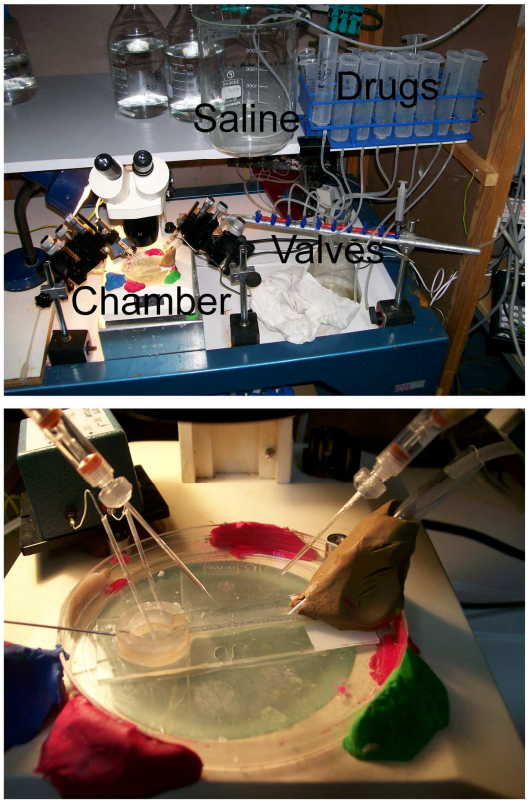

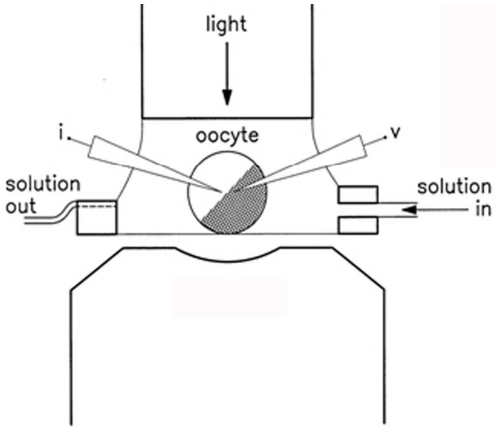

Figure 2.1 Standard TEVC setup. Left: TEVC rig with gravity driven saline perfusion and drug valves for smooth saline/drug transitions (above). Oocyte is immobilised by a small piece of copper wire in the recording bath and impaled by borosilicate pipettes (below). **Right:** TEVC rig schematic

GABA (Sigma) was diluted in recording saline and applied to the bath using a simple row of valve switches (See Fig. 2.1). Doses of GABA were applied successively to achieve a concentration-response curve.

Concentration–response data were normalised to maximal current (I_{MAX}) fitted to the four-parameter logistic equation using GraphPad PRISM version 4.03 for Windows (GraphPad USA, http://www.grphpad.com). Significance was calculated using a one-way ANOVA or an unpaired t-test (Prism v3.02).

$$I = I_{MIN} + (I_{MAX} - I_{MIN})/[1 + 10^{\log}(EC_{50}-[A])^{nH}]$$

Where I_{MAX} = maximal response plateau

I_{MIN} = minimum response plateau

[A] is the concentration of agonist, and

n_H is the Hill coefficient

Four-parameter logistic equation

Automated TEVC was carried out using the MultichannelSystems© *Robocyte R8* electrophysiology platform. This system allows pre-injected oocytes to be loaded individually into a 96-well plate with V-shaped wells (Greiner) for high-throughput automated recording. Supplier's ready-made measuring heads were used; each head comprises two glass microelectrodes, two silver/silver chloride (Ag/AgCl) reference electrodes, and a perfusion inlet and outlet. Recording protocols can be defined in simple scripts – small text files written in the dedicated *Roboocyte* scripting language. Based on preselected parameters, the program decides whether a cell is suitable for further recording, and, if not, the *Roboocyte* simply proceeds to the next oocyte in the well plate to continue the measurements. The *Robocyte* system can thus operate continuously without any supervision until all tests are performed or all cells within the 96-well plate are tested. For a comprehensive review of the *Robocyte* system, see Leisgen *et al.* (2007).

2.6 Sequence alignment

The *Drosophila melanogaster* (GRBDROME) subunit was aligned with the sequence of the AChBP (primary accession number P58154) using FUGUE (Shi *et al.*, 2001). FUGUE is an alignment program which assesses sequence similarity as well as quantifying this in the context of three-dimensional (3D) structure. FUGUE defines the conformation of the aligned protein considering main chain conformation, secondary structure, solvent accessibility and also H-bonding. FUGUE considers the local environment to calculate the likelihood of amino-acid substitutions, insertions and deletions and uses this information to determine the scoring system of the alignment.

2.7 Modelling

A 3D model of the extracellular domain of the RDL receptor was created using MODELLER (Sali and Blundell, 1993), based on the AChBP (PDB accession number 1i9b) crystal structure. A dimer was generated by superimposing the modified monomer onto two protomers of the AChBP.

A model of the transmembrane regions of RDL was generated using the sequence of GLIC, a prokaryotic pentameric ligand-gated ion channel from *Gloebacter violaceus* (GLIC) (PDB ID: 3EAM). Homology models of mutant receptors were generated by the same method, by manually mutating the sequence of RDL before aligning using FUGUE.

Models were analysed using RAMPAGE (http://raven.bioc.cam.ac.uk/rampage.php)(Lovell *et al.*, 2003). Amino acids found in the unfavoured regions of this plot were visually inspected using ViewerLite (www.accelrys.com), to determine if their orientation will affect the binding site model.

2.8 Ligand docking

Binding site ligand structures generated using ChemBio3D Ultra 11.0 were energy minimised using the MM2 force field. Docking of the ligands into the RDL receptor homology model was carried out using GOLD 4.0. The binding site was defined using the αC atoms of the conserved aromatics F206, Y254 and Y109, with a binding site radius of 10 Å. Ten genetic algorithm runs were performed on each docking exercise, giving a total of 10 solutions for each analogue. The structures were analysed using the implemented GoldScore fitness function to identify the most accurate simulation. Special attention was paid to GABA folding and conformation as well as positioning relative to conserved binding site residues and experimental evidence. Hydrogen bonding interactions between ligands and binding site residues were identified using the hydrogen bond monitor function in ViewerLite (www.accelrys.com).

For channel-blocking antagonists, the PDB structures for ligands were downloaded from the CCDC (Cambridge Crystallographic Data Centre) database (http://www.ccdc.cam.ac.uk/). Compounds were docked into the homology model of the RDL transmembrane domain using the program GOLD 4.0. Ten docking experiments were performed for each compound.

2.9 Quantum mechanical ab-initio calculations for ligands

Molecular modelling was carried out with ChemBio3D Ultra 11.0 (CambridgeSoft, UK; http://www.cambridgesoft.com). Ligand structures were generated in the charged zwitterionic state using the ChemDraw program. Ligands structures were energy minimized using the MM2 force field and Mulliken charges (partial atomic charges) were calculated using the GAMESS interface. Dipole distances were calculated using the atomic distance tool in ChemBio3D Ultra 11.0.

2.10 Site directed mutagenesis

2.10.1 Primer design

Mutagenic primers containing the mutation and flanking complementary sequence were designed manually. Primers were designed to be 25-45 bases in length with the mutation in middle with at least 10-15 bases either side. GC content was at least 40% and T_m was typically ~80°C. Primers were terminated with one or more C/G at either end. A local restriction site was also disrupted using a silent base substitution where applicable. Where no restriction sites could be removed a restriction site was inserted. This facilitates quick detection of mutant clones. All primers were obtained from Sigma-Aldrich.

Table 2.1 Oligonucleotide primers used

Mutant	*Forward primer (5'->3')*	*Reverse primer (5'->3')*
F206A	GAAATCGAAAGTGGCGGTTACAC	GTGTAACCGCCACTTTCGATTTC
F206Y	GAAATCGAAAGTTACGGTTACAC	GTGTAACCGTAACTTTCGATTTC
Y254F	GGCAACTTTTCTCGTTAGCCTGC	GCAGGCTAACGAGAAAAGTTGCC
Y254A	GGCAACGCTTCTCGTTTAGCCT	AGGCTAAACGAGAAGCGTTGCC
E204D	GCCAGCTGTGCCACATTGAAATCGATAGCTTCGG	CCGAAGCTATCGATTTCAATGTGGCACAGCTGGC
E204A	GCCAGCTGTGCCACATTGAAATCGCAAGCTTCGG	CCGAAGCTTGCGATTTCAATGTGGCACAGCTGGC
S205T	GCCAGCTGTGCCACATTGAAATCGAAACCTTCGG	CCGAAGGTTTCGATTTCAATGTGGCACAGCTGGC
S205A	GCCAGCTGTGCCACATTGAAATCGAAGCCTTCGG	CCGAAGGCTTCGATTTCAATGTGGCACAGCTGGC
Y208S	GCCACATTGAAATCGAGAGCTTCGGTTCTACGATGCGAGATATCCG	CGGATATCTCGCATCGTAGAACCGAAGCTCTCGATTTCAATGTGGC
Y208F	GAAAGTTTCGGTTTCACGATGCGA	TCGCATCGTGAAACCGAAACTTTC
R111A	GGACTTCACATTGGATTTTTACTTTGCTCAGTTTTGGACCGATCC	GGATCGGTCCAAAACTGAGCAAAGTAAAAATCCAATGTGAAGTCC
R111K	GGACTTCACATTGGATTTTTACTTTAAGCAGTTTTGGACCGATCC	GGATCGGTCCAAAACTGCTTAAAGTAAAAATCCAATGTGAAGTCC
Y109F	GGACTTCACATTGGATTTTTTCTTTCGTCAGTTTTGGACCGATCC	GGATCGGTCCAAAACTGACGAAAGAAAAAATCCAATGTGAAGTCC
Y109S	CACATTGGATTTTAGCTTTCGTCAGTTTTGG	CCAAAACTGACGAAAGCTAAAATCCAATGTG
Y109A	GGACTTCACATTGGATTTTGCCTTTCGTCAGTTTTGGACCGATCC	GGATCGGTCCAAAACTGACGAAAGGCAAAATCCAATGTGAAGTCC
Y109R.R111Y	GGACTTCACATTGGATTTTCGCTTTTATCAGTTTTGGACCGATCC	GGATCGGTCCAAAACTGATAAAAGCGAAAATCCAATGTGAAGTCC
S176T	CGTAGTAAGACCTTGCTATTGTTC	GAACAATAGCAAGGTCTTACTACG
S176A	CGTAGTAAGACCTCGCTATTGTTC	GAACAATAGCGAGGTCTTACTACG
A302S	GCAACGCCGGCGCGTGTGTCGCTCGGTGTGACAAC	GTTGTCACACCGAGCGACACACGCGCCGGCGTTGC
T306S	TGCAACGCCGGCGCGTGTGGCTCTCGGTGTGAGTACCGTGTTG	TGGTCATTGTCAACACGGTACTCACACCGAGAGCCACACGCGC
T306V	TGCAACGCCGGCGCGTGTGGCTCTCGGTGTGGTAACCGTGTTG	TGGTCATTGTCAACACGGTTACCACACCGAGAGCCACACGCGC
L314Q	GAC AAT GAC CAC TCA GAT GTC GTC AAC AAA TGC	GAC AAT GAC CAC TCA GAT GTC GTC AAC AAA TGC
R256A	CCTAACCACAGGCAACTATTCGGCTTTAGCCTGCG	CGCAGGCTAAAGCCGAATAGTTGCCTGTGGTTAGG
R256K	CCTAACCACAGGCAACTATTCGAAATTAGCCTGCG	CGCAGGCTAATTTCGAATAGTTGCCTGTGGTTAGG
T306V.A302S	GGCGCGTGTGTCGCTCGGTGTGGTAACCGTGTTG	CAACACGGTTACCACACCGAGCGACACACGCGCC

2.10.2 PCR

Polymerase chain reaction (PCR) was carried out using a high-fidelity *Pfu* DNA polymerase (Stratagene) and mutagenesis reactions were made up in a 1.5 mL Eppendorf tube as follows:

5 µL (10x) Buffer
1 µL Template DNA (100 ng)
1 µL (25 mM NTPs) (Stratagene)
3 µL Oligo (F) (150 ng)
3 µL Oligo (R) (150 ng)
32 µL dH_20
5 µL DMSO*
1 µL *Pfu* turbo

Covered with 50 µL mineral oil

**10% DMSO was added as it was found to greatly boost the PCR product*

PCR was carried out using standard protocol (QuikChange, Stratagene). Annealing temperatures were modified as required for successful incorporation of the mutation. A melting temperature of T_m Oligo - 5ºC was routinely used. This temperature was altered arbitrarily (± 5ºC) where reactions failed to produce a product. *Dpn*1 digestion (1 µL *Dpn*1 (NEB)/mutagenesis reaction) at

37°C for 2 h was carried out to eliminate methylated template DNA from the PCR products. 1 µL of the reaction was run on a 1% agarose gel for 20 min to visualise any PCR product.

Cycling Parameters
95°C for 1 minute
22 Cycles of: 1. 95°C for 1min
2. 60°C for 1min
3. 72°C for 10 min (or 2 min/kb DNA)
72°C for 7min (extension time after cycles)
4°C for infinity

2.10.3 Preparation of electrocompetent E.coli

A 3 mL culture of DH5α *E.coli* was grown over night in LB in an incubator shaker at 37ºC. A 300 mL flask of LB was inoculated with the 3 mL culture and was incubated at 37°C in incubator-shaker until the OD_{600} was 0.5. The culture was then chilled on ice for 15 min and then spun at 2,500 g (JA-14 rotor) for 15 min at 4ºC. The supernatant was decanted and discarded and cells were rinsed in 300 mL ice cold dH_2O. Cells were then re-spun as before and the supernatant discarded again. Cells were then rinsed in 100 mL ice cold dH_2O, respun as before and then resuspended in 30 mL ice cold 10% glycerol and transferred to 50 mL Falcon tubes. Cells were then spun at 2,500 g for 15 min at 4ºC. Cells were finally resuspended in 2 mL 10% glycerol. Aliquots of 90 µL were pipetted into 1.5 mL Eppendorfs on dry ice. Samples were stored at -80°C.

2.10.4 Transformation of DH5α cells

45 µL of DH5α cells were electroporated (200 Ω, 1.8 kV, tau value 3 msec) with 1-7 µL mutagenesis reaction and 200 µL LB (at RT) was added immediately afterwards. The cell suspension was then incubated at 37°C for 1 h. Cells were plated out on LB + amp (100 µg/mL) plates and placed in an incubator over night.

2.10.5 Plasmid minipreps and restriction digests

Colonies from the transformed DH5α plate were selected and grown over night at 37°C in 2 mL LB + ampicillin (100 μg/mL) in an incubator shaker. Plasmid DNA samples were extracted (QIAGEN Miniprep) and 5 μL of DNA was used to set up restriction digest. Samples were then stored at –20°C. Restriction digests were set up in 1.5 mL Eppendorf tubes according to the table:

Vector DNA	5 μL
10X Buffer	1 μL
Restriction enzyme	1 μL
ddH_2O	3 μL

Digests were incubated for at least 1 hour at 37°C. Loading buffer, 5 μL, was added and samples were run on a 1% agarose gel with ethidium bromide added. Gels were viewed on a UV bed and photographs were taken.

2.11 Assessment of antagonists using TEVC

TEVC was performed using the method outlined in section 2.5. Oocytes showing steady GABA-evoked responses were selected before antagonists were applied. All recordings were carried out at EC_{50} concentrations of GABA. Antagonists were co-applied with GABA at a range of antagonist concentrations and responses were measured yielding IC_{50} values (the concentration of antagonist (M) at which half-maximal inhibition is achieved).

2.12 Mutant cycle analysis

Mutant cycle analysis can be used to investigate interactions between pairs of residues in proteins as well as interactions between residues and molecular groups on ligands (Hidalgo and MacKinnon, 1995). When assessing the effect of molecular groups on ligands the effect on ligand affinity of changing a ligand group or a protein residue, either individually or both together, is measured. If the individual effects are independent and additive, indicating no effective interaction between the two groups, then the coupling coefficient (Ω), defined in eqn. 1 below, will be equal to one.

$$\Omega = \frac{(IC_{50\,WT.L1}).(IC_{50\,MUT.L2})}{(IC_{50\,WT.L2}).(IC_{50\,MUT.L1})}$$

The subscripts WT and MUT represent the wild type and mutant receptor, respectively, and L1 and L2 denote the two ligands being compared. Values of $\Omega > 2.5$ have been shown to identify direct interactions between molecular groups (Schreiber and Fersht, 1995). The interaction energy, $\Delta\Delta G_{int}$, between the two substituted groups is given by $RT\ln\Omega$, where R is the gas constant (8.314 $JK^{-1}M^{-1}$) and T is temperature (293 K). Ω values < 1 were normalised by the function Ω^{-1}.

2.13 Whole insect Bioassays

Bioassays were carried out by Mirel Puinean and Martin Williamson at Rothamsted Research, Hertfordshire. *N.lugens*, the brown planthopper was chosen as it is a typical crop pest. Adult brachypterous (short-winged) susceptible females were used to assess responses to compounds. Bioassays consisted of 3 replicates per dose, each one with 10-20 individual insects. Insects were removed directly from rearing cages, lightly anaesthetised with CO_2 and dosed on the prothorax using 0.25 µL of acetone as the solvent carrier. Endpoint readings were taken at 48 h. Bioassays for 50 ppm and 1000 ppm were carried out.

2.14 Culture of HEK293 cells

Human embryonic kidney (HEK) 293 cells were maintained on 90 mm tissue culture plates at 37 °C and 7% CO_2 in a humidified atmosphere. They were cultured in DMEM: F12 (Dulbecco's Modified Eagle Medium/Nutrient Mix F12 (1:1)) with Glutamax I™ containing 10% foetal calf serum and passaged when confluent.

2.15 FlexStation recording

2.15.1 HEK293 transfection

Cells were stably transfected with pcDNA3.1 (Gibco: Invitrogen) containing the complete coding sequences for the human 5-HT3A receptor subunit (Genbank accession number P46098), as previously described (Hargreaves *et al.*, 1996). For heteromeric receptors, approx 10^6 HEK293 cells (stably expressing human 5-HT_3A receptors) were transfected (electroporation: 1300 V, 30 ms) with 5 μg of human 5-HT3B subunit DNA (Genbank accession number O95264; pcDNA3.1, Invitrogen) using the microporator system (DigitalBio, Labtech), as per manufacturer's instructions. Cells were then plated (approximately 3×10^4 cells/well) onto black sided, clear bottomed, 96 well plates (Greiner) for FlexStation assays. Cells were incubated 1–2 days before assay.

2.15.2 Recording

HEK293 cells in each well were briefly washed once with 100 μL flex buffer (115 mM NaCl, 1 mM KCl, 1 mM $CaCl_2$, 1 mM $MgCl_2$, 10 mM glucose, 10 mM HEPES pH 7.4) at room temperature, and then incubated for 1 h at 37 °C in 100 μL flex buffer containing 1% v/v membrane potential dye (Reagent A-Blue Kit, Labtech). Fluorescence was measured every 2 s for 200 s and, at 20 s, 50 μL of agonist or flex buffer was added to each well. Softmax Pro (Molecular Devices, UK) or Prism (GraphPad, USA) was used for data analysis. The percent change in fluorescence, which was calculated as F (peak fluorescence) minus F_0 (baseline fluorescence at 20 s) divided by agonist F_{max} (peak fluorescence), and was compared across agonist concentrations yielding data points to be plotted as a concentration-response curve.

2.16 Single-channel electrophysiology

HEK293 cells were transfected with subunit cDNA for human 5-HT3A and 5-HT3B subunits (pcDNA3.1, Invitrogen) using calcium phosphate precipitation as previously described (Corradi *et al.*, 2009). For a 35 mm dish of cells, the

total amount of cDNA was 5 µg, and the ratio of A to B subunit cDNA was 1:5. Single-channel recordings were obtained from HEK293 cells one or two days after transfection in the cell-attached configuration (Corradi *et al.*, 2009; Hamill *et al.*, 1981) at a membrane potential of -70 mV, -100 mV and -120 mV at 20°C. The bath and pipette solutions contained 142 mM KCl, 5.4 mM NaCl, 0.2 mM $CaCl_2$, and 10 mM HEPES, pH 7.4. Solutions free of magnesium and with low-calcium were used to minimize channel block by divalent cations. Patch pipettes were pulled from 7052 capillary tubes (Garner Glass) and coated with Sylgard (Dow Corning). Pipette resistances ranged from 5 to 7 MΩ. 5-HT was added to the pipette solution at roughly EC_{50} concentration.

Single-channel currents were recorded using an Axopatch 200 B patch-clamp amplifier (Molecular Devices, US), digitized at 5 µs intervals with the PCI-6111E interface (National Instruments), recorded to the computer hard disk using the program Acquire (Bruxton Corporation), and detected by the half-amplitude threshold criterion using the program TAC 4.0.10 (Bruxton Corporation) at a final bandwidth of 10 kHz (Gaussian digital filter).

Chapter 3

Biophysical properties of RDL receptors

3.1 Introduction

Oocytes from the African clawed frog, *Xenopus laevis*, are a favoured heterologous expression system amongst electrophysiologists working on ion channels. Two-electrode voltage clamping (TEVC) of the oocyte allows any changes in current that result from an ion channel opening event to be observed and quantified. This technique allows the response following agonist application to be monitored, yielding quantitative results within real time. Responses for a range of agonist concentrations can be recorded from the same oocyte, allowing concentration-response curves to be generated, yielding an EC_{50} value for the agonist. Here I determine the EC_{50} value for GABA at RDL receptors using conventional TEVC as well as the automated *Robocyte R8* system.

By measuring the amplitude of maximal currents elicited from oocytes expressing RDL receptors over a time course, we can determine the optimum incubation time for conducting electrophysiological experiments. Here I measure the maximal currents over a 72 hour period post-injection.

RDL receptors are GABA-activated chloride channels. Allowing the passage of anions into the cell allows the generation of IPSPs, facilitating inhibitory neurotransmission under normal physiological conditions. By reducing the chloride concentration in the extracellular saline, changes in the reversal potential for the receptor can be used to determine the charge selectivity of the channel pore. This strategy has been employed in determining the charge selectivity of the acetylcholine receptor (Galzi *et al.*, 1992). Here I have reduced the chloride concentration in the extracellular saline by 90%, substituting chloride ions with the large isethionate anion, to determine the effect of chloride concentration on channel currents.

Changes in the extracellular pH have been shown to affect the maximal currents of $GABA_A$ receptors in a subunit dependant manner (Krishek *et al.*, 1996a). Here I investigate the effect of a change of pH on RDL receptors currents.

The aims of this chapter were to characterise the biophysical properties of RDL GABA receptors expressed in *Xenopus* oocytes, specifically determining the GABA EC_{50} value, the expression rate, the ionic selectivity of the channel pore and the sensitivity of the receptor to changes in pH.

3.2 Results

In order to test RDL receptor function in *Xenopus* oocytes, the *rdl* gene was subcloned from pcDNA3.1 into the oocyte expression vector pGEMHE. The *rdl* gene was excised from pcDNA3.1 using the restriction enzymes *Afl*II and *Xba*I (Fig. 3.1) and cloned into pGEMHE using the same restriction sites.

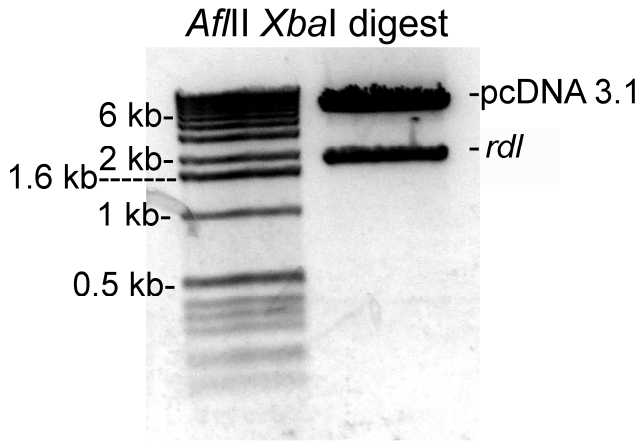

Figure 3.1 *Afl*II *Xba*I excision of *rdl* from pcDNA3.1.

3.2.1 Expression of RDL receptors in Xenopus oocytes

Application of GABA to *Xenopus* oocytes expressing RDL receptors elicited concentration-dependant inward currents (Fig. 3.2). Little desensitisation occurred when GABA was applied successively to an oocyte expressing RDL receptors. RDL receptors recovered quickly following withdrawal of agonist allowing successive applications of agonist to be applied generating a concentration-response course. Plotting current amplitude against a range of GABA concentrations revealed an EC_{50} of ~20 μM (Fig. 3.3) which is similar to previously published results (10-31 μM) (Belelli *et al.*, 1996; Hosie *et al.*, 2001; Hosie and Sattelle, 1996a; McGurk *et al.*, 1998). The dose response profiles as yielded by the automated *Roboocyte R8* system and by conventional

TEVC are identical, giving confidence that an accurate EC_{50} value has been arrived at (Table 3.1).

Although the *Robocyte* system allows accurate and reliable measurements of receptor function, it was felt that conventional TEVC allows more user control and adaptability. For cases where oocyte health varies or where immediate control of drug/wash is required, conventional TEVC affords the user greater control to quickly alter the recording protocol. For these reasons, unless otherwise stated, all further experiments in this dissertation were carried out using conventional TEVC.

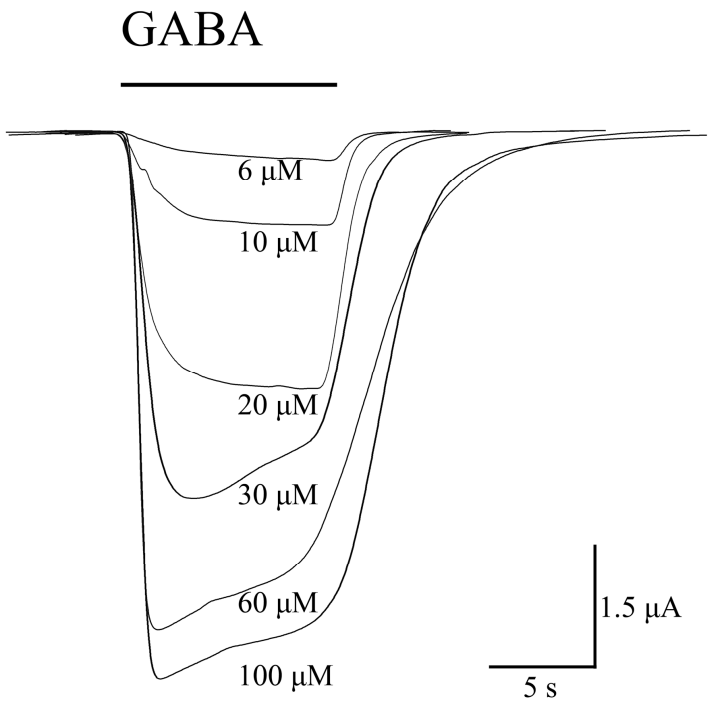

Figure 3.2 Electrophysiological traces from wild-type RDL receptors expressed in *Xenopus laevis* oocytes using conventional TEVC. Inward currents are evoked when GABA is applied. A range of doses of GABA were applied yielding data to plot a concentration-response curve.

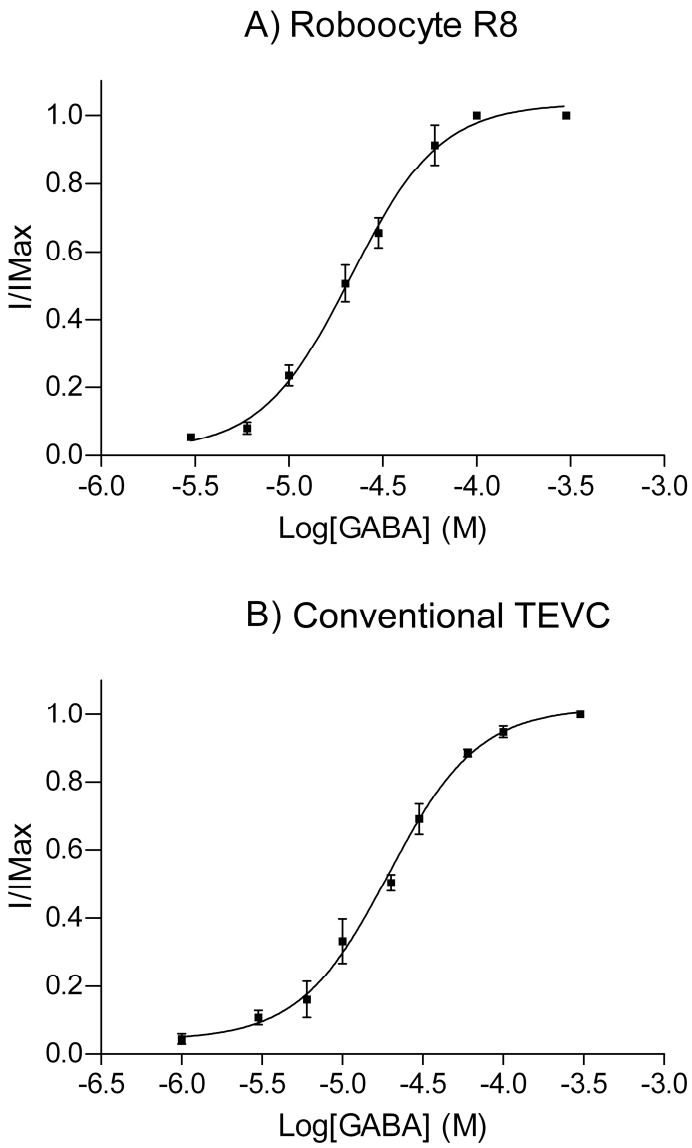

Figure 3.3 Concentration-response curves for RDL receptors expressed in *Xenopus* oocytes for both the automated electrophysiology system (*Robocyte R8*) and conventional TEVC. The concentration-response curves for the automated system (*Robocyte R8*) and conventional TEVC are similar.

Table 3.1 Parameters derived from concentration-response curves.

Recording system	pEC_{50} ± SEM	EC_{50} (µM)	n_H ± SEM	n
Robocyte R8	4.671 ± 0.042	21.3	1.8 ± 0.3	6
TEVC	4.705 ± 0.039	19.7	1.8 ± 0.2	19

Data = mean ± SEM, n_H is the Hill coefficient, n indicates number of replicates. Data are not significantly different (p=0.93, Student's t-test).

3.2.2 RDL expression rate

To determine the stability of receptor expression and to detect any decay of current amplitude occurs, EC_{50} currents were measured over a twenty minute period, a time scale representative of a typical experiment on a single oocyte. No decrease in current amplitude was detected over twenty minutes, confirming that receptors express stably (Fig. 3.4).

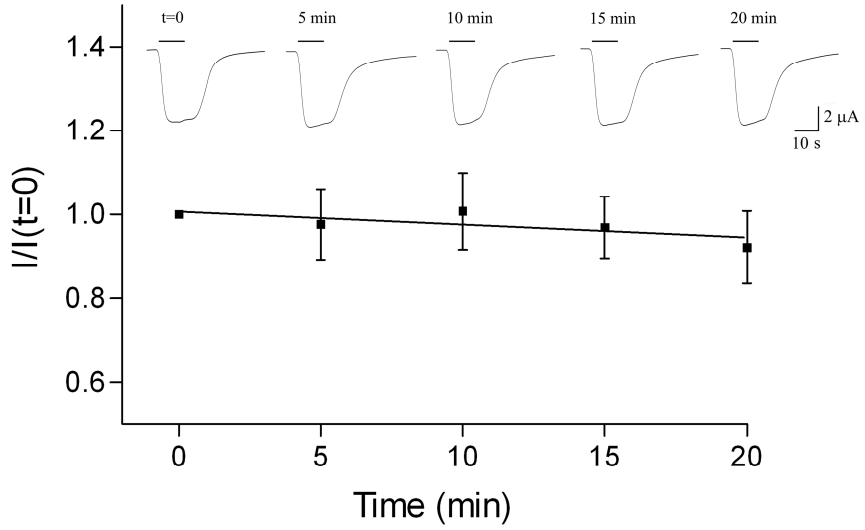

Figure 3.4 EC_{50} current amplitudes from RDL receptors expressed in *Xenopus* oocytes over 20 min. RDL EC_{50} currents do not decay over a 20 min period as demonstrated by sample electrophysiological traces (above) and a graph of mean currents (± SEM) (n≥5 oocytes).

RDL receptor maximal currents (evoked by 100 µM GABA) were recorded over a 72 hour period (post injection of cRNA) to determine expression rate in *Xenopus* oocytes. No response was observed at 6 h. At 60 hours no currents could be recorded and the oocytes health had deteriorated with a high membrane leak (>200 nA). Maximal currents (~7 µA) were observed at 40 h (Fig. 3.5).

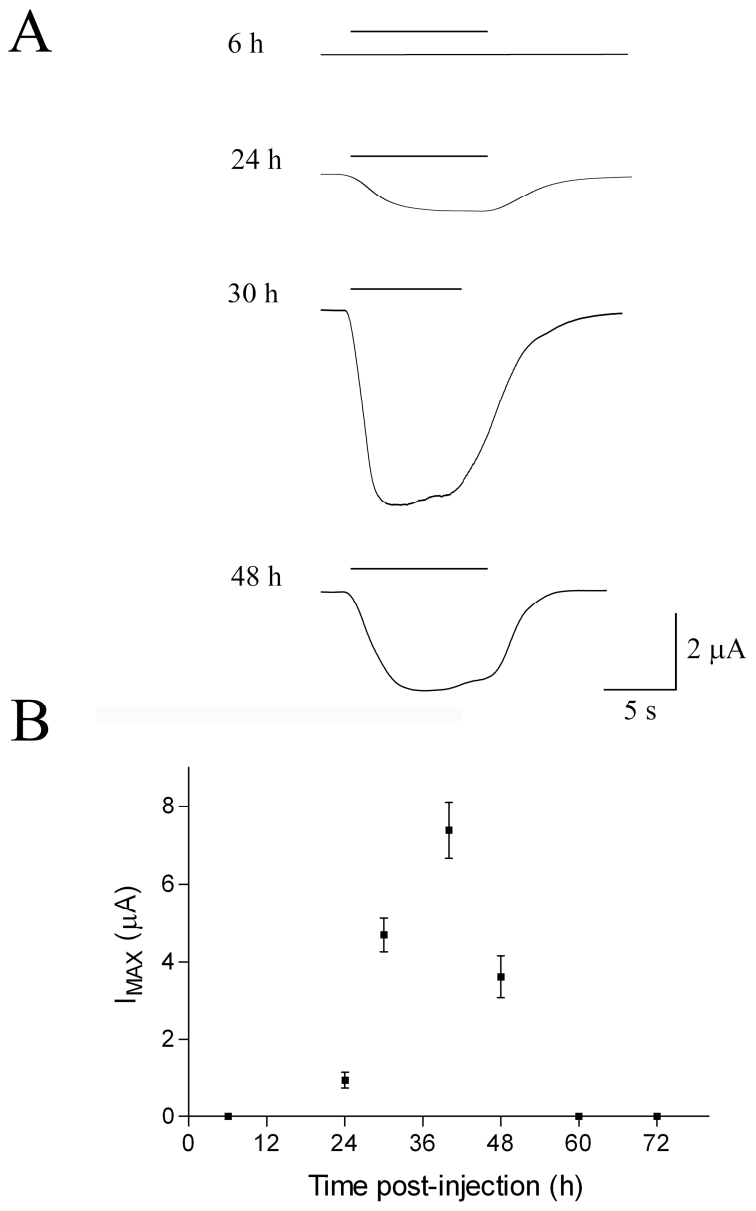

Figure 3.5 Maximal currents from RDL receptors expressed in *Xenopus* oocytes over 72 h. A Sample current traces for 100 µM GABA (I_{Max}) at 6 h, 24 h, 30 h and 48 h. **B** Maximal current amplitudes over 72 h (n≥6 oocytes for each data point).

3.2.3 Ionic selectivity of RDL receptors

Maximal GABA currents were recorded over a range of voltages, in both standard ND96 saline (96 mM NaCl, 2 mM KCl, 1 mM $MgCl_2$, 5 mM HEPES, pH 7.4), as well as a low chloride substitute (6 mM NaCl, 2 mM KCl, 1 mM $MgCl_2$, 5 mM HEPES, 90 mM Na-Isethionate, pH 7.4).

Reducing the chloride concentration resulted in an increase in the voltage reversal potential as evinced by a shift to a higher voltage of the IV curve, as characteristic for a chloride selective channel (Fig. 3.6). Published values for the internal ion concentrations for the *Xenopus* oocyte are: $[K^+]$, $[Na^+]$ and $[Cl^-]$; 110, 10 and 38 mM respectively (Costa *et al.*, 1989). Since the internal chloride concentration of the *Xenopus* oocyte has been determined to be close to 40 mM (Costa *et al.*, 1989), we can use the Goldman-Hodgkin-Katz Equation (Fig. 3.6) to determine the relative permeability of cations and anions through the channel pore.

$$V_m = \frac{RT}{F} \ln\left(\frac{p_K[K]_o + p_{Na}[Na]_o + p_{Cl}[Cl]_i}{p_K[K]_i + p_{Na}[Na]_i + p_{Cl}[Cl]_o} \right)$$

Figure 3.6 The Goldman-Hodgkin-Katz Equation. V_m is the membrane reversal potential. R is the universal gas constant (8.314 $J.K^{-1}.mol^{-1}$), T is the temperature in Kelvin (°K = °C + 273.15), F is the Faraday's constant (96485 $C.mol^{-1}$), p_K is the membrane permeability for K^+, p_{Na} is the relative membrane permeability for Na^+, p_{Cl} is the relative membrane permeability for Cl^-, $[K]_o$ is the concentration of K^+ in the extracellular fluid, $[K]_i$ is the concentration of K^+ in the intracellular fluid, $[Na]_o$ is the concentration of Na^+ in the extracellular fluid, $[Na]_i$ is the concentration of Na^+ in the intracellular fluid, $[Cl]_o$ is the concentration of Cl^- in the extracellular fluid and $[Cl]_i$ is the concentration of Cl^- in the intracellular fluid.

A reversal potential of -22.2 mV was determined for receptors in ND96 saline and +11.2 mV in low chloride (10 mM) saline (Fig. 3.7). Such an increase in the reversal potential is characteristic of a chloride selective channel as shown by the Goldman-Hodgkin-Katz Equation rationale. Taking the combined extracellular concentrations of potassium and sodium together the relative permeability of cations to anions was calculated for both experiments. The

relative permeability of cations and anions was determined to be 0.07:1 and 0.26:1 in ND96 and low chloride saline respectively.

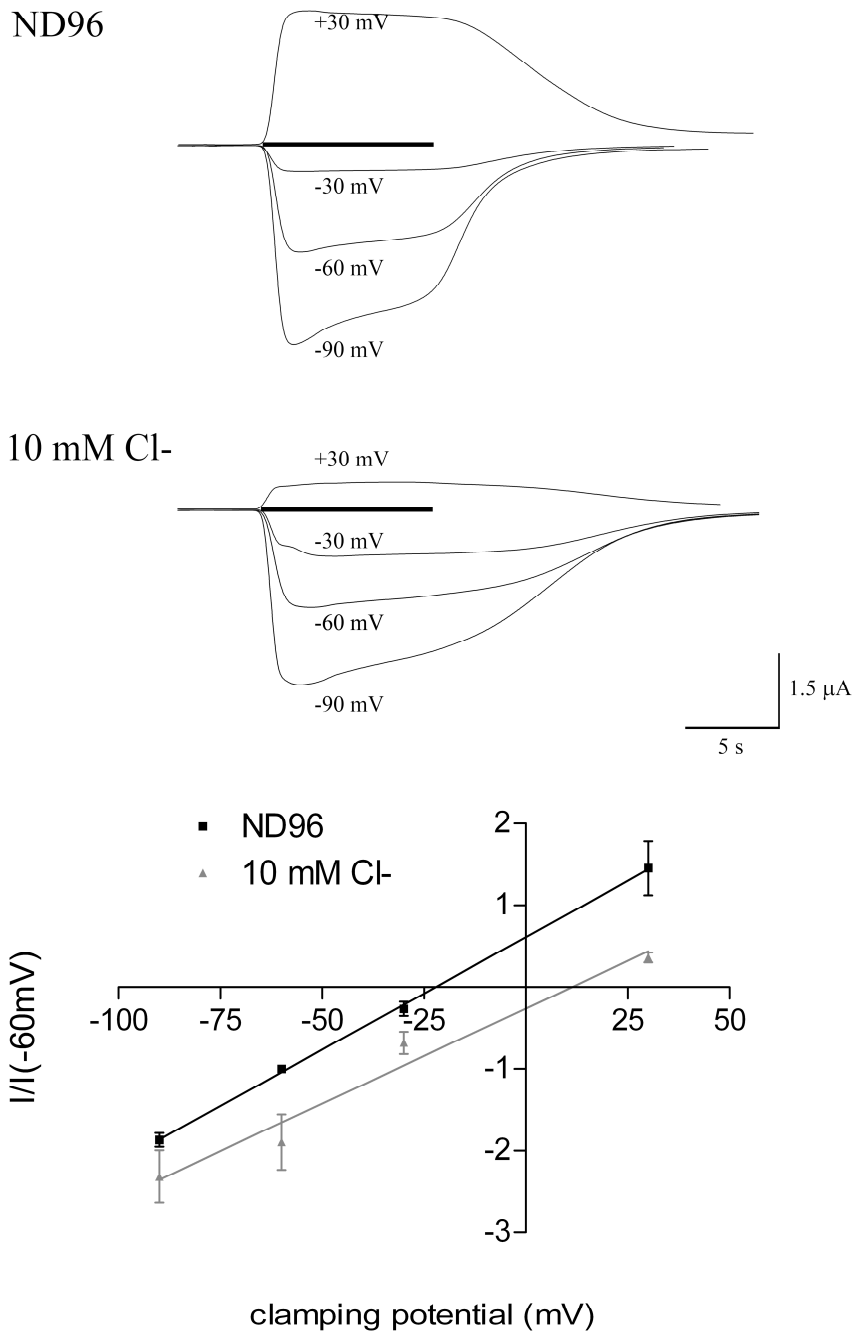

Figure 3.7 Voltage-reversal experiments for RDL receptors in ND96 and low chloride saline. Above: Sample current traces for RDL receptors (maximal currents [GABA] = 100 µM) in normal ND96 and low chloride (10 mM) saline. **Below:** IV curves for normal and low chloride saline. Data = mean ± SEM for at least four oocytes. An increase in the reversal potential as shown with the reduced chloride saline is characteristic of a chloride selective channel. Reversals potentials were significantly different (p=0.03, paired t-test) and slopes were not significantly different (p=0.16, paired t-test).

3.2.4 pH sensitivity of RDL receptors

Since GABA itself is an acid I felt it important to assess the affect of GABA on the pH of a solution and to determine if perturbations in pH have an affect on receptor function.

The concentration-pH relationship for GABA in aqueous solution was determined using the program ChemBuddy (www.chembuddy.com) (Fig. 3.8). RDL receptors reach maximal activation at 100 µM GABA. At this concentration of GABA the pH of an unbuffered aqueous solution is 4.2. If high concentrations of GABA were to be reached in the synaptic cleft or the extrasynaptic milieu, local pH perturbations may play a role in modulating receptor function. Solutions of GABA in buffered recording saline (pH 7.4) were tested for changes in pH with the addition of GABA. Concentrations as high as 1 mM GABA effected no change in the pH of the saline.

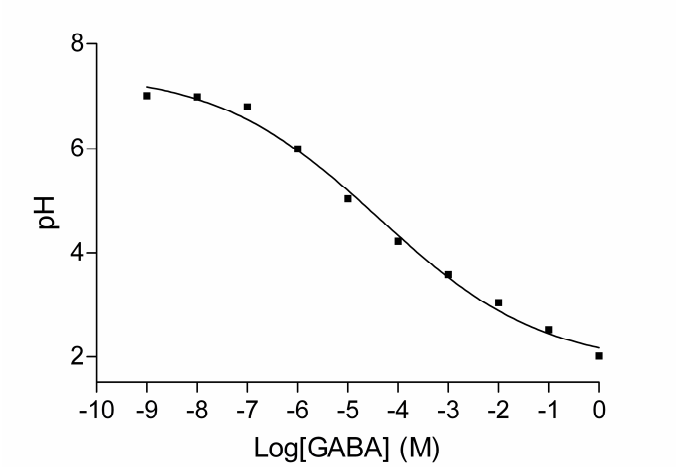

Figure 3.8 pH of an aqueous solution of GABA. Concentration-pH relationship for GABA (pK_a 4.03 (Huxtable *et al*, 1987)) in aqueous solution. Generated using the ChemBuddy program (www.chembuddy.com).

The effect of ten and one hundred-fold changes in extracellular pH on RDL receptor function was determined. An increase in the extracellular pH to 8.5 and 9.5 caused a decrease in the EC_{50} current of approximately 10% and 20% respectively. A decrease in the pH to 6.5 and 5.5 caused no decrease in the EC_{50} current (Fig. 3.9).

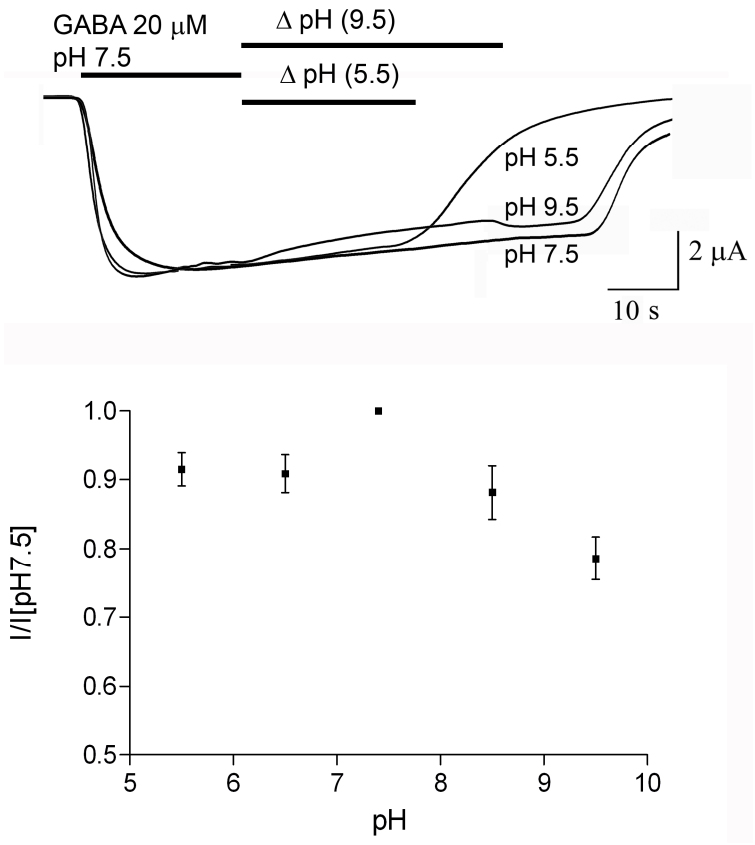

pH	mean current	SEM	n
5.500	0.915	0.024	6
6.500	0.909	0.028	7
7.500	1.000	0.000	6
8.500*	0.881	0.038	8
9.500*	0.786	0.031	6

Figure 3.9 The effect of a pH change on the current amplitude of RDL receptors. Above: Sample traces showing the effect of a change in pH during a non-desensitising EC_{50} response. Changing the pH to 9.5 during the course of the receptor response decreased the current amplitude within ten seconds, whilst a decrease in pH to 5.5 had no effect. **Below** The effect of a change in pH upon GABA EC_{50} currents. Data = mean ± SEM for at least six oocytes. Currents at pH 5.5 and 6.5 are not significantly different from pH 7.5 ($p>0.05$, t-test).

* denotes currents at pH 9.5 and 8.5 are significantly different from pH 7.5 ($p<0.05$, t-test).

3.3 Discussion

In this chapter I have assessed the biophysical properties of RDL receptors expressed in *Xenopus* oocytes. I have determined the GABA EC_{50} and I have assessed the rate at which the oocyte expresses RDL receptors. I have demonstrated the anionic selectivity of RDL receptors and I have also assessed the sensitivity of these receptors to changes in extracellular pH.

The RDL subunit, an insect $GABA_A$ –like receptor, can be expressed readily in the *Xenopus* oocyte expression system. Maximal current responses were detected ~40 h post-injection. To facilitate experiments it was deemed optimal to inject in the morning and to record responses the following day, i.e. 24 h later, thus utilising the greatest window of opportunity for measuring robust current responses.

The MultichannelSystems© *Robocyte R8* automated TEVC electrophysiology platform yielded an EC_{50} value not significantly different to those arrived at using conventional TEVC. The GABA EC_{50} value is in line with previously published values (Hosie *et al.*, 2001; Hosie and Sattelle, 1996a). This makes the *Robocyte R8* a useful and reliable tool for studying ligand-gated ion channels.

Cys-loop receptors elicit a cellular response by allowing the passage of cations or anions either into or out of the cell in an agonist dependant manner. The selectivity of the channel to cations/anions determines whether the effect of channel opening will lead to EPSPs or IPSPs, respectively. The ion selectivity filter is located close to the second transmembrane region of the receptor and residues that line the pore have been indentified to be responsible for charge selectivity in these receptors (Galzi *et al.*, 1992; Gunthorpe and Lummis, 2001; Keramidas *et al.*, 2000; Thompson and Lummis, 2003) (Fig. 3.10).

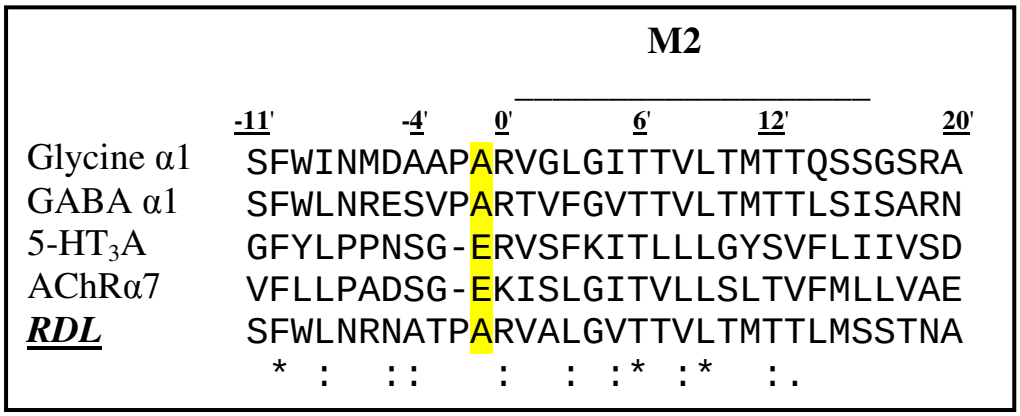

Figure 3.10 Alignment of M2 regions of RDL and other Cys-loop receptors. The -1' residue (highlighted) has been shown to be responsible for ionic selectivity in the 5-HT_3A receptor (Gunthorpe and Lummis, 2001; Thompson and Lummis, 2003), the nAChR (Galzi *et al.*, 1992) and the glycine receptor (Keramidas *et al.*, 2000). RDL, like the glycine and $GABA_A$ receptors, has an alanine residue at the -1' position suggesting that the channel is also anion selective.

RDL receptors are similar to other anionic selective channels, with neutral residues at the -1' position, and the findings here show that the channel is indeed selective for anions. My results here show that the channel is predominantly anion selective and that at low chloride levels, cations may compete for passage through the channel pore. A mutagenesis study of the β subunit of $GABA_A$ receptors has shown that mutating the residues at positions -5' to 0' to those of the α7 nicotinic acetylcholine receptor subunit converts the channel from being anion selective to cation selective (Jensen *et al.*, 2002). This study fits with other work which showed that the ionic selectivity filter lies in the M1-M2 cytoplasmic loop of acetylcholine receptors (Wilson and Karlin, 2001; 1998). Similar studies on the 5-HT_3R have highlighted the critical role of the -1' residue (Gunthorpe and Lummis, 2001; Thompson and Lummis, 2003) and proximal mutations (0, -1' and -2' residues) have been shown to convert GlyRs from anionic to cationic selective (Keramidas *et al.*, 2000), with the converse mutations rendering the acetylcholine receptor anion selective (Galzi *et al.*, 1992). Given the critical role of this region in determining the ionic selectivity of Cys-loop receptors, it is unsurprising that

RDL receptors are anion selective, given their similarity to their vertebrate orthologues.

Changes in external pH are a feature of certain pathological processes such as ischaemia, anoxia and epileptiform activity (Chen and Chesler, 1992; Chesler, 1990; Kraig *et al.*, 1983; Urbanics *et al.*, 1978) and therefore inhibitory neurotransmission may be affected by such biophysical perturbations. Additionally, activation of $GABA_A$ receptors may change the external pH following bicarbonate efflux through the integral anion selective channel (Kaila, 1994; Kaila and Voipio, 1987) and this phenomenon could lead to physiological changes in GABA signalling. Indeed α1β1 $GABA_A$ receptors EC_{50} currents are potentiated by lowering the pH of the external medium from 7.4 to 5.4 by (73 ± 10%, mean ± SEM). In contrast, increasing the pH from 7.4 to 9.4 resulted in a reduction (36 ± 11%) in the response to GABA (Wilkins *et al.*, 2005). While an increase in pH has been shown previously to have little or no affect on $GABA_AR$ currents (Huang *et al.*, 1999; Krishek *et al.*, 1996a), Wilkins *et al.* (2005) showed that GABA-activated currents are potentiated at pH 8.4 for both αβ and αβγ subunit-containing receptors, but only at GABA concentrations below the EC_{40}. This same study also identified a critical role of the 24' lysine residue in the M2-M3 extracellular linker in the modulation of GABA currents. A prior study of GABA receptors has shown that this pH modulation is subunit dependent (Krishek *et al.*, 1996a), with a histidine residue at the 17' position in the β subunit being critical to modulation at low pH (Wilkins *et al.*, 2002). The homologous residue in RDL is different (17'S) while the 24' residue is conserved (24'K) so it is possible that the protonation state of this residue could affect channel gating. However, RDL receptors displayed relative resistance to changes in extracellular pH when compared to their vertebrate orthologues, with no potentiation observed at higher or lower pH. In fact current reduction was observed at higher pH (pH 8.5 and 9.5) with no change at lower pH (pH 6.5 and 5.5), distinguishing RDL receptors from $GABA_A$ receptors. These results demonstrate that a large change in pH has only a small effect on RDL receptor function and this finding may have wider implications for insect physiology and neural signalling.

3.4 Conclusions

RDL receptors express stably in *Xenopus* oocytes with large currents (~ 5 μA) detectable at ~30 h. The *Robocyte R8* is an effective automated electrophysiology platform for testing Cys-loop receptor function, post mRNA injection, and it is a reliable accompaniment to standard TEVC, yielding identical EC_{50} values. RDL receptors are predominantly chloride selective ion channels, highlighting their important role in inhibitory neurotransmission. RDL receptors are resistant to changes in extracellular pH, with only moderate effects at pH 8.5 and pH 9.5. These findings provide a biophysical profile for the functioning of RDL receptors, showing their agonist sensitivity, ionic selectivity and insensitivity to pH modulation. These findings may contain useful information for further studies on the physiological properties of insect GABA receptors.

Chapter 4

Molecular characterisation of agonists that bind to RDL receptors

---

4.1 Introduction

Cys-loop receptors, such as $GABA_A$, $GABA_C$ (a subclass of $GABA_A$), glycine, 5-HT_3, and nicotinic acetylcholine (nACh) receptors, have homologous regions which form their agonist binding sites. These are located in the extracellular domain and are comprised of six discontinuous loops, named A-F (See Fig. 1.12). There are as yet no high resolution structural data of a complete vertebrate Cys-loop receptor, but the lower resolution nACh receptor structure, and homologous structures, such as those from the related acetylcholine binding protein (AChBP), have been useful for creating homology models (Brejc *et al.*, 2001; Miyazawa *et al.*, 2003; Sixma *et al.*, 2003; Unwin *et al.*, 2002). Homology models have been created for many different vertebrate Cys-loop receptors including nACh, 5-HT_3, GABA and glycine receptors (Bartos *et al.*, 2009b; Padgett *et al.*, 2007; Pless *et al.*, 2008; Thompson *et al.*, 2008), but invertebrate Cys-loop receptors have been largely ignored. The lack of models for these proteins is surprising, as these proteins are the targets of a number of invertebrate specific ligands, such as insecticides, and a better understanding of critical binding site features could assist the development of novel, more effective compounds (Casida, 1993; 2009). Some information, however, can be extrapolated from vertebrate models, which supports previous mutagenesis and labelling studies in showing that aromatic residues in the binding loops contribute to the formation of an "aromatic box" that is important for ligand binding in all of these receptors (Beene *et al.*, 2002; Beene *et al.*, 2004; Harrison and Lummis, 2006; Padgett *et al.*, 2007; Pless *et al.*, 2007). However, critical residues are not necessarily equivalent for different receptors; even in the closely related $GABA_A$ and $GABA_C$ receptors, for example, GABA has different orientations in the binding pocket: in the former there is a cation-π interaction between GABA and a tyrosine residue in loop A, while in the latter this interaction is with a tyrosine in loop B (Lummis *et al.*, 2005b; Padgett *et al.*, 2007). Nevertheless, in both these receptors, there is evidence that the

carboxylate residue is close to arginine residues in loop D (Harrison and Lummis, 2006; Wagner *et al.*, 2004), suggesting that GABA has broadly similar orientations in both GABA receptor binding sites.

There are a range of invertebrate Cys-loop receptors that are activated by GABA, but, as mentioned above, we know little about the molecular details of insect GABA receptor binding sites. The aim of this study was to identify the molecular determinants of agonist binding and potential interactions with binding site residues in RDL receptors, one of the best studied classes of insect GABA receptor.

4.2 Results

4.2.1 Functional responses:

A range of GABA analogues was tested for activity at RDL receptors (Fig. 4.1). The most potent of these were muscimol, TACA and isoguvacine (Table 4.1; Fig. 4.2). THIP and β-alanine are weaker agonists with EC_{50} s of 220 and 800 μM respectively, while 5-aminovaleric acid (5-AV) and taurine were very weak agonists with EC_{50} values of 1.1 mM and > 10 mM respectively. GHB, a $GABA_B$ receptor agonist, and 3-APP, a $GABA_C$ and $GABA_B$ receptor antagonist, had no activating effect at RDL receptors. Glycine, 4-AB, PABA, and tyramine also failed to activate RDL receptors when applied at concentrations up to 10 mM. EC_{50} values for previously tested analogues (muscimol, β-alanine, TACA and isoguvacine) are close to published values (Hosie and Sattelle, 1996a). None of the compounds tested were antagonists of RDL receptors.

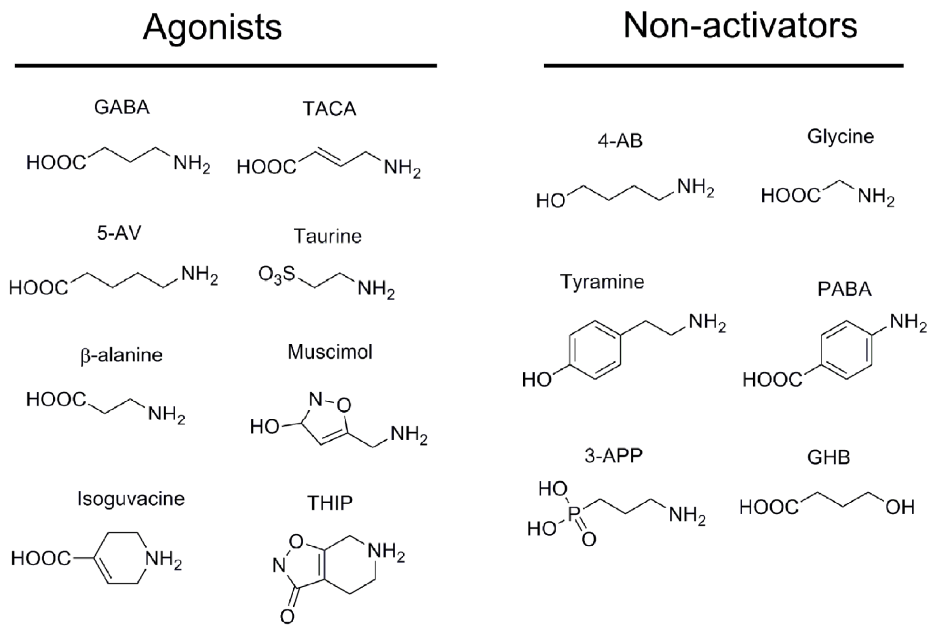

Figure 4.1 Chemical structures of GABA analogues examined in this study. Taken from McGonigle and Lummis, 2010, with copyright permission from *ACS Biochemistry*.

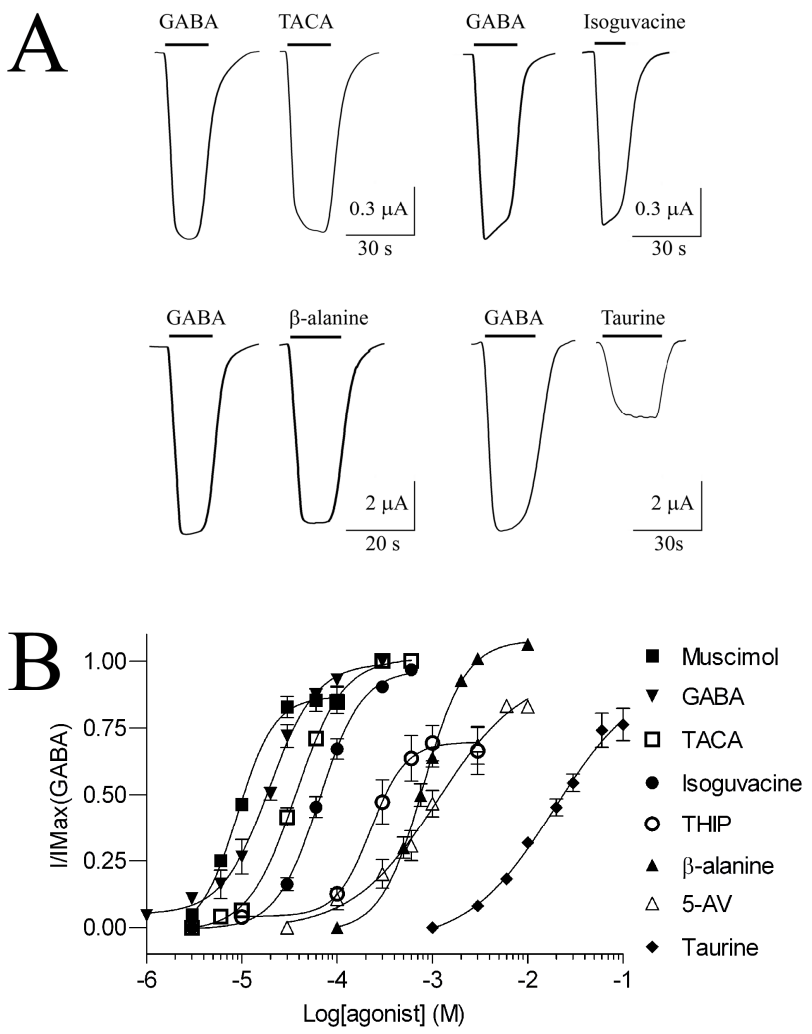

Figure 4.2. **A. Electrophysiological traces showing maximal currents elicited by agonists tested at RDL receptors**; GABA (100µM), TACA (300 µM), Isoguvacine (600 µM), β-alanine (10 mM) and Taurine (10 mM). **B. Concentration-response curves** showing the relative potencies of GABA and GABA analogues at wild-type RDL receptors expressed in *Xenopus* oocytes. EC_{50} values for analogues tested: Muscimol < GABA < TACA < isoguvacine < THIP < 5-AV < β-alanine < taurine. Data represent mean ± SEM, $n \geq 3$. Taken from McGonigle and Lummis, 2010, with copyright permission from *ACS Biochemistry*.

Table 4.1 Parameters derived from concentration-response curves.

Agonist	pEC_{50} ± SEM	EC_{50} (μM)	n_H ± SEM	n	I_{Max}/I_{Max}GABA
Muscimol	5.044 ± 0.04	9.04	2.2 ± 0.6	5	0.87 ± 0.03
GABA	4.705 ± 0.04	19.7	1.8 ± 0.2	19	1.0 ± 0.06
TACA	4.435 ± 0.02	36.7	1.8 ± 0.2	3	1.0 ± 0.02
Isoguvacine	4.188 ± 0.03	64.9	1.9 ± 0.2	5	0.97 ± 0.03
THIP	3.645 ± 0.10	226	2.4 ± 1.0	5	0.57 ± 0.06
β-alanine	3.096 ± 0.03	801	2.0 ± 0.3	10	1.0 ± 0.03
5-AV	2.950 ± 0.15	1120	1.0 ± 0.3	4	0.85 ± 0.1
Taurine	< 2.0	> 10,000	-	3	-
GHB	N/R	-	-	-	-
3-APP	N/R	-	-	-	-
Glycine	N/R	-	-	-	-
4-AB	N/R	-	-	-	-
PABA	N/R	-	-	-	-
Tyramine	N/R	-	-	-	-

Data = mean ± SEM**;** N/R indicates no response, n_H is the Hill coefficient, n indicates number of replicates. I_{Max}/I_{Max}GABA indicates the maximal response compared to GABA. Taken from McGonigle and Lummis, 2010, with copyright permission from *ACS Biochemistry*.

4.2.2 Computational ligand analysis

The atomic distance between the ammonium nitrogen and the carboxylate oxygen, or its equivalent substituent, was calculated for all ligands tested. Comparing these data to the ligand EC_{50} values (Table 4.2) indicates that the most potent activators have a dipole separation distance of ~5 Å. Glycine has a dipole separation distance of 2.35 Å, and may be too short to activate RDL receptors, while for tyramine the distance was 7.94 Å, thus this molecule may be too long to fit into the binding site cleft. GHB and 3-APP, however, which have dipole separation distances of 5.1 Å and 4.5 Å respectively, are not agonists, while 5-AV, which has a dipole separation distance of 6.5 Å, can activate receptors. These data suggest that other factors also play a role. One of these may be charge distribution; partial atomic charge calculations suggest there is a dependence on the electrostatic potentials of atomic groups at either end of the ligand. Partial atomic charges of + 0.3 at ammonium hydrogen atoms and - 0.5 to - 0.6 on carboxylate oxygen atoms were common amongst the most potent ligands (Table 4.2). However for 3-APP and 4-amino-1-butanol (4-AB), which do not activate receptors, the charges on phosphonic acid and hydroxyl oxygens are -1.2 and - 0.4 respectively. Additionally, 4-AB and GHB are not zwitterions and thus carry no formal charge, and so even if their length is close to optimal for receptor activation, their inactivity could be attributed to the absence of charge at either end of the ligand. The hydroxyl of GHB cannot substitute the ammonium of GABA, confirming the importance of this group for ligand binding at RDL receptors.

Table 4.2 Dipole separation distances of GABA analogues.

Ligand	*Potency* pEC_{50}	*Dipole separation (Å)*	Carboxylate Oxygens*	Ammonium Hydrogens
Muscimol	5.04	5.22	-0.26 (Isox-N), -0.47	0.32, 0.32, 0.30
GABA	4.71	4.83	-0.60, -0.54	0.31, 0.31, 0.29
TACA	4.44	4.88	-0.57, -0.53	0.31, 0.31, 0.29
Isoguvacine	4.19	4.86	-0.55, -0.53	0.29, 0.31, 0.29
THIP	3.65	5.14	-0.25 (Isox-N), -0.46	0.29, 0.31, 0.31
β-alanine	3.09	4.37	-0.58, -0.51	0.29, 0.29, 0.29
5-AV	3.06	6.47	-0.61, -0.56	0.31, 0.31, 0.30
Taurine	< 2.0	4.46	-1.11, -1.12	0.30, 0.30, 0.28
GHB	N/R	5.10	-0.61, -0.61	-0.38 (Hydroxyl-O) †
3-APP	N/R	4.50	-1.23, -1.23 (Phos-O)	0.29, 0.31, 0.31
Glycine	N/R	2.35	-0.47, -0.57	0.32, 0.32, 0.27
4-AB	N/R	6.20	-0.38 (Hydroxyl-O)	0.19, 0.20, 0.24
PABA	N/R	6.39	-0.54, -0.54	0.30, 0.30, 0.30
Tyramine	N/R	7.94	-0.47 (Hydroxyl-O)	0.31, 0.30, 0.30

Mulliken charges of GABA analogues calculated using the GAMESS interface. Ammonium hydrogens and carboxylate oxygens, or their equivalent substituents for the dipole, are listed. *Ligands without carboxyl groups were assessed by their equivalent groups: Isoxazole nitrogens in THIP and muscimol, phosphate oxygen in 3-APP, and hydroxyl oxygen in 4-AB and tyramine. † GHB does not have an ammonium group. The charge on the hydroxyl oxygen is negative. Taken from McGonigle and Lummis, 2010, with copyright permission from *ACS Biochemistry*.

4.2.3 Homology modelling and docking

Homology modelling of the extracellular domain of RDL was based on the crystal structure of AChBP and analogue docking was ranked based on the GOLDscore fitness function, which ranks simulations by comparing interaction energies by consideration of predicted protein-ligand hydrogen bond energy, protein-ligand van der Waals energy, ligand internal van der Waals energy and ligand torsional strain energy, and has been established as an accurate method for scoring ligand-protein docking (Verdonk *et al.*, 2003). The most favored orientation for GABA in the binding site was with the ligand in the cleft between loops B, C, and D (Fig. 4.3). The carboxyl group of GABA was deepest in the cleft, located close to residues Y109 and R111 in loop D. The ammonium was located between aromatic residues contributed by loop B (F206) and loop C (Y254), suggesting a cation-π interaction with one or both of these residues. A hydrogen bond was predicted between the ammonium of GABA and the backbone carbonyl of S205. 5-AV docked in a similar orientation with a hydrogen bond predicted at the same location. β-alanine was found to dock in two almost equally favored orientations. One of these was similar to the orientation of GABA described above, with the carboxyl deep in the cleft and the ammonium sandwiched between F206 and Y254. In this orientation there was a hydrogen bond between the ligand ammonium and the S205 backbone carbonyl oxygen. In the second orientation β–alanine was close to S131 above loop E, and there was a hydrogen bond between the ligand ammonium and the side chain hydroxyl.

All other agonists docked with the ammonium moiety oriented close to loop B residues E204 and S205, with hydrogen bonds predicted between these residues and TACA and taurine (Table 4.3). Muscimol and isoguvacine were predicted to hydrogen bond with residues L249 and Y254 respectively. These orientations also position their carboxylate moieties close to loop D residue R111.

Table 4.3 Hydrogen bonding partner residues predicted from docking of functional GABA analogues.

Analogue	H-bonding residues predicted
GABA	S205
β-alanine	S205
5-AV	S205
Muscimol	L249
Isoguvacine	Y254
TACA	S205, E204
Taurine	S205, E204
THIP	None detected

Taken from McGonigle and Lummis, 2010, with copyright permission from *ACS Biochemistry*.

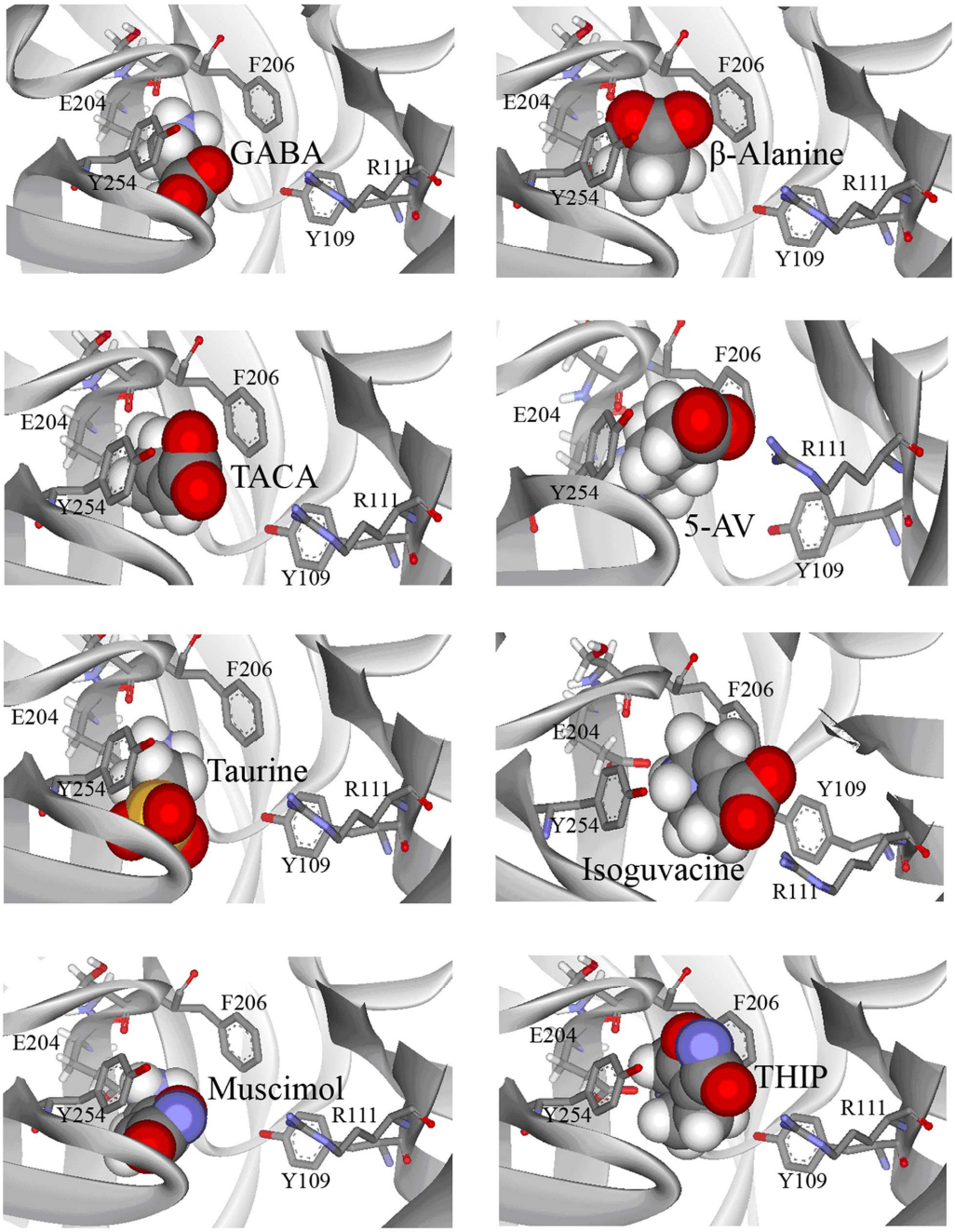

Figure 4.3 Docking of GABA and active analogues (β-alanine, TACA, 5-AV, taurine, isoguvacine, muscimol and THIP) into the RDL binding site. Analogues docked with the ammonium group located deep in the cleft formed between loop B and loop C aromatic residues. The carboxylate moiety or equivalent substituent was predicted to be located facing towards R111. Atomic colour scheme: Grey (Carbon); Red (Oxygen); Blue (Nitrogen); White (Hydrogen); Orange (Sulphur). Taken from McGonigle and Lummis, 2010, with copyright permission from *ACS Biochemistry*.

4.3 Discussion

In the present study I have examined the characteristics of agonist binding in RDL receptors, which are GABA-gated chloride selective Cys-loop receptors found in insect nervous systems. They are important to understand as insecticidal targets, and knowledge of their structure and function could clarify how these receptors function in other species. I have created a homology model of the RDL binding site, and demonstrated that GABA and a range of GABA analogues can dock into this site with a range of potential interactions with binding site residues. I have also examined the characteristics of the agonists and, using functional and modelling data, described the critical features required to activate these receptors.

The GABA-gated chloride channels produced when RDL subunits are expressed in *Xenopus* oocytes have distinct pharmacological characteristics to the vertebrate $GABA_A$ receptors: they are activated by GABA with an EC_{50} of ~20 μM; they exhibit minimal desensitization; they can be inhibited by PTX but not by bicuculline and they can be activated by the $GABA_A$ receptor agonist muscimol and the $GABA_C$ receptor agonist TACA. Muscimol, which is a full agonist of $GABA_A$ receptors and a partial agonist of $GABA_C$ receptors, is a full agonist at RDL receptors, while THIP, which is a full agonist of $GABA_A$ receptors and an antagonist of $GABA_C$ receptors, is a partial agonist at RDL receptors. These characteristics are similar to GABA-gated receptors in cockroach neurons as previously reported (Sattelle *et al.*, 1988; Schnee *et al.*, 1997). Other GABA-gated channels that have been heterologously expressed include those from *Musca* (MdRdl) and *Laodelphax*, where GABA-gated anion channels were identified with similar GABA EC_{50} values; these findings are similar to GABA-gated chloride channels in lobster, cockroach, and crab neurons and are in contrast to those of GABA-gated cation channels that have been identified in *Caenorhabditis elegans*, small crab, and *Drosophila* (Beg

and Jorgensen, 2003; Duan and Cooke, 2000; Eguchi *et al.*, 2006; Gisselmann *et al.*, 2004; Swensen *et al.*, 2000).

Our examination of the GABA agonists suggests that GABA activates RDL receptors in the extended conformation, with agonist optimum length of ~5Å. This is similar to the extended conformation of GABA at $GABA_C$ receptors but differs to the partially folded conformation of GABA at $GABA_A$ receptors (Verdonk *et al.*, 2003). 5-AV, which is one CH_2 longer than GABA, and β-alanine, which is one CH_2 shorter, can also activate the receptors, suggesting that they are both close enough in size to generate essential contacts within the binding site, although the potencies of both these compounds (EC_{50} ~1 mM) are considerably less than GABA. Glycine, which is two CH_2 groups smaller than GABA, is inactive, as is tyramine, which is considerably larger than GABA. Similarly, a correlation between agonist affinity and agonist length has been previously shown in $GABA_A$ receptors where affinity is correlated with ligand length, with a decreased binding rate for shorter ligands, suggesting a length-based selectivity mechanism at these receptors (Jones *et al.*, 1998).

Replacement of the ligand carboxylate group with a hydroxyl, as in 4-AB, results in an inactive ligand, confirming the requirement for an anionic group at this point of the ligand. Taurine, which is an analogue of β-alanine with the carboxylate replaced by a sulphonate, can also act as an agonist, although its low potency indicates that sulphonate does not substitute very effectively for carboxylate. Replacement of the carboxylate with a phosphoric acid group, however, as in 3-APP, results in an inactive ligand, demonstrating that the type of acidic group is important. 3-APP also had no antagonistic properties at RDL receptors which is in contrast to $GABA_C$ receptor data, where replacement of the carboxylic acid group of GABA with a phosphonic acid, phosphinic acid or sulphonic group produces potent antagonists (Woodward *et al.*, 1993).

The ammonium group is also critical. GHB, the well known “date rape” drug, is an analogue of GABA with the ammonium group replaced by a hydroxyl. This compound had no activity at RDL receptors.

The data therefore support the requirement for a charged dipole for receptor activation, suggesting electrostatic interactions with binding site residues are important. Computational ligand calculations reveal a partial negative charge at the carboxylate moiety and a partial positive charge at the ammonium moiety for all active agonists. Thus, since the most potent ligands have a dipole distance close to 5 Å, and both ends of the ligand are thought to interact with the receptor, we can assume that the agonist binding site lies at the cleft between the binding loops with a distance of ~5 Å from one another. This suggests that loops B, C, and D comprise the part of the binding site with which agonists interact in this receptor, as placement of ligands between the other loops would require a longer ligand. This hypothesis is supported by the model which shows that loops B, C, and D form a clearly defined pocket in which the ligands bind (Fig. 4.3).

Docking of ligands identified several residues with hydrogen bonding potential, in particular in loops B and C, which have been shown to have important contact points for ligands in 5-HT_3, nACh, glycine and $GABA_C$ receptors (Beene *et al.*, 2002; Lummis *et al.*, 2005b; Pless *et al.*, 2008; Thompson *et al.*, 2008). Most of the agonists (GABA, β-alanine, TACA and taurine) could form a hydrogen bond with S205 (loop B), and TACA and taurine could also form H-bonds with E204 (also loop B). Muscimol and isoguvacine could form H-bonds with loop C residues L249 and Y254 respectively.

The ammonium group of all the functional agonists docked between loop B and loop C aromatics (F206 and Y254 respectively) suggesting a cation-π interaction. All Cys-loop receptors studied to date have been shown to have a cation-π interaction with an aromatic residue in the binding pocket and the ammonium of their natural ligand, although the location of the interacting residue varies from receptor to receptor. Such interactions have mostly been with loop B aromatics (in nACh, 5-HT_3, Gly and $GABA_C$ receptors), but interactions with loop C (MOD-1) and loop A ($GABA_A$) aromatics have also been reported (Mu *et al.*, 2003; Padgett *et al.*, 2007).

4.4 Conclusions

In conclusion, I have identified the charge and dipole requirements for agonist recognition in RDL receptors and have identified residues within loop B, loop C and loop D which could interact with agonists. I have also shown that loop B and/or loop C aromatic residues could contribute to the binding and/or function of the receptor via a cation-π interaction. The data therefore provide a model of the agonist binding site, which can be used for further structure activity studies and rational drug design.

Chapter 5

Investigating the GABA binding site of RDL receptors

5.1 Introduction

The aim of this chapter was to characterise putative binding site residues in order to assess the accuracy of my binding site model. I use mutagenesis to assess the effect of altering the side chains of residues identified as potentially important in agonist binding. The effects of these substitutions are assessed by TEVC, monitoring changes in the concentration-response relationship with GABA.

'Binding' residues in the homologous $GABA_A$ receptor have been identified within the extracellular loops using mutagenesis, single-channel analysis and homology modelling: several aromatic residues form an 'aromatic box,' a hydrophobic surface favourable for ligand stabilisation. Hydroxylated residues and charged residues are also involved in GABA binding through direct salt-bridge or hydrogen bonding interactions (Amin and Weiss, 1993; Boileau *et al.*, 2002; Newell and Czajkowski, 2003; Wagner *et al.*, 2004; Westh-Hansen *et al.*, 1997; Westh-Hansen *et al.*, 1999). Furthermore, aromatic residues from loops A, B, C and D have been found to form an aromatic box stabilising ligand binding in other Cys-loop receptors and several studies have in fact identified these regions as the binding site (Bartos *et al.*, 2009b; Lummis, 2009; Lummis *et al.*, 2005b; Melis *et al.*, 2008; Padgett *et al.*, 2007; Pless *et al.*, 2008; Thompson *et al.*, 2008; Wagner *et al.*, 2004; Xiu *et al.*, 2009).

Homology modelling and docking experiments on RDL receptors in Chapter 4 led to the identification of several candidate binding residues (See Fig. 5.1). These residues are in similar regions to binding residues in the homologous $GABA_A$ receptor. I determine the importance of Loop B residues F206, Y208, E204 and S205, assessing the role of aromaticity, hydroxylation and charge. Loop C residues Y254 and R256 as well as Loop D residues Y109 and adjacent residue R111 are investigated, as well as Loop A aromatic residues F146 and F147. The aromatic residues investigated here are conserved across many of the Cys-loop receptors (See Fig. 1.2) and may well be important in ligand

binding. Indeed, in all of the mammalian Cys-loop receptors studied to date, a cation-π interaction with the native ligand has been identified, highlighting the importance of aromatic residues in ligand-binding. Additionally, charged residues may be involved in salt-bridge or electrostatic interactions with the charged ends of GABA and the charged residues investigated here may be involved in such interactions. Such interactions seem likely, given the requirement for a charged dipole as shown in the previous chapter. Thus, here I aim to identify the partner binding residues for GABA in the RDL binding site.

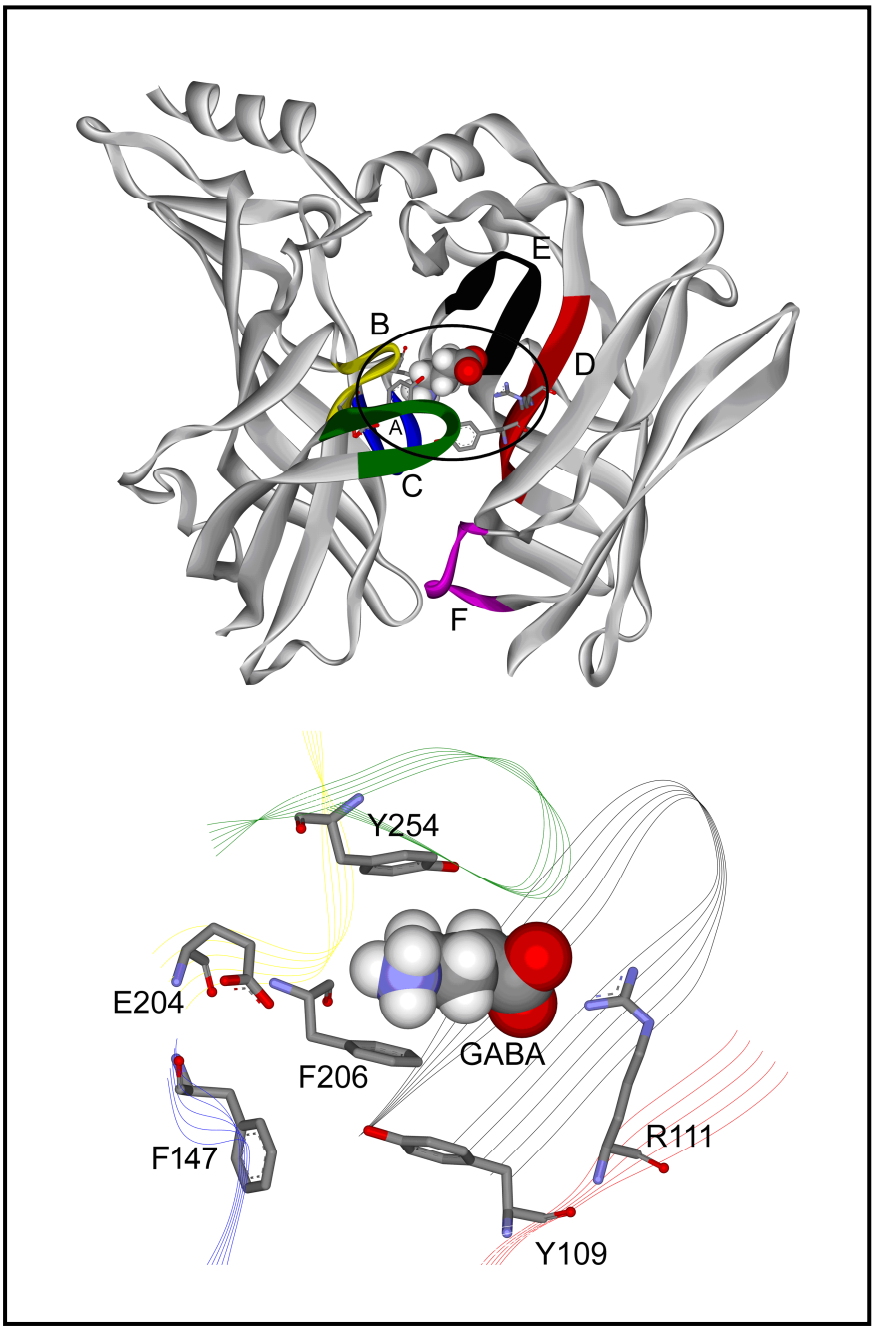

Figure 5.1 Binding site model. Above: Ribbon model of the RDL extracellular domain with GABA docked into its binding site. Loops A (Blue), B (Yellow), C (Green), D (Red), E (Black) and F (Purple) are highlighted. **Below:** Close up view of the putative agonist binding site with GABA docked and important residues labelled. Atomic colour scheme: Red (Oxygen); Blue (Nitrogen); Grey (Carbon); White (Hydrogen). Loops A-E are shown in wire format and coloured as above.

5.2 Results

5.2.1 Molecular biology

Mutagenesis PCR reactions yielded a DNA product of the expected size (6 kb), confirming the successful amplification of the pGEMHE vector (Fig. 5.2). Digestion of mini-prep DNA from *E.coli* colonies transfected with PCR product allowed the identification of mutant DNA samples (Fig. 5.3).

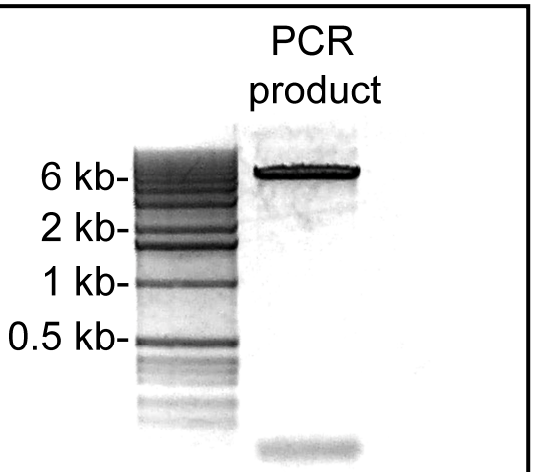

Figure 5.2 Gel screen showing PCR product

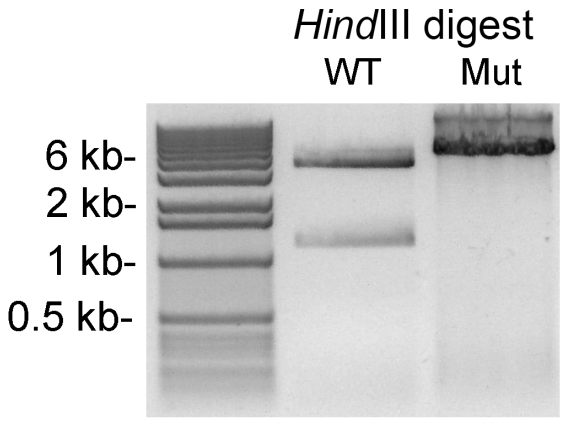

Figure 5.3 Analysis of wild-type (WT) and mutant (Mut) DNA as revealed by the mutagenic removal of a reporter restriction site (*Hind*III). Samples show the removal of a *Hind*III site in the mutant DNA (mut), confirming the mutation has been incorporated.

5.2.2 Loop B mutants

Loop B is an important region of the Cys-loop receptor binding site and residues in this loop have been shown to be critical for ligand binding and/or receptor activation; specifically, aromatic residues in loop B have been shown to be critical, forming a cation-π interaction with the native ligand in the 5-HT_3, Glycine, $GABA_C$ and nACh receptors (Beene *et al.*, 2002; Thompson *et al.*, 2008; Lummis *et al.*, 2005b; Zhong *et al.*, 1998; Pless *et al.*, 2008). Furthermore, charged residues in loop B have also been shown to be critical for receptor function in the 5-HT_3 receptor (Thompson *et al.*, 2008). For these reasons, charged and aromatic residues in RDL loop B were investigated.

F206

Mutation of F206 to alanine (F206A) resulted in an increase in EC_{50} for GABA (53 μM), from 20 μM in wild-type receptors, and a reduced Hill coefficient of 0.9 (Fig. 5.4; Table 5.1) (Hill coefficient is 1.8 in wild type receptors). The reduction in the Hill coefficient to 0.9 would suggest that cooperativity within the receptor has been reduced.

Mutation of F206 to tyrosine (F206Y) resulted in an EC_{50} of 0.5 μM (a 38-fold decrease from wild type). There was no significant change in Hill coefficient for F206Y, which would suggest that cooperativity has not been altered. β-alanine was tested on this mutant to assess whether the gain of function was GABA specific or observable for other agonists. β-alanine had an EC_{50} of 17 μM, which is a 47-fold decrease in EC_{50}, comparable to the change for GABA (Table 5.1). Since β-alanine showed a near parallel shift in EC_{50} with GABA, it is likely that the biophysical affects of the F206Y mutation affect these two ligands similarly. Such a large gain in agonist sensitivity would suggest that this residue may contribute to ligand binding and/or receptor gating.

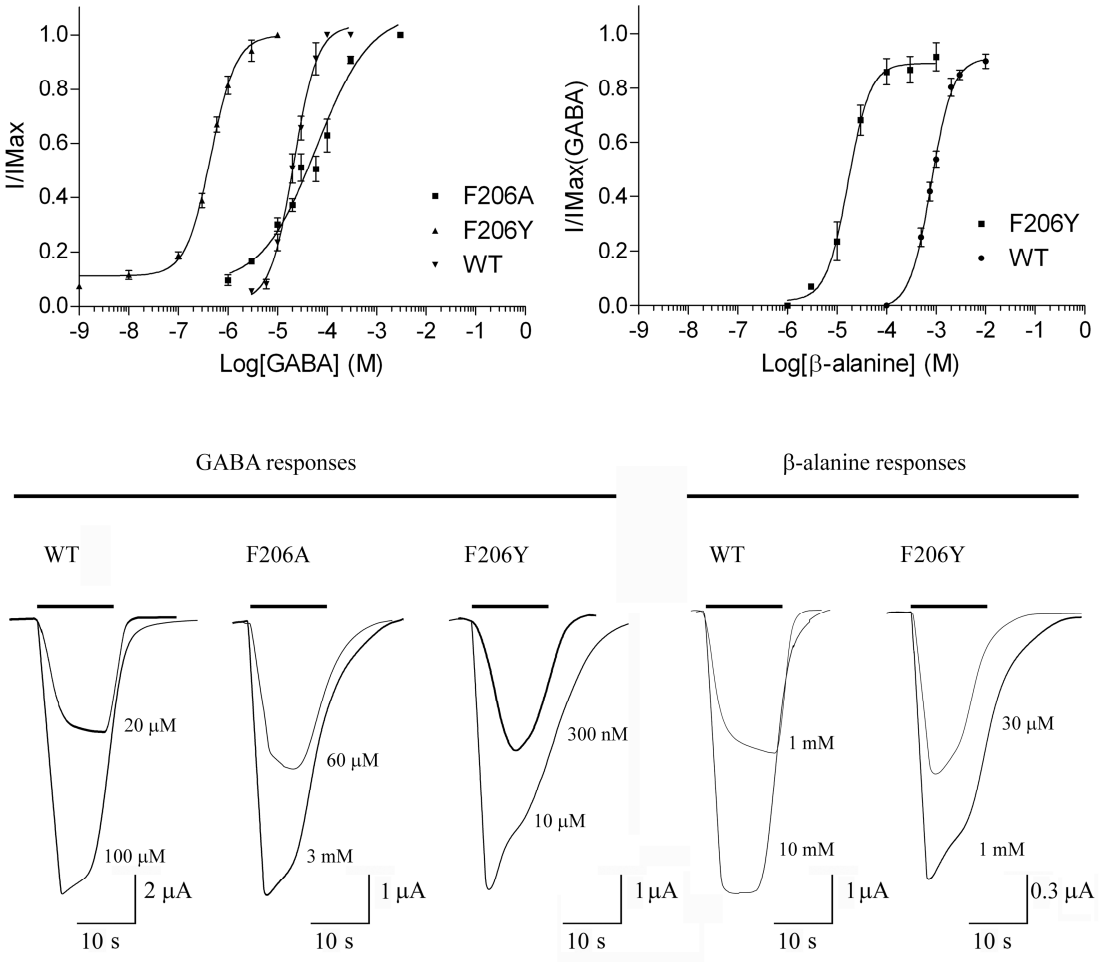

Figure 5.4 Concentration-response curves for F206 mutations. Above: GABA and β-alanine concentration-response curves for F206A, F206Y and wild type (WT) receptors. Each data point is the mean ± SEM for at least four oocytes. **Below:** Sample electrophysiological traces showing maximal and approximately EC_{50} currents from wild type and mutant receptors.

Y208

Loop B residue Y208 did not feature prominently in the binding site model, however its proximity to F206 prompted close attention to this region. Y208 was predicted to point away from the GABA binding site, pointing inwards towards the core of the extracellular domain. The effect of mutating this residue and also coupling the Y208F mutation to the F206Y mutation was assessed to identify potential interactions between these residues. Mutation of Y208 to phenylalanine (Y208F) yielded functional receptors with a GABA EC_{50} of 71 μM (a 3.7-fold increase from wild type) with no significant change in the Hill coefficient. This mutation increased the EC_{50} for β-alanine to 2.8 mM (a 3.5-fold increase from wild type). Similarly, mutation of Y208 to serine (Y208S) resulted in a GABA EC_{50} of 47 μM (a 2.5-fold increase from wild type), with no change in Hill coefficient (Fig. 5.5; Table 5.1).

The double mutant F206Y.Y208F had a GABA EC_{50} of 3.6 μM, with a Hill coefficient of 1.1. Double mutant cycle analysis of these two residues shows that they are coupled with interaction energy of 1.7 kJ/mol (Fig. 5.6).

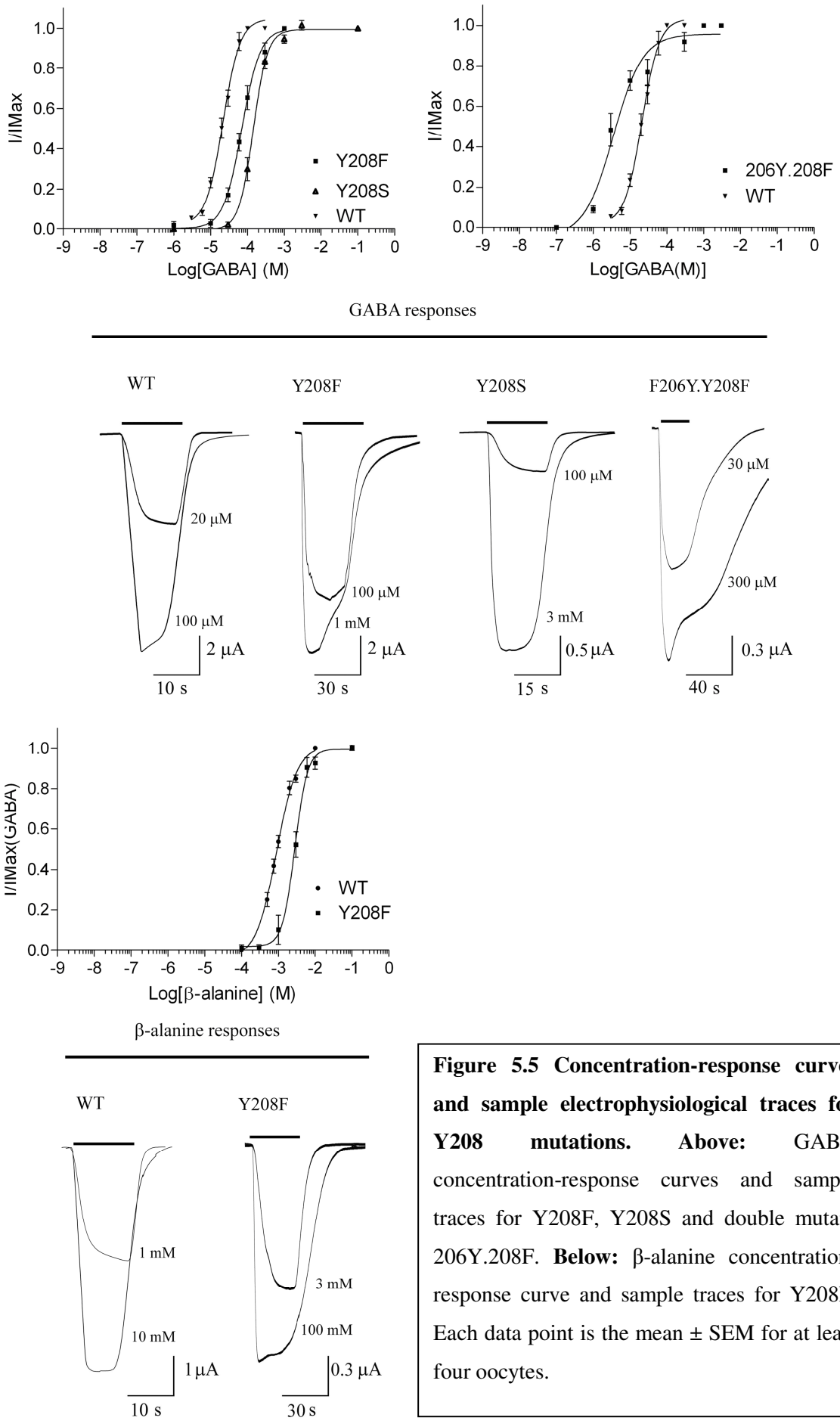

Figure 5.5 Concentration-response curves and sample electrophysiological traces for Y208 mutations. Above: GABA concentration-response curves and sample traces for Y208F, Y208S and double mutant 206Y.208F. **Below:** β-alanine concentration-response curve and sample traces for Y208F. Each data point is the mean ± SEM for at least four oocytes.

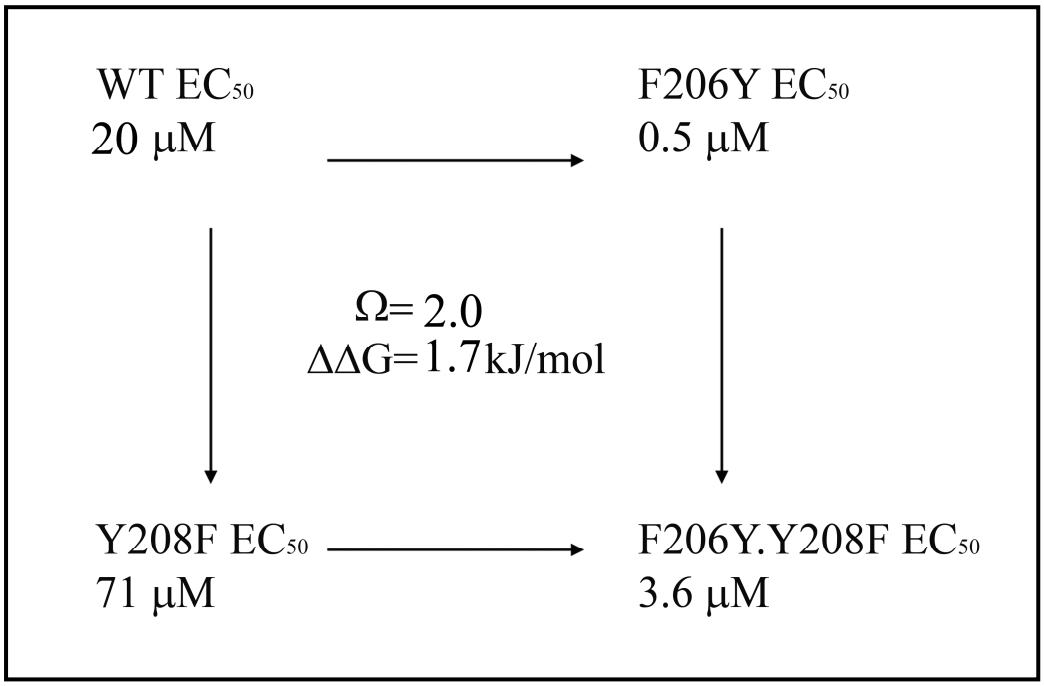

Figure 5.6 Mutant cycle analysis for mutants Y208F, F206Y and double mutant F206Y.Y208F. A coupling energy of 1.7 kJ/mol suggests that the effects of these mutations on receptor function are coupled. This suggests that these residues are situated close together in an orientation which may contribute to the GABA binding site. Values of $\Omega > 2.5$ have been shown to identify direct interactions between molecular groups (Schreiber *et al.*, 1995).

E204

Loop B glutamate (E204) was mutated to alanine (E204A) and aspartate (E204D). *Xenopus* oocytes injected with 50 ng of cRNA for these mutants failed to give responses to GABA, suggesting that GABA binding or gating has been disrupted.

S205T

Loop B serine (S205) was mutated to threonine (S205T) and alanine (S205A), to test whether this residue is critical to receptor function. Oocytes injected with 50 ng of cRNA for these mutants failed to give responses to GABA.

5.2.3 Loop C mutants

Loop C is an important part of the ligand binding site in Cys-loop receptors; recent studies have suggested that loop C moves in a 'capping motion' during agonist binding (Ulens *et al.*, 2009; Hansen *et al.*, 2005) and previous studies have demonstrated a role for aromatic and charged residues in agonist binding in the related 5-HT_3, $GABA_A$ and $GABA_C$ receptors (Padgett *et al.*, 2007; Beene *et al.*, 2007; Harrison and Lummis, 2006). For these reasons, aromatic and charged residues in RDL loop C were investigated to determine their role in agonist binding.

Y254

Loop C tyrosine (Y254) was mutated to alanine (Y254A) and phenylalanine (Y254F). Oocytes injected with Y254A cRNA failed to give responses to GABA. Y245F mutant receptors had an increased GABA EC_{50} of 124 μM (6.5-fold greater than wild-type), with no significant change in Hill coefficient. Testing of β-alanine on this mutant revealed an EC_{50} of 1800 μM, a 2.2-fold increase compared with wild-type receptors (Fig. 5.7; Table 5.1).

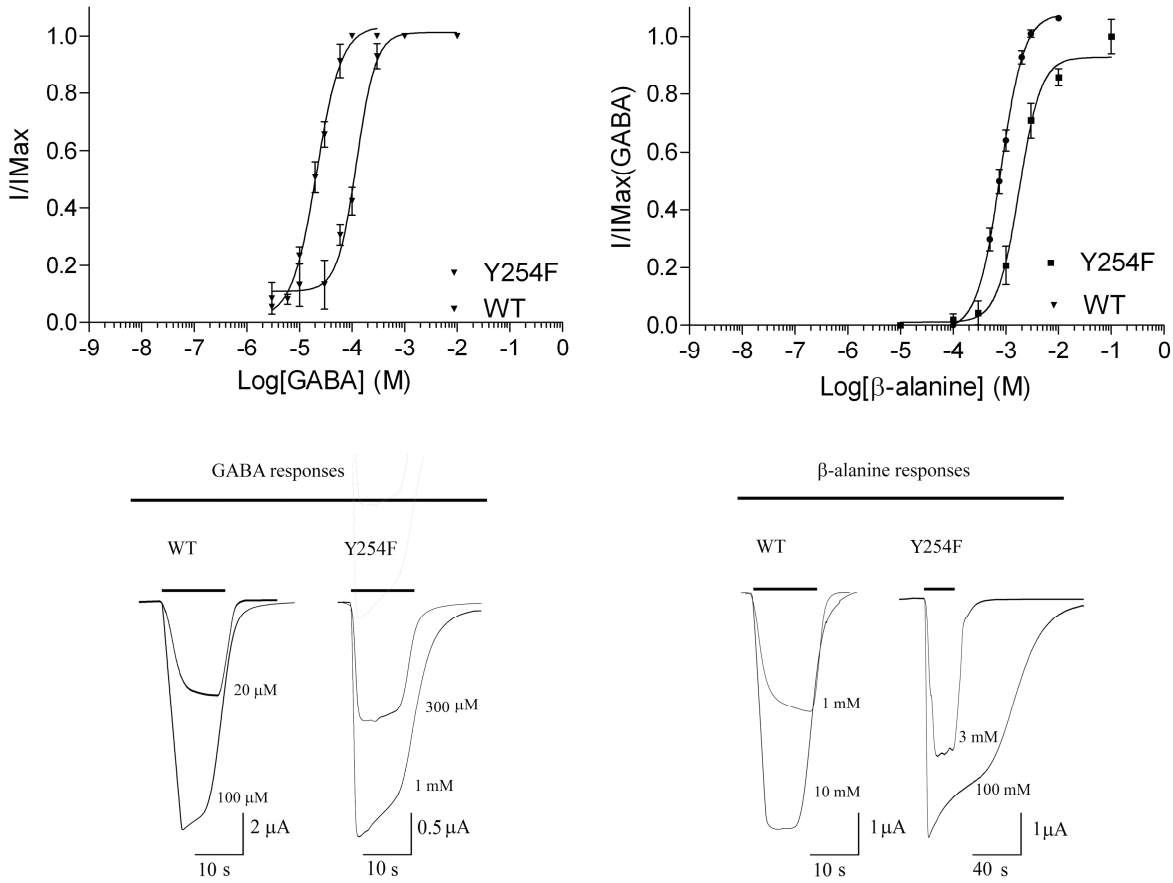

Figure 5.7 Concentration-response curves for mutant Y254F. Above: GABA and β-alanine concentration-response curves for Y254F mutant receptors. Each data point is the mean ± SEM for at least four oocytes. **Below:** Sample electrophysiological traces.

R256

Functional responses from mutant receptors R256K and R256A could not be detected following 50 ng RNA injection, suggesting that binding and/or gating has been disrupted.

5.2.4 Loop D mutants

Loop D forms part of the agonist binding site in Cys-loop receptors (Akabas, 2004); in the $GABA_A$ receptor an aromatic residue (α1Phe65) has been shown to form part of the "aromatic box," allowing ligand binding, and in the $GABA_C$ receptor, a charged residue (R104) was shown to be critical to agonist binding (Harrison and Lummis, 2006). The homologous residues to these in RDL (Y109 and R111) were mutated to determine their role in ligand binding.

Y109

Mutation of Loop D tyrosine residue Y109 to alanine (Y109A) failed to give responses following injection of 50 ng cRNA. Similarly, mutation of the same residue to a serine (Y109S) also failed to give responses. However, mutation to phenylalanine (Y109F) resulted in functional receptors with a GABA EC_{50} of 398 μM (21-fold increase from wild type), but with no change in Hill coefficient (Fig. 5.8; Table 5.1).

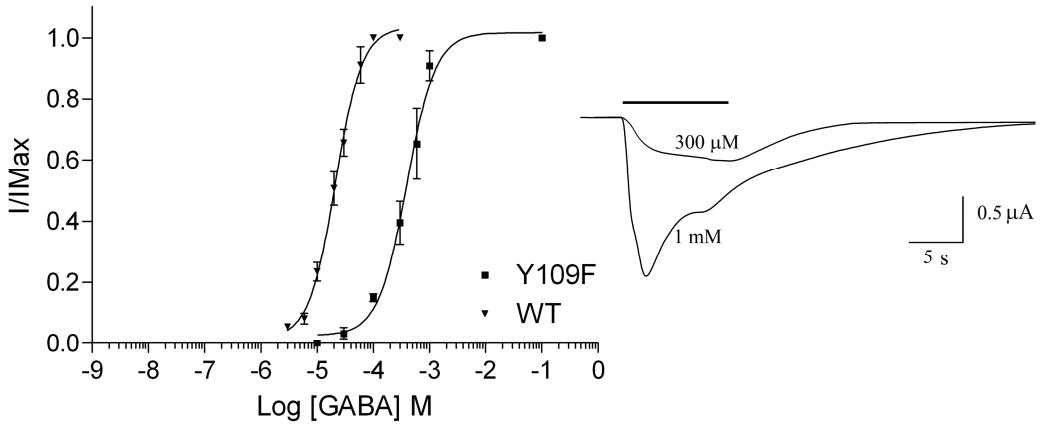

Figure 5.8 Concentration-response curve and sample traces for mutant Y109F. Each data point is the mean ± SEM for at least four oocytes.

R111

Mutation of Loop D arginine residue R111 to alanine (R111A) or lysine (R111K) failed to give responses following injection of 50 ng cRNA.

Since R111 is positioned next to Y109 in a β-sheet region it was suspected that these residues may be interacting with each other via a cation-π interaction. This is a likely interaction, as there is on average 1 cation-π interaction for every 77 amino acids in the protein data bank. Also, it is known that Tyr/Trp···Lys/Arg motifs contribute significantly to stabilising protein secondary structure (Dougherty, 2007). As part of an Arg-X-Tyr motif, this residue is likely to be involved in an interaction with Y109. However, responses could not be detected from R111Y.Y109R injected oocytes, suggesting that functional receptors could not be formed.

5.2.5 Loop A mutants

A loop A aromatic residue (β_2Tyr97) has been shown to be important in the human RDL orthologue, the $GABA_A$ receptor, where a cation-π interaction between the ammonium of GABA and β_2Tyr97 has been detected (Padgett *et al.*, 2007). Although in my homology model the candidate loop A aromatic residue (F147) was predicted to be quite distant from the ammonium of GABA (See Fig. 5.1), it was thought important to investigate this residue in order to validate my model.

F146

F146 was assessed to determine if it is involved in agonist binding and/or receptor activation. Mutation of this phenylalanine residue to alanine (F146A) resulted in a GABA EC_{50} of 90 µM, with no change in Hill coefficient (Fig. 5.9; Table 5.1).

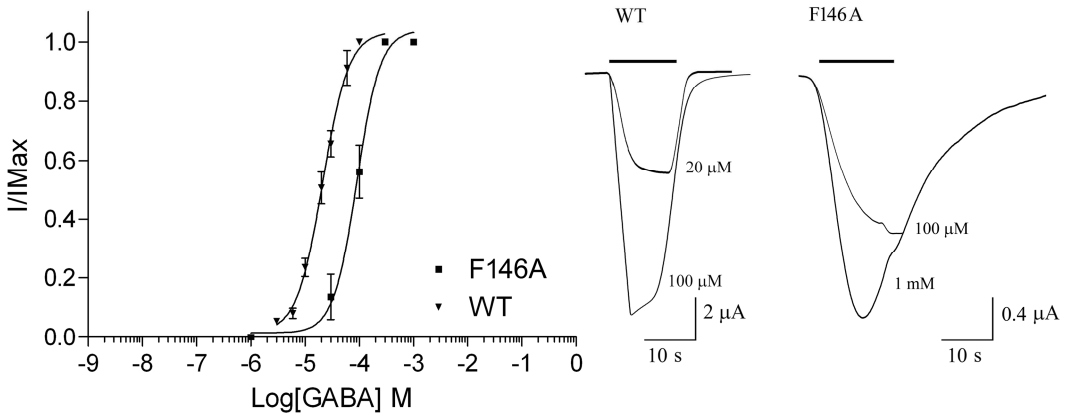

Figure 5.9 Concentration-response curve and sample traces for mutant F146A. Each data point is the mean ± SEM for at least four oocytes.

F147

F147 is positioned adjacent to F146 in the β-sheet region of loop A. The side chain of F147 was predicted by my homology model to face towards the central core of the protein, away from the binding site cleft. This residue was mutated to alanine but no responses were detected from this mutant.

Table 5.1 Parameters derived from concentration-response curves.

Mutant	pEC_{50}(μM) ± SEM	EC_{50}(μM)	n_H ± SEM	n
GABA evoked responses				
WT	**4.705 ± 0.039**	**19.7**	**1.8 ± 0.2**	**19**
F206A	4.278 ± 0.063*	53	0.9 ± 0.1*	5
F206Y	6.342 ± 0.026*	0.5	1.7 ± 0.2	8
Y208F	4.149 ± 0.032*	71	1.7 ± 0.3	6
Y208S	3.839 ± 0.029*	47	2.2 ± 0.3	5
F206Y. Y208F	5.447 ± 0.078*	3.6	1.1 ± 0.2	6
E204D	N/R	-	-	-
E204A	N/R	-	-	-
S205T	N/R	-	-	-
S205A	N/R	-	-	-
Y254F	3.910 ± 0.041*	124	2.3 ± 0.5	5
Y254A	N/R	-	-	-
R256K	N/R	-	-	-
R256A	N/R	-	-	-
Y109F	3.400 ± 0.060*	398	1. 7 ± 0.4	4
Y109S	N/R	-	-	-
Y109A	N/R	-	-	-
R111K	N/R	-	-	-
R111A	N/R	-	-	-
Y109R. R111Y	N/R	-	-	-
F146A	4.044 ± 0.061*	90	2.0 ± 0.6	4
F147A	N/R	-	-	-
β-alanine evoked responses				
WT	**3.096 ± 0.030**	**801**	**2.0 ± 0.3**	**10**
F206Y	4.770 ± 0.058*	17	2.0 ± 0.4	4
Y208F	2.567 ± 0.035*	2835	2.6 ± 0.5	4
Y254F	2.745 ± 0.050*	1800	2.1 ± 0.4	6

N/R indicates no response, n_H is the Hill coefficient, n indicates number of replicates. * denotes significance from WT ($p<0.05$, t-test).

5.2.6 Probing binding site mutations using the gain of function mutant L314Q

The RDL mutation L314Q (M2 14' residue) was reported by Hosie *et al.* to induce spontaneous channel opening with a 200-fold decrease in GABA EC_{50} (Biochemical Society Summer Meeting, St Andrews, July 2009). The 14' residue lies close to the 16' residue in the adjacent subunit and he proposed that the interaction of these residues could influence closed state stability. Cysteine substitution of 14' and 16' markedly reduced the amplitude of GABA responses. Reduction of disulphide bonds with DTT restored large amplitude GABA responses suggesting these residues are interacting directly. Spontaneously open channels can be detected by applying picrotoxin (PTX) in the absence of agonist. A rise in the baseline current is indicative of open channels being blocked by PTX.

I felt that the L314Q mutation would make a useful reporter for changes in the intrinsic open channel probability of the receptor. By coupling a gain/loss of function mutation to the L314Q mutation, changes in the proportion of open channels, as measured by PTX block, can be used to indicate whether the mutation of interest can affect gating in an agonist independent manner.

L314Q

Cells expressing L314Q mutant receptors displayed a large leak current. GABA evoked responses recovered very slowly when compared to wild type. PTX induced a rise in the current indicative of channel block and channels recovered slowly requiring several agonist applications (Fig. 5.10).

F206Y.L314Q

F206Y.L314Q receptors displayed a large leak current and GABA evoked very small or no currents (Fig. 5.10). Mean maximal GABA currents were compared to the amplitude of PTX induced block to give an estimation of the proportion of channels that are spontaneously open (Fig. 5.10). The open channel population for F206Y.L314Q was compared to that for L314Q (Fig. 5.11). This ratio was found to be 2.9, indicating that the introduction of the F206Y mutation increased the proportion of open channels by 2.9-fold.

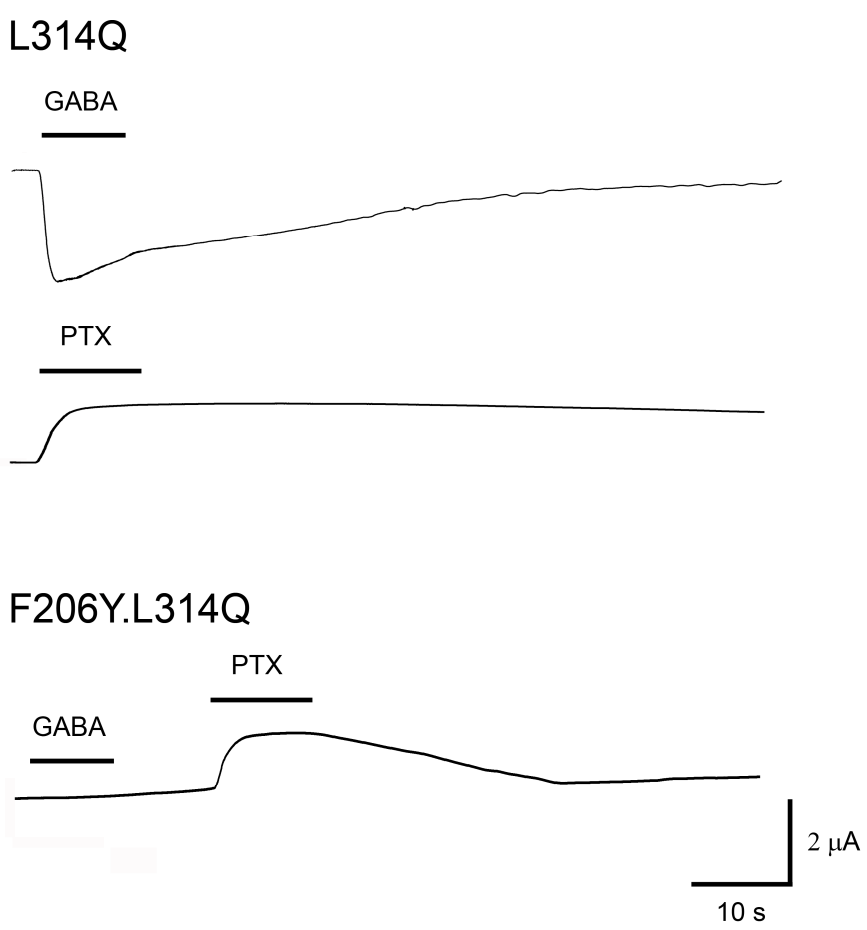

Figure 5.10 Electrophysiological traces for L314Q and F206Y.L314Q mutations. GABA and PTX were applied at EC_{100} and IC_{100} concentrations (100 μM).

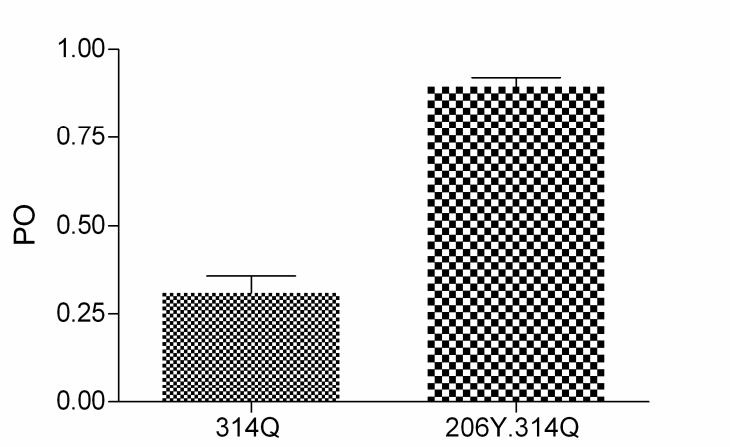

$$PO = A/(A+B)$$

$$\Delta PO = [A/(A+B)]_{mut2} / [A/(A+B)_{mut1}]$$

$$\Delta G = RT\ln \{ [A/(A+B)]_{mut2} / [A/(A+B)]_{mut1} \}$$

Figure 5.11 F206Y.L314Q open channel proportions. Above: Changes in open channel proportions (PO) with F206Y mutation. Above: Relative amplitudes of maximal GABA currents (**B**) and PTX induced block (**A**) for L314Q and F206Y.L314Q mutants were calculated and open proportions were plotted as [A/(A+B)] . Data points are mean ± SEM, n≥10. Data are significantly different ($p<0.0001$, t-test). **Below: Open channel proportions (PO) calculation and Gibbs free energy of gain/loss of function.** Where **A** is $I[PTX]_{Max}$, **B** is $I[GABA_{Max}]$, **R** is the universal gas constant (8.314 $J.K^{-1}.mol^{-1}$), **T** is the temperature in Kelvin (°K = °C + 273.15), where mut2 is the double mutant and mut1 is the L314Q mutant.

If the increase in PTX-induced block is a direct reflection of an increase in the proportion of receptors in the open state then we can use the relative open proportions for the mutant and wild type receptors to calculate the free energy of gating associated with the mutation of interest. This value is an indirect measure of the effects on intrinsic receptor gating, as introduced by the F206Y mutation (Fig. 5.11). This energy should therefore represent an interaction between mutant residue F206Y and another extracellular domain residue, since no agonist is present in this experiment.

The change in Gibbs free energy for activation of mutant F206Y receptors is 8.9 kJ/mol (RTln[38]), as calculated using the 38-fold increase in GABA EC_{50} (EC_{50}Mut/EC_{50}WT). This value is close to the value for a single hydrogen bond. This finding led to the hypothesis that the mutant residue F206Y is interacting with another residue in the ECD in a fashion that favours receptor activation. Since the phenolic oxygen is capable of such an interaction, a hydrogen bond acceptor residue is a likely candidate for interaction. This prompted a further analysis of the RDL ECD homology model, identifying Loop E residue S176, which is predicted to lie close, within 3.1 Å, of F206 (Fig. 5.12).

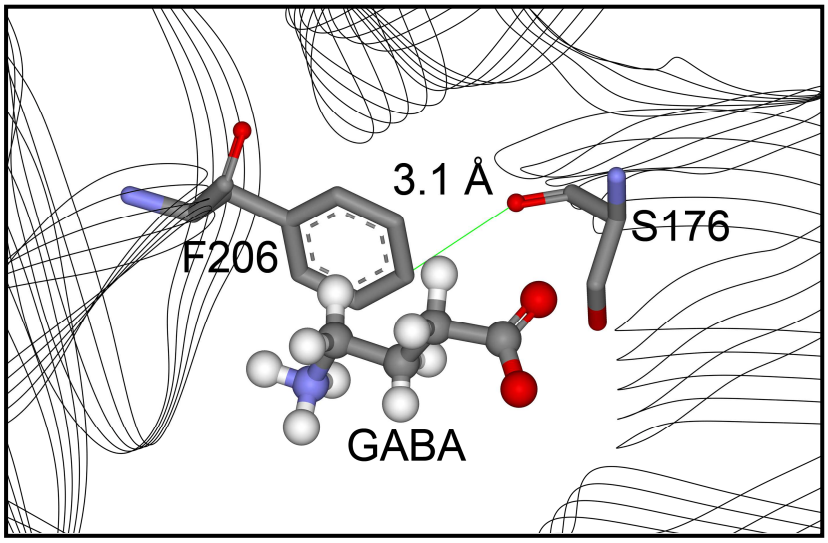

Figure 5.12 Distance between loop B F206 and Loop E S176. F206 is predicted to lie 3.1 Å from S176. With the addition of the phenolic hydroxyl, as in the mutation F206Y, an interaction, such as a hydrogen bond, may occur between S176 and Y206.

The F206Y mutation increased the open proportion of receptors by 2.9-fold. This increase in intrinsic gating conferred by the 206Y mutation does not fully account for the 38-fold gain of function, as revealed by EC_{50} value for GABA. This suggests that though the addition of a hydroxyl group can confer a gain of function, the intrinsic gating component does not fully account for the much larger decrease in agonist (GABA and β-alanine) EC_{50} values. This finding therefore supports the hypothesis that F206 forms part of the agonist binding site, possibly via a cation-π interaction with the ammonium of GABA.

According to the Del Castillo-Katz receptor activation scheme, receptor activation involves distinct steps of agonist binding and receptor gating (K and Ø) (Fig. 5.13) (Del Castillo and Katz., 1957). This basic theory has been since expanded upon to include many more hypothetical states but its basic premise remains widely accepted (Burzomato *et al.*, 2004; Corradi *et al.*, 2009; Miller and Smart, 2010). The open probability of the channel is therefore the product of both of these hypothetical biophysical properties, binding and gating. If the gain of function from the F206Y mutation is the product of both an increase in binding energy as well as an decrease in gating energy, we can use the Del Castillo-Katz equation to calculate the value of these separate components. The change in binding energy for GABA with the F206Y mutation was thus calculated to be 3.4 kJ/mol (Fig. 5.13).

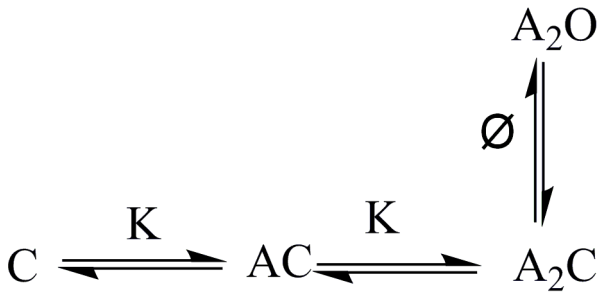

Del Castillo-Katz

K x Ø = RTln[38]
K x Ø = 8.9 kJ/mol
K x RTln[2.89] = 8.9 kJ/mol
K x 2.6 kJ/mol = 8.9 kJ/mol
K = 3.4 kJ/mol

Figure 5.13 Change in binding energy for the F206Y mutation. Above: Del Castillo-Katz equation. **Ø** is the gating coefficient. **K** represents the equilibrium constant for ligand binding steps. While in this scheme only two agonist binding events are displayed, a theoretical maximum of five agonists may bind a receptor. This simple scheme shows how binding of an agonist precedes channel opening. **Below:** Calculation of binding energy using the Del Castillo-Katz rationale and the Gibbs free energy equation where, **R** is the universal gas constant (8.314 $J.K^{-1}.mol^{-1}$), **T** is the temperature in Kelvin (°K = °C + 273.15), **Ø** represents the gating energy and **K** represents the change in binding energy for GABA.

Y254F.L314Q

Y254F.L314Q mutant receptors displayed a large leak current and significant GABA evoked currents could not be detected (Fig. 5.14). Y254F mutant receptors showed an increase in the intrinsic gating pathway with a theoretical open channel proportion of 100%.

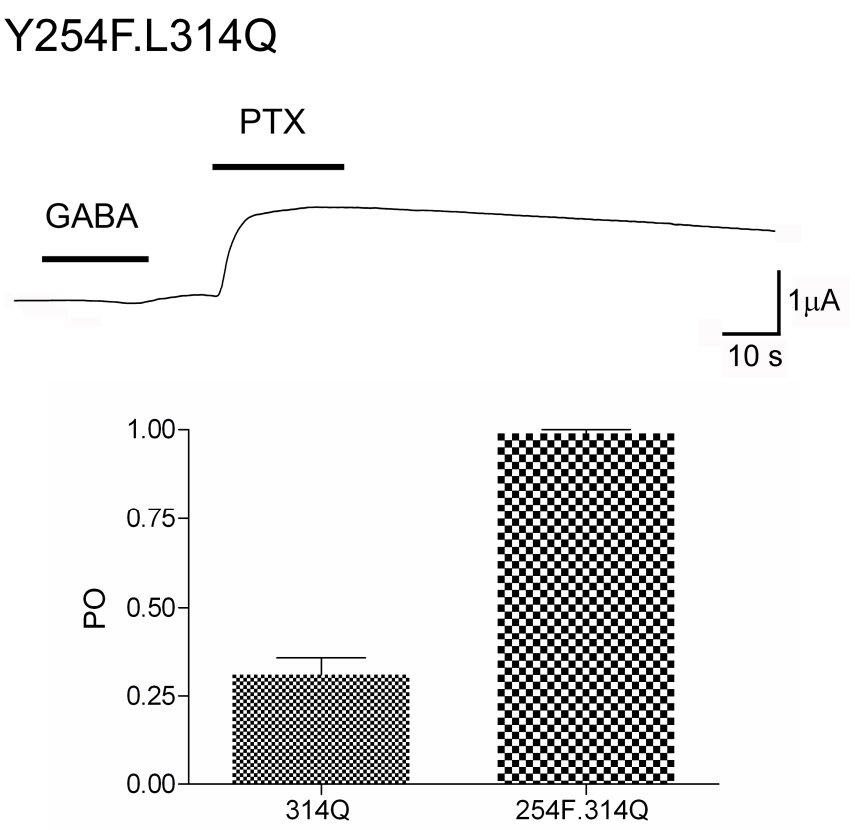

Figure 5.14 254F.314Q open channel proportions. Above: Relative amplitudes of maximal GABA currents and PTX induced block for 314Q and 254F.314Q mutants. Data points are mean ± SEM, n≥4. Data are significantly different ($p<0.0001$, t-test). **Below:** Relative open channel proportions (PO) of receptors.

The change in Gibbs free energy for the Y254F mutation is -4.6 kJ/mol, as calculated using the 6.5-fold increase in EC_{50} for GABA (Fig. 5.15). Using the Del Castillo-Katz rationale to calculate the change in GABA binding energy with this mutation, taking **Ø**, the gating coefficient to be equal to the open probability, revealed a change in binding energy of -1.6 kJ/mol (Fig. 5.15).

$$K \times Ø = RT\ln[-6.5]$$
$$K \times Ø = -4.6 \text{ kJ/mol}$$
$$K \times RT\ln[3.2] = -4.6 \text{ kJ/mol}$$
$$K \times 2.9 \text{ kJ/mol} = -4.6 \text{ kJ/mol}$$
$$K = -1.6 \text{ kJ/mol}$$

Figure 5.15 Loss in binding energy for 254F mutation. Calculation of binding energy using the Del Castilo-Katz rationale and the Gibbs free energy equation where, **R** is the universal gas constant (8.314 $J.K^{-1}.mol^{-1}$), **T** is the temperature in Kelvin (°K = °C + 273.15). **Ø** represents the gating energy and **K** represents the binding energy.

Y109F.L314Q

No GABA currents could be detected from oocytes injected with Y109F.L314Q mutant cRNA. Additionally no PTX induced change in current could be detected and oocytes displayed a low level of leak current, indicating that receptors were not being expressed or that channels could not be opened. This suggests that these two mutations, although individually both resulting functional receptors, when combined have deleterious effects on receptor expression. This finding would suggest that these mutations disrupt receptor folding or trafficking to the cell surface.

5.3 Discussion

In this chapter I have characterised the agonist binding site of RDL receptors. I have used mutagenesis to determine which residues are critical to ligand binding. I have focused on residues in loops A, B, C and D, regions which are known to contain binding residues in several other Cys-loop receptors.

Loop B residue F206 was found to be sensitive to mutation, with an alanine substitution disrupting cooperativity, as evinced by a reduced Hill coefficient, and with a tyrosine mutation greatly increasing agonist sensitivity. This residue is equivalent in location to conserved aromatic residues in 5-HT_3, $GABA_A$, $GABA_C$ and nACh receptors, where the equivalent residues have been shown to be key binding residues and specifically forming a cation-π interaction with the native ligand in 5-HT_3 and $GABA_C$ receptors (Beene *et al.*, 2002; Lummis *et al.*, 2005b; Padgett *et al.*, 2007; Thompson *et al.*, 2008; Zhong *et al.*, 1998). Further analysis of F206, by incorporating the L314Q reporter mutation, which causes spontaneous channel opening, revealed that this residue plays a role in both ligand binding as well as channel gating in RDL receptors. The change in binding energy for GABA associated with the F206Y mutation was found to be 3.4 kJ/mol. This value is greater than the difference in cation-π forming ability of tyrosine and phenylalanine (Dougherty, 1996; Mecozzi *et al.*, 1996), suggesting that a direct interaction between the phenolic oxygen of mutant residue F206Y and GABA may occur. This finding fits well with work on the homologous residue in other Cys-loop receptors and suggests that RDL receptors bind GABA in a similar fashion to the binding of ligands in vertebrate Cys-loop receptors.

Loop B residue Y208 was found not to be a binding residue, however it is energetically coupled to F206 and plays a role in receptor gating. These results suggest that this region of loop B is involved in receptor activation and is sensitive to mutation. This finding fits well with a recent structure-function study of loop B in the related 5-HT_3R, which showed that many residues in

loop B are essential for receptor function via both structural stabilisation of loop B and direct ligand binding (Thompson *et al.*, 2008). The position of Y208 as predicted by my homology model, facing into the hydrophobic core of the extracellular domain, is consistent with such a structural stabilisation.

The Loop B residue E204 was found to be critical to receptor function. Currents could not be recorded from mutants E204D or E204A. Since neither of these mutants responded, it seems likely that this residue is important for receptor activation or receptor folding. E204 is situated close to F206, which is important in receptor activation. It thus seems probable that this region of Loop B is sensitive to mutations and those residues likely to be involved in structural roles, such as charged residues, cannot be mutated without deleterious effects. Mutation of the homologous residue in the 5-HT_3R (a threonine) to either an alanine or a serine resulted in non-functional receptors, although receptors expressed and formed a binding site and radioligand binding studies (using an antagonist) showed a six-fold increase in binding affinity for the alanine mutation and no change for the serine mutant when compared to wild type receptors (Thompson *et al.*, 2008). This suggests a critical role for this residue in receptor activation. My results are therefore similar to those of Thompson *et al.* (2008), since no functional receptors could be detected. Docking simulations from the previous chapter show the ammonium of GABA to be positioned 6.7 Å from E204 (Fig. 5.16). Although the distance here exceeds the predicted length of a salt-bridge of ~4 Å (Kumar and Nussinov, 2002) this finding should leave open the possibility for such an interaction.

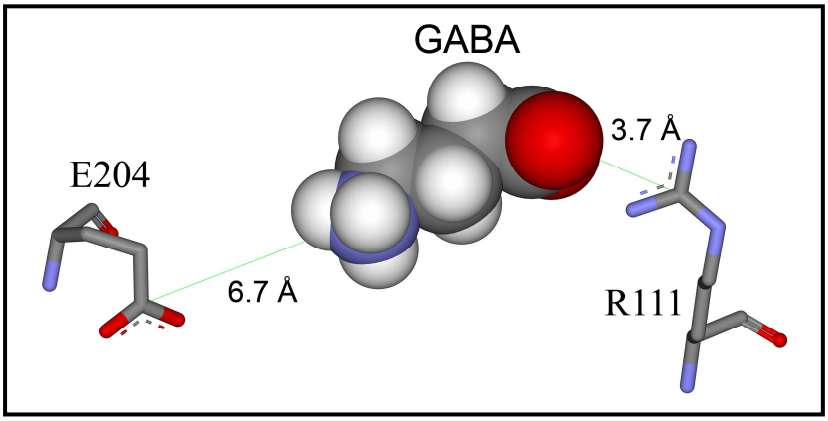

Figure 5.16 Electrostatic polarity of GABA within the binding site. GABA docked with the carboxylate group 3.7 Å from Loop D residue R111 and with the ligand ammonium 6.7 Å from Loop B residue E204.

Loop B residue S205 is one of very few residues conserved across the Cys-loop receptor family (See Figure 1.2). It is thus unsurprising that mutations made to this residue are not tolerated. This residue is located next to F206, which has proven to be a key determinant of agonist sensitivity. It is probable that mutations at position 205 disrupt the structure of Loop B, since even the conservative mutant S205T failed to respond. Mutation of the homologous residue in the 5-HT_3 receptor (also a serine) to both alanine and threonine resulted in a two and four-fold decrease in binding affinity respectively, with only the threonine mutant showing functionality, with a three-fold increase in EC_{50}. Further investigations into this residue should utilise unnatural amino acids which can monitor very subtle changes in side chain chemistry without the deleterious effects observed here.

Loop C residue Y254 was found to be important in ligand binding. Mutation of Y254 to alanine (Y254A) resulted in non-functional receptors. This is unsurprising since Y254 is a conserved residue across many Cys-loop receptors, suggesting an important functional or structural role. The Y254F mutation however, resulted in an increase in GABA EC_{50}, suggesting that subtle changes at this location can affect receptor function. Additionally, this result supports the hypothesis that the tyrosine phenolic hydroxyl group is involved in ligand binding and/or receptor activation. Analysis with the

reporter mutation L314Q revealed that the energy of binding between GABA and Y254 is less than a single hydrogen bond, suggesting that a cation-π interaction may occur here. Furthermore, docking simulations in the previous chapter, placed the ammonium of GABA between F206 and Y254 (Fig. 5.17), suggesting that Y254 may well form a cation-π interaction with the ammonium of GABA. This would be similar to the interaction observed in the *C.elegans* 5-HT-gated channel MOD-1 (Mu *et al.*, 2003). Proximal Loop C residue R256 was also found to be critical to receptor activation and/or formation. Since this residue was not prominent in docking simulations carried out in the previous chapter, I feel that this residue is more likely to be involved in receptor structure rather than ligand binding. However, in a study of the homologous residue in the $GABA_C$ receptor, R249 was substituted with alanine, glutamate, or aspartate with relatively small (4–30-fold) increases in GABA EC_{50} (Harrison and Lummis, 2006). This would suggest that this residue may play different roles in different receptors, with it perhaps being more important in RDL.

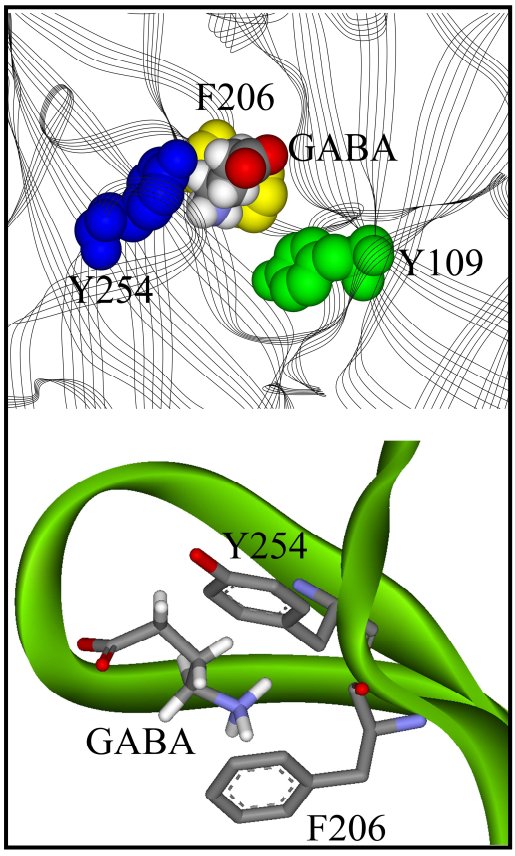

Figure 5.17 Aromatic box residues. Above: Wire diagram of the binding site with aromatic box residues Y109, F206 and Y254 in space filling representation, with GABA docked. **Below:** Close up view of GABA docked with the ammonium group sandwiched between the faces of aromatic residues F206 and Y254.

Mutation of Loop D residue Y109 to alanine resulted in non-functional receptors and the conservative phenylalanine mutation resulted in a large rise in GABA EC_{50}. This residue is thus critical to GABA sensitivity. Indeed, the homologous residue in the $GABA_A$ receptor (α_1Phe65) has been shown to be involved in ligand binding by increasing the "general hydrophobicity of the region," showing a requirement for aromaticity at this position (Padgett *et al.*, 2007). However another study of the same residue in $GABA_A$ receptors showed that mutation to leucine increased the GABA EC_{50} from 6 to 1260 μM, with the IC_{50} values of bicuculline and SR95531 (competitive antagonists) increasing by similar amounts (Sigel *et al.*, 1992). This would suggest an important role in ligand binding. The position of this residue in the ECD homology model supports the hypothesis that this residue forms part of the aromatic box in this receptor, providing a hydrophobic surface for water exclusion and ligand stabilisation close to the predicted GABA binding location (Fig. 5.17). The adjacent residue R111 was found to be a key binding residue in RDL receptors with R111K and R111A mutants failing to respond. R111 is predicted to lie 3.7 Å from the carboxylate of GABA, based on docking simulations (Fig. 5.16). A salt bridge interaction is likely to occur if the simulation is accurate. Furthermore, it has been shown in the $GABA_C$ receptor that the homologous residue (R104) is critical to receptor activation: when R104 is substituted with alanine or glutamate an increase in GABA EC_{50} >10,000-fold was observed. In the same study, molecular modelling indicated a role of this residue in binding GABA (Harrison and Lummis, 2006).

Loop A aromatic F146 was found not to be a binding residue in RDL receptors. Referring to the model predicted that the ammonium of GABA is 9.7 Å from the aromatic side chain of F146 (Fig. 5.18). The model is consistent with the observed experimental evidence in this chapter and suggests that this residue is not close enough to interact directly with GABA. Conversely however, this residue is of central importance to GABA binding in the $GABA_A$ receptor, where the equivalent aromatic residue (β_2Tyr97), is involved in a cation-π interaction with the ammonium of GABA (Padgett *et al.*, 2007). This would

suggest that GABA binds in a different position in RDL than in $GABA_A$ receptors. Adjacent residue F147 is predicted to face into the hydrophobic core of the extracellular domain (Fig. 5.18). Alanine substitution (mutation F147A) resulted in nonfunctional receptors. It is possible that the alanine substitution alters the tertiary structure of the β-sheet backbone of Loop A resulting in misfolded protein. The hydrophobic nature of this residue may be important in maintaining receptor structure or correct receptor folding.

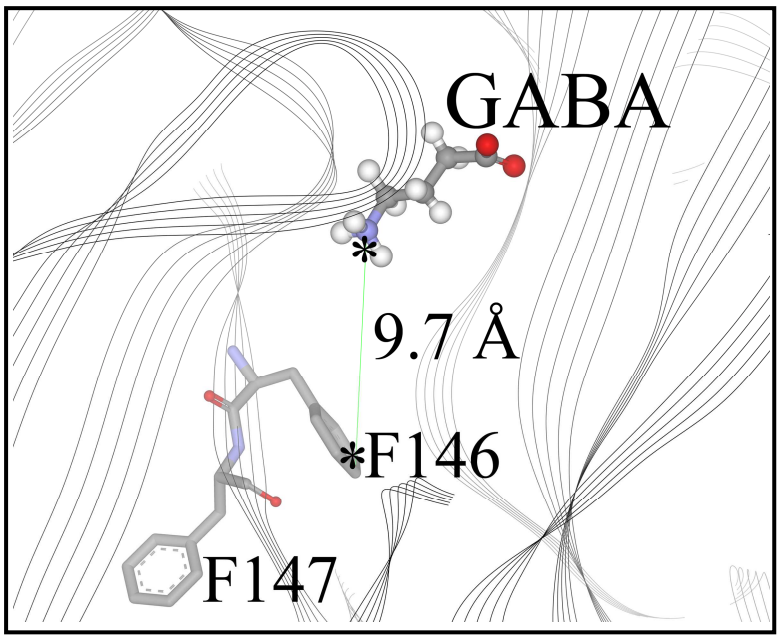

Figure 5.18 Loop A aromatic residues F146 & F147. GABA is positioned in its predicted binding orientation with its distance from F146 labeled.

5.4 Conclusions

RDL receptors are sensitive to mutations in Loop B, Loop C and Loop D aromatic residues (F206, Y254 and Y109 respectively), suggesting that these residues form the aromatic box involved in stabilising ligand binding. Furthermore, Loop B aromatic residues F206 and Y208 are energetically coupled, suggesting an interaction during receptor activation. However, Loop A aromatic residues are unlikely to be involved in GABA binding.

Loop B glutamate and serine residues E204 and S205 may play important structural roles as well as being directly involved in ligand binding. In particular, the negatively charged side chain of E204 is likely to be involved in a salt-bridge interaction with the positive ammonium of GABA.

A Loop D arginine residue (R111) is also critical to RDL receptor function and modelling and docking experiments predict a direct role for this residue in GABA binding.

The mutation F206Y causes a large gain of function and this residue is predicted to form a cation-π interaction with the ammonium of GABA. Additionally, Loop C aromatic Y254 is sensitive to mutations and is predicted to interact with GABA, also via a cation-π interaction. Molecular modelling supports this hypothesis and this should be further tested using unnatural amino acid mutagenesis.

Chapter 6

Characterisation of Ginkgo biloba extracts on RDL receptors

6.1 Introduction

The *Ginkgo biloba* tree has been used in Chinese medicine for over 2,500 years (Drieu *et al.*, 2000) and is amongst the most used herbal medicines today. *Ginkgo biloba* extracts contain flavonoids (22-24%) and terpene trilactones (6-8%) (DeFeudis and Drieu, 2000). *Ginkgo biloba* extracts are also potent insecticides, e.g. bilobalide has an LD_{50} of 0.26 ng/insect when tested on planthoppers, while ginkgolide A and ginkgolide B had values of 64 and 16 ng/insect respectively (Ahn, 1997). These terpene trilactone compounds have been shown to be non-competitive antagonists of vertebrate glycine and $GABA_A$ receptors with IC_{50} values in the low micromolar range (Ivic *et al.*, 2003; Huang *et al.*, 2004; Kondratskaya *et al.*, 2004). Ginkgolides and bilobalide are therefore pharmacologically similar to picrotoxin (PTX) a non-competitive antagonist of $GABA_A$ and glycine receptors (Ivic *et al.*, 2003; Li and Slaughter, 2007). PTX has been well characterised as binding close to the 2' channel-lining residue (Chen *et al.*, 2006; Das and Dillon, 2005; Olsen, 2006). Similarly, molecular modelling of the glycine receptor pore has yielded insight into the binding parameters of ginkgolide B, implicating a role for the 6' and 2' channel-lining residues (Hawthorne *et al.*, 2006; Heads *et al.*, 2008).

The aim of this study was to assess the potency of ginkgolide A, ginkgolide B, bilobalide and picrotoxin (Fig. 6.1) on RDL receptor function and to determine the role of the 2' and 6' channel-lining residues.

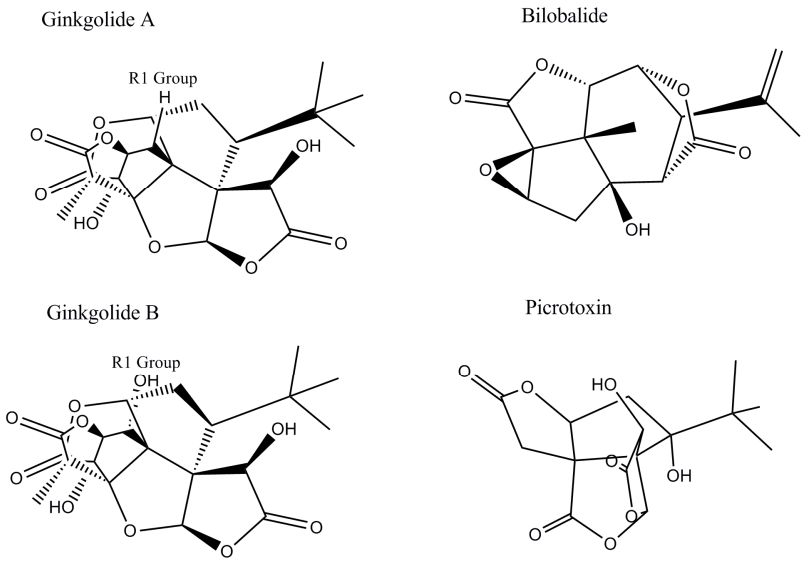

Figure 6.1 Structures of picrotoxin (picrotoxinin) and ginkgolides. Ginkgolide A and ginkgolide B differ only by a single atom, the R1 group being a hydrogen atom and hydroxyl group respectively. Ginkgolides, bilobalide and picrotoxinin are all caged compounds.

6.2 Results

6.2.1 Ginkgolides are antagonists of RDL receptors

Co-application of ginkgolides and bilobalide with GABA resulted in diminished currents (Fig. 6.2), while pre-application (30 µM for 30 s) had no effect on subsequent GABA responses. Concentration-inhibition curves were prepared (Fig. 6.2) and IC_{50} values were 0.95 µM, 0.69 µM, 0.25 µM and 1.1 µM for GA, GB, BB and PTX respectively (Table 6.2).

Following ginkgolide inhibition (10 µM antagonist), receptors recovered slowly, with the effects of inhibition not fully reversed after twenty minutes of washout and four GABA applications (EC_{50}) (Fig. 6.3).

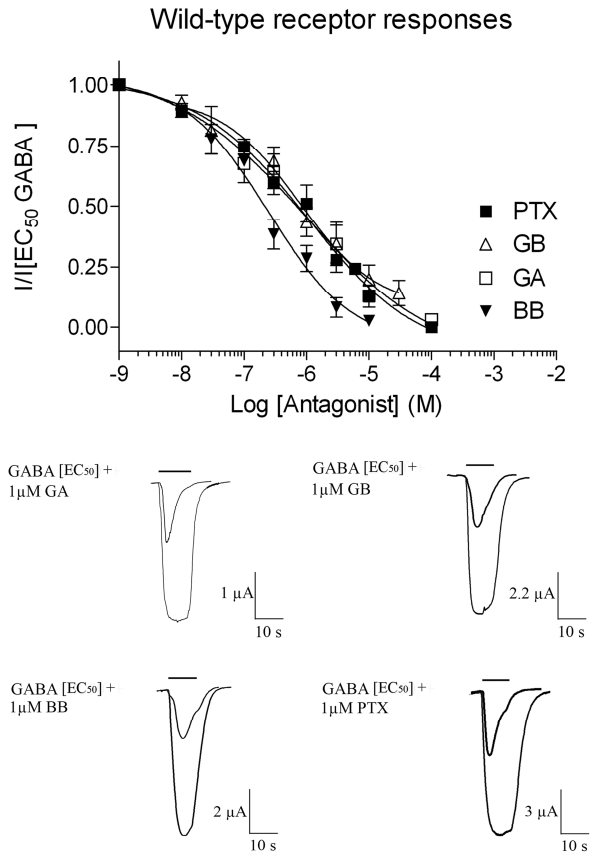

Fig. 6.2 Ginkgolides are antagonists of RDL receptors. Concentration-inhibition curves and sample electrophysiological traces showing the effects of ginkgolide A (GA), ginkgolide B (GB), bilobalide (BB) and picrotoxin (PTX) on GABA (EC_{50}) evoked currents. GABA evoked responses are diminished in the presence of all compounds.

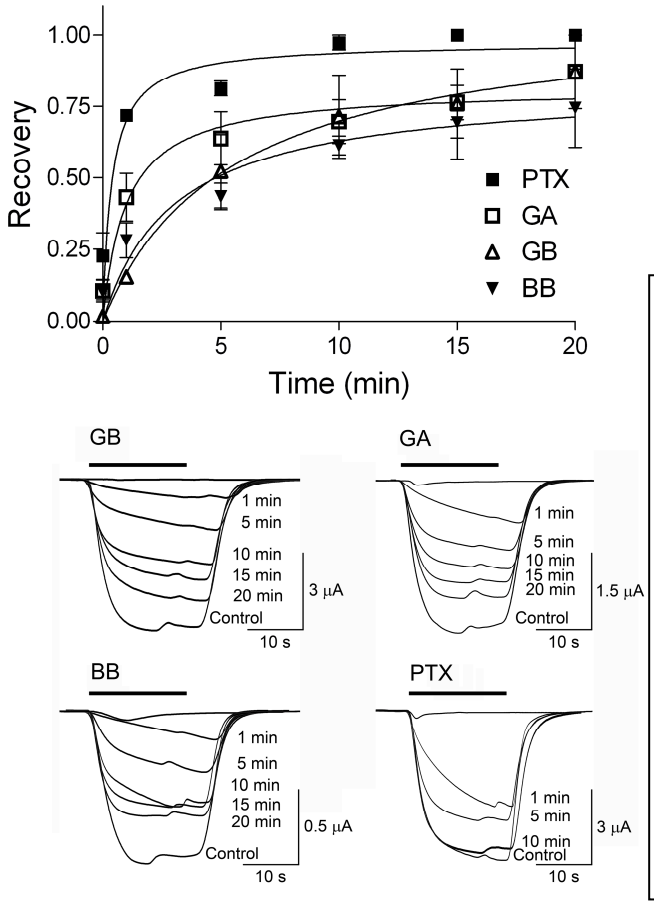

Figure 6.3 RDL receptor recovery following ginkgolide inhibition. Above: Recovery time of wild-type RDL receptors following GA, GB, BB and PTX inhibition. PTX, BB, GB and GA inhibition (10 μM antagonist) was not fully reversed following four applications of GABA [EC_{50}] and twenty minutes of saline washout. Each data point is mean ± SEM from at least three oocytes. **Below:** Electrophysiological traces showing recovery from inhibition.

6.2.2 Mutant receptors are resistant to antagonists

Mutant receptors A2'S, T6'V and double mutant A2'S T6'V formed functional receptors with EC_{50} values of 23 µM, 75 µM and 21 µM respectively (Fig. 6.4) (Table 6.1). Both T6'V and A2'S mutant receptors showed decreased sensitivity to all compounds: IC_{50} values for T6'V were > 100 µM, 260 µM, > 1 mM and 1.1 mM for GA, GB, BB and PTX respectively; IC_{50} values for A2'S were 2.8 µM, 10.1 µM, 160 µM and 260 µM for GA, GB, BB and PTX respectively (Table 6.2; Fig. 6.5). Double mutant A2'S T6'V was resistant to all compounds, with no effects observable with 100 µM antagonist. A2'S and T6'V mutant receptors also displayed accelerated recovery from antagonists when compared to wild type. Following antagonist withdrawal, A2'S and T6'V mutant receptors recovered fully with a subsequent GABA application.

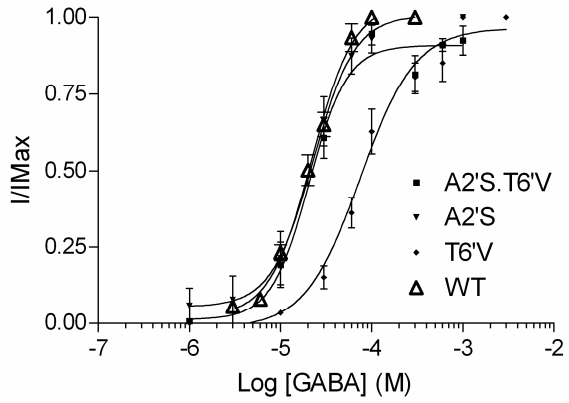

Figure 6.4 Concentration-response curves for mutants used in this study. Each data point is the mean ± SEM of at least three different oocytes

Table 6.1 Parameters derived from concentration-response curves.

Mutant	EC_{50} ± SEM	EC_{50} (µM)	n_H ± SEM	n
WT	**4.71 ± 0.04**	**19.7**	**1.8 ± 0.2**	**19**
A2'S	4.64 ± 0.06	22.7	1.9 ± 0.4	4
T6'V	4.13 ± 0.06*	74.6	1.4 ± 0.3	9
A2'S.T6'V	4.69 ± 0.06	20.6	2.1 ± 0.5	5

n_H is the Hill coefficient, n indicates number of replicates. * denotes significance from WT ($p<0.05$, t-test).

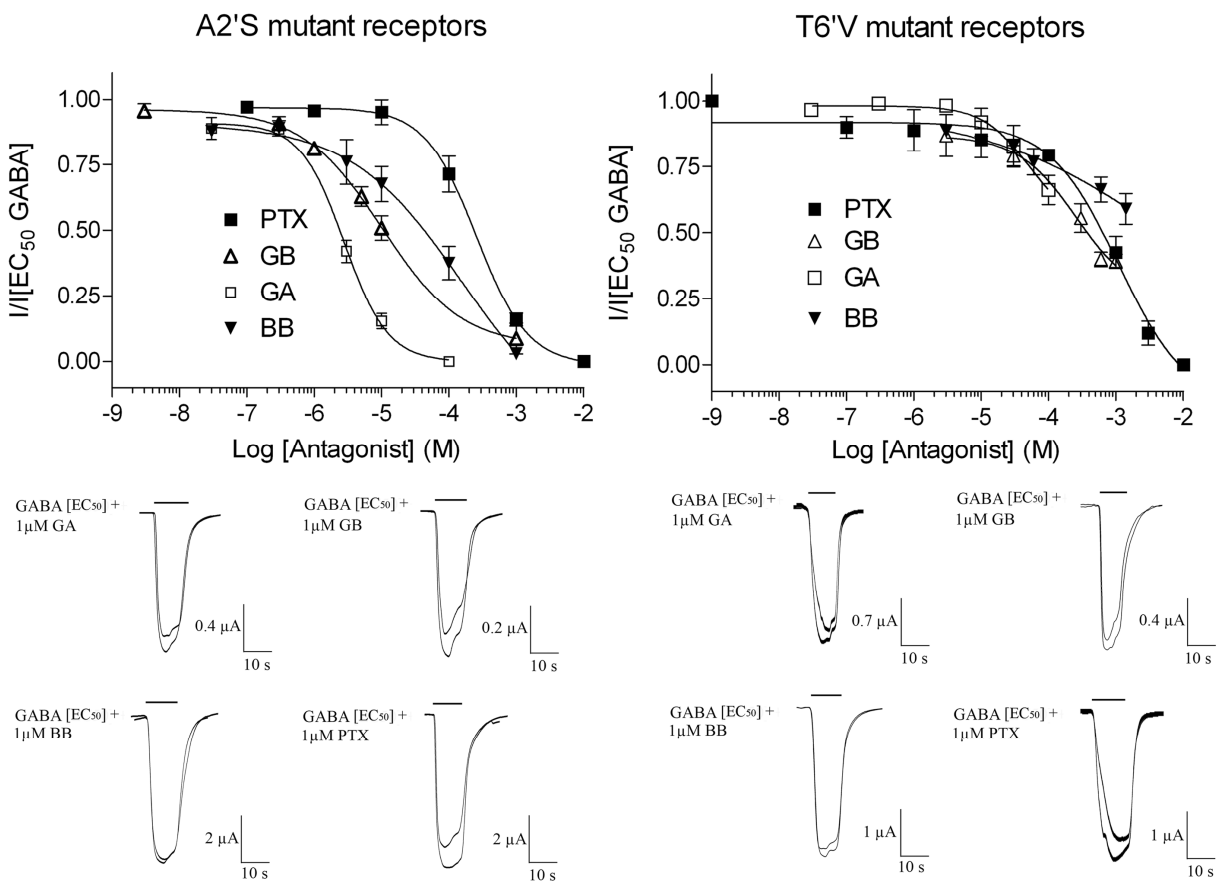

Figure 6.5 Ginkgolide inhibition of mutant RDL receptors. Above: Concentration-inhibition curves prepared from mutant receptor responses. Antagonist was co-applied with GABA (EC_{50} concentration) and the inhibited response was normalised to response in the absence of antagonist. Each data point is the mean ± SEM of at least three different oocytes. **Below: Electrophysiological traces showing the effects of 1 μM ginkgolide A (GA), ginkgolide B (GB), bilobalide (BB) and picrotoxin (PTX) on GABA (EC_{50}) evoked currents.** A2'S and T6'V mutant receptors show resistance to these compounds.

Table 6.2 Parameters derived from concentration-inhibition curves.

Antagonist	pIC_{50} ± SEM	IC_{50} (μM)	n_H ± SEM	n
Wild-type receptors				
PTX	5.976 ± 0.165	1.1	0.5 ± 0.1	3
GA	6.024 ± 0.371	0.95	0.5 ± 0.2	3
GB	6.118 ± 0.222	0.69	0.7 ± 0.3	4
BB	6.610 ± 0.167	0.25	0.7 ± 0.2	4
A2'S receptors				
PTX	3.593 ± 0.082*	260	1.1 ± 0.2	4
GA	5.555 ± 0.052	2.80	1.3 ± 0.2	3
GB	4.997 ± 0.111*	10.1	0.7 ± 0.2	4
BB	3.800 ± 0.787*	160	0.5 ± 0.2	3
T6'V receptors				
PTX	2.961 ± 0.185*	1090	0.9 ± 0.2	5
GA	≤4	-	-	3
GB	3.588 ± 0.362*	260	1.0 ± 0.7	4
BB	≤3	-	-	4

n_H is the Hill coefficient, n = number of replicates. * denotes significance from wild-type ($p<0.05$, unpaired t-test).

6.2.3 Mutant cycle analysis

Mutant cycle analysis was carried out using IC_{50} values arrived at from concentration-inhibition curves. By assessing the effect of changing a single chemical group on the ligand both on wild-type and mutant receptors we can determine how coupled these two atomic groups are by calculating a coupling coefficient. Coupling coefficients suggest a positive interaction between the R1 group of ginkgolide B and both the 2' and 6' residues. Interaction energies ($\Delta\Delta G.int = -RT\ln\Omega$) of 3.9 and 4.8 $kJ.mol^{-1}$ for 2' and 6' residues respectively suggest a non-covalent interaction between ligand and receptor at this position (Fig. 6.6). This prediction at 6'T is in line with the expected energy of a single hydrogen bond (5-30 $kJmol^{-1}$).

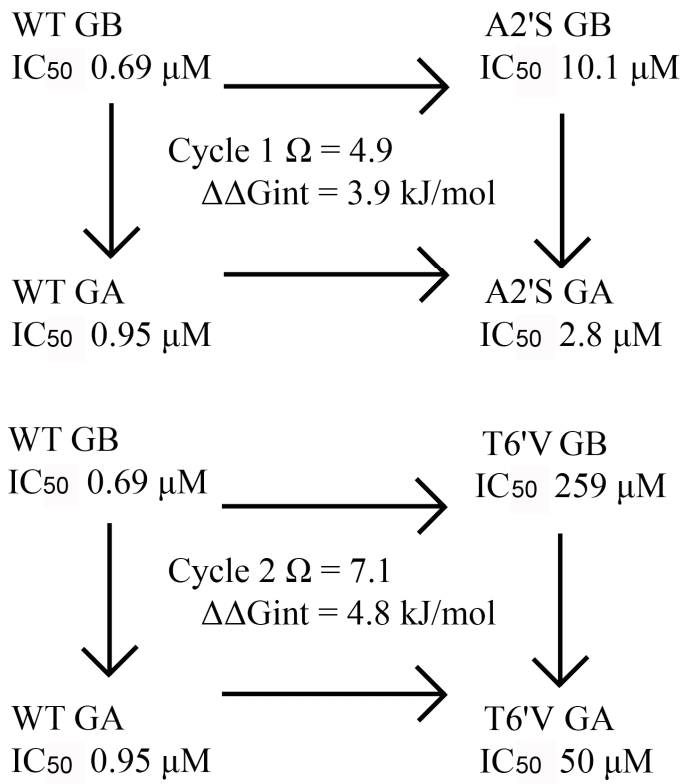

Figure 6.6 Mutant cycle analysis. For the 6' threonine residue the coupling energy (ΔΔG.int = -RTlnΩ) was 4.8 kJmol^{-1}. For the 2' alanine it was 3.9 kJmol^{-1}.

6.2.4 Molecular modelling and docking

Ginkgolide A and ginkgolide B docked into the channel close to the 6'T residue (Fig. 6.7). Both compounds docked towards two of the M2 helical bundles. Hydrogen bonding with the carbonyl oxygen of the 6'T residue was detected for Ginkgolide A. Ginkgolide B docked into the same location in a similar orientation but the same H-bonding interaction with this residue was not detected. Picrotoxinin and bilobalide also docked within 5 Å of the 6' and 2' channel-lining residues of contiguous subunits; however no specific interactions were detected. In A2'S receptors, both ginkgolide A and ginkgolide B showed hydrogen bonding interactions with the 2'S residue whilst hydrogen

bonding at the 6'T residue was absent. Furthermore, both ginkgolide compounds docked in the same orientation at 2'S receptors, orientations distinct from that observed at wild type receptors, with both compounds inverted and lower in the channel. In T6'V receptors no hydrogen bonding interactions were observed for any compounds.

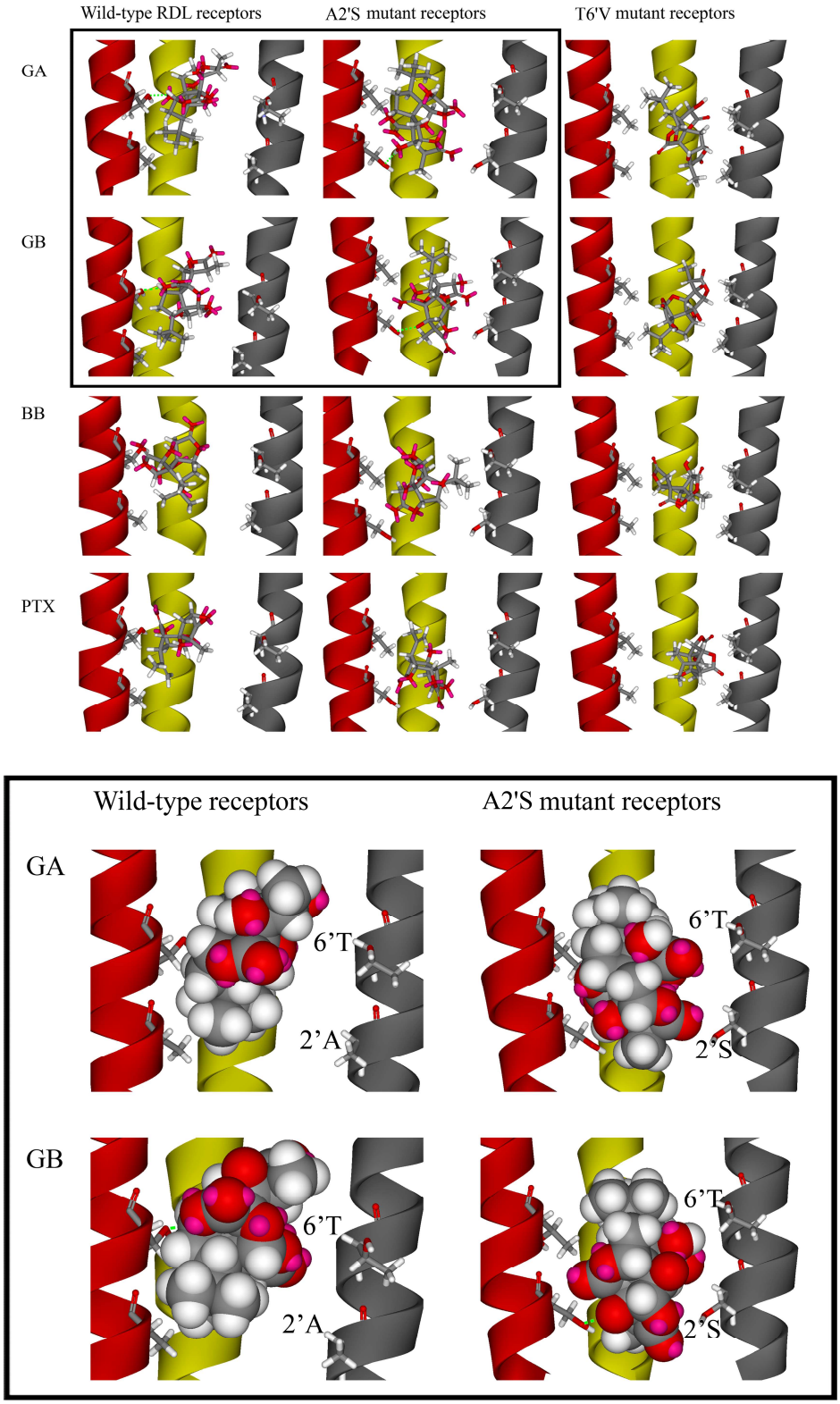

Figure 6.7 Homology models of the RDL transmembrane domain and docking simulations. A homology model of the full RDL pentamer based on *Gloebacter violaceus* (GLIC) (PDB: 3EAM). Two subunits were removed for the purpose of this figure, revealing the binding orientation within the pore. M2 transmembrane regions are α-helical (red, grey and green; denoting separate subunits)**. Above:** GA, GB, BB and PTX docked into WT, A2'S and T6'V mutant receptors. **Below:** Close up view of GA and GB binding orientations in WT and A2'S mutant receptors, where hydrogen bonds were detected.

6.2.5 Insect bioassays

Bioassays were carried out by Mirel Puinean and Martin Williamson at Rothamsted Research, Hertfordshire. After 48 h with an application of 1000 ppm compound, two out of four compounds (BB and GA) produced 100% mortality. The difference between these compounds and GB and PTX could be observed after 1 h when most of the individuals dosed with BB and GA, although alive, had their hind legs paralyzed while the insects dosed with GB and PTX, although affected, could still move all their legs. However, after 48 h at this high dose 100% of the individuals were killed ($p<0.05$, Student's t-test) (Fig. 6.8).

A further bioassay using 50 ppm solutions of the tested compounds produced a better resolution between their toxicity. BB and GA emerged as the most toxic with 100% mortality ($p<0.05$, Student's t-test). GB and PTX were significantly less potent yielding 60% and 34% mortality respectively, and significantly different to control treated insects ($p>0.05$, Student's t-test).

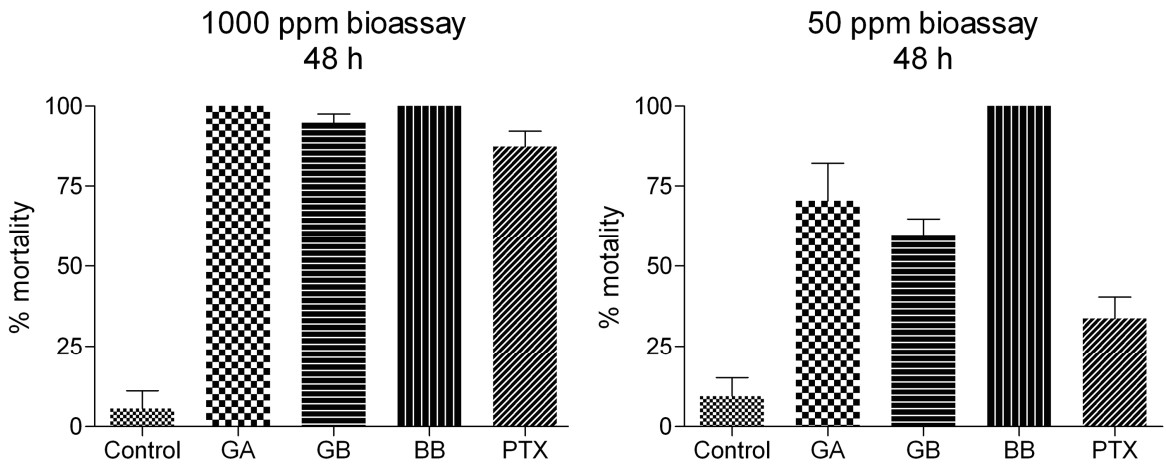

Figure 6.8 Whole insect toxicity bioassays for GA, GB, BB and PTX on *N.lugens*. Each experiment consisted of ten insects being dosed with compound. Data is mean ± SEM for three experiments.

6.3 Discussion

I have shown that ginkgolide A, ginkgolide B and bilobalide are antagonists of RDL receptors with IC_{50} values in the sub-micromolar range. Reversal from inhibition is slow, requiring >20 min to wash out. This distinguishes the ginkgolides from picrotoxin, which washes out within 10 min. This behaviour of ginkgolides differs from that reported at glycine receptors, where recovery is observed following one minute of washout (Ivic *et al.*, 2003). An investigation into the role of the 6'T and 2'A channel-lining residues using mutagenesis studies revealed that these residues are critical to the ginkgolide sensitivity of RDL receptors, suggesting that ginkgolides bind in the channel close to these residues.

Modelling of the transmembrane domain of homomeric RDL receptors reveals that the 6'T and 2'A residues are amongst the channel-lining M2 residues which face into the channel pore. Docking of ginkgolides into the channel identified a hydrogen bond interaction between ginkgolides A and B and the hydroxyl oxygen of the 6'T residue. This binding location is supported by mutant cycle analysis which suggested an interaction between ginkgolides and the 6'T. This binding site is similar to that reported for ginkgolide binding in the glycine receptor pore (Hawthorne *et al.*, 2006; Heads *et al.*, 2008). Bilobalide also docked close to the 6'T but no specific interactions were observed. Docking of these compounds into the A2'S mutant receptor revealed hydrogen bonding between ginkgolides and the 2'S hydroxyl, while hydrogen bonding with the 6'T residue was absent. T6'V mutant receptors showed no hydrogen bonding interactions, suggesting that this mutation disrupts binding and that this residue may be the principal attachment point for ginkgolides. Since the 6'T residue and the mutant A2'S residues have hydroxyl groups on their side chains and both of these residues showed H-bonding interactions in the docking simulations, it may be that interactions with these side chains is a determinant of ginkgolide binding. Indeed, the A2'S “resistance to dieldrin” mutation

caused ginkgolides to dock lower in the channel, in what may be a lower affinity binding site. Such an altered binding position may underlie the decreased ginkgolide sensitivity conferred by this mutation.

Picrotoxin inhibits both cation-selective (nACh and 5-HT_3 receptors) and anion-selective ($GABA_A$, $GABA_C$, GlyR, and GluCl receptors) receptor channels (Das *et al.*, 2003; Erkkila *et al.*, 2004; Etter *et al.*, 1999; Schmieden *et al.*, 1989; Zhang *et al.*, 1995a). Picrotoxin is an equimolecular complex of picrotoxinin and picrotin (Curtis and Johnston, 1974) and picrotin is inactive in inhibiting $GABA_A$Rs and $GABA_C$Rs, indicating that the inhibitory effect of picrotoxin is related to the picrotoxinin component (Curtis *et al.*, 1974; Qian *et al.*, 2005). Conversely picrotoxinin and picrotin are equally potent in inhibiting α_1 homomeric GlyR activation (Lynch *et al.*, 1995). RDL receptors are also inhibited by picrotoxin (Hosie *et al.*, 1995), however the blocking effect at RDL receptors is mediated solely by picrotoxinin as RDL receptors are resistant to picrotin (Shirai *et al.*, 1995). This finding shows RDL receptors to be more $GABA_A$-like than GlyR-like in terms of picrotoxin sensitivity. So far, ginkgolides have only been shown to inhibit anion selective receptors (Ivic *et al.*, 2003; Huang *et al.*, 2004; Kondratskaya *et al.*, 2004) and more recently Jensen *et al.* (2010) described how ginkgolide X, a synthetic ginkgolide derivative, is selective for glycine receptors, and suggested a distinct binding mode for ginkgolides at anionic receptors.

The ginkgolides and picrotoxin block RDL receptors with similar IC_{50} values to those at vertebrate $GABA_A$ receptors (Huang *et al.*, 2004; Krishek *et al.*, 1996b). What is surprising, however, is that picrotoxin is a convulsant but the ginkgolides are not, and instead have neuro-protective, anxiolytic and other beneficial properties (Ahlemeyer and Krieglstein, 2003; Mdzinarishvili *et al.*, 2007; Zhu *et al.*, 2004). The reasons for this are still unclear, but may include differences in bioavailability as well as differences in insect and human GABA receptor structure. Other properties of these compounds include symptomatic relief from Alzheimer disease and a reduction in the effects of dementia (DeFeudis and Drieu, 2000). Furthermore, a study on human volunteers, using

a computer-analysed electroencephalogram, showed that *Ginkgo biloba* extract (EGb) has effects similar to those of cognitive enhancers as well as tacrine (an anticholinesterase), a marketed antidementia drug currently available in the United States (Itil *et al.*, 1996). A more established property of *Ginkgo biloba* extract is its potent insecticidal activity. For many decades leaves from the *Ginkgo biloba* tree have been used in books to prevent insect activity, and more recent studies to determine potency have shown excellent activity on a range of insects (Sun *et al.*, 2006; Ahn, 1997). One potential mode of action is via insect GABA receptors, as many insecticidal compounds are known to exert their effects through these proteins. My data showing moderate potency of ginkgolides at RDL receptors, and perhaps more importantly, slow reversibility, indicates that these receptors could indeed be the insecticidal target of these compounds. This would be a mechanism of action that fits well with reported potencies (Sun *et al.*, 2006; Ahn, 1997), with bilobalide being the most potent insecticide and also the most potent RDL receptor antagonist. Insecticides which act on GABA receptors such as hexachlorocyclohexanes, polychloroboranes and chlorinated cyclodienes (such as lindane, toxaphene and endosulfan respectively) were used widely as pesticides before their GABAergic mechanism of action was revealed (Casida, 1993). Fipronil is still one of the most common insecticides (used mainly for pest control), with 119,000 lbs being used in California in 2006 (http://cdpr.ca.gov/). Identifying compounds which selectively block insect GABA receptors could facilitate novel insecticide design. The environmental and economic benefits of developing bio-organic insecticides which poses little toxicological threat to humans are great. Selective toxicity is the ultimate goal of the pesticide industry, whilst ever progressively, environmentalism is in the sights of modern industry. For these reasons, I deem *Ginkgo biloba* extracts to be an underexploited bio-organic alternative to current pesticide strategies. This study provides chemical insight into their action which will facilitate further development of these “green” insecticides.

6.4 Conclusions

Ginkgolide A, ginkgolide B and bilobalide are antagonists of RDL GABA receptors and recovery from inhibition is slow. These compounds block the channel of RDL receptors, binding close to the 2' and 6' residues. Interaction energies between ginkgolides and their binding residues are in the region of a single hydrogen bond and the expected interaction includes a hydrogen bond with the 6'T hydroxyl side chain. I hypothesise that the blocking action of ginkgolides at RDL receptors is the mechanism underlying their potent insecticidal activity.

Chapter 7

Single-channel analysis of heteromeric 5-HT_3 receptors

7.1 Introduction

5-HT_3 receptors are 5-hydroxytryptamine-gated Cys-loop receptors that are largely sodium selective. Receptor activation results in a rapidly activating and then desensitising inward current resulting in depolarisation of the cell. Thus far, five 5-HT_3 receptor genes have been identified (subunits A-E), and functional receptors containing each of these have been expressed (Davies *et al.*, 1999; Niesler *et al.*, 2003; Niesler *et al.*, 2007). Only A subunits can form functional homomeric receptors, but other subunits can combine with A subunits to form heteromeric complexes. Isoforms of the human A-subunit have also been described, and recently two novel transcriptional variants of the B subunit (Brain-1 and Brain-2) have also been cloned (Bruss *et al.*, 2000a; Bruss *et al.*, 2000b; Tzvetkov *et al.*, 2007). RNA for these B variants has been quantified using real-time RT-PCR showing that the B subunit is abundantly expressed in the human brain as well as in the colon and small intestine (Fig. 7.1). Tzvetkov *et al.* (2007) reported that in the brain less than 1% of the 5-HT3B subunit RNA coded for the conventional B-subunit, while the remaining B-subunit RNA was accounted for by approximately 75% Brain-2 and 24% Brain-1.

Protein sequences have been predicted from the alternative transcripts, and compared to the canonical 5-HT3B subunit (Tzvetkov *et al.*, 2007) (Fig. 7.1). The Cys-loop, four transmembrane domains (designated TM1 to TM4) and the HA-stretch are common to all three 5-HT3B isoforms. The HA-stretch is responsible for the higher conductance of 5-HT3B-containing heteromeric receptors (Kelley *et al.*, 2003) (Fig. 7.2). The N-terminal localisation signal and the β1–β2 loop structure mediating channel gating (Reeves *et al.*, 2005) are missing in the Brain-2 isoform. The six amino acids of the N-terminus of the Brain-1 isoform differ from the canonical form.

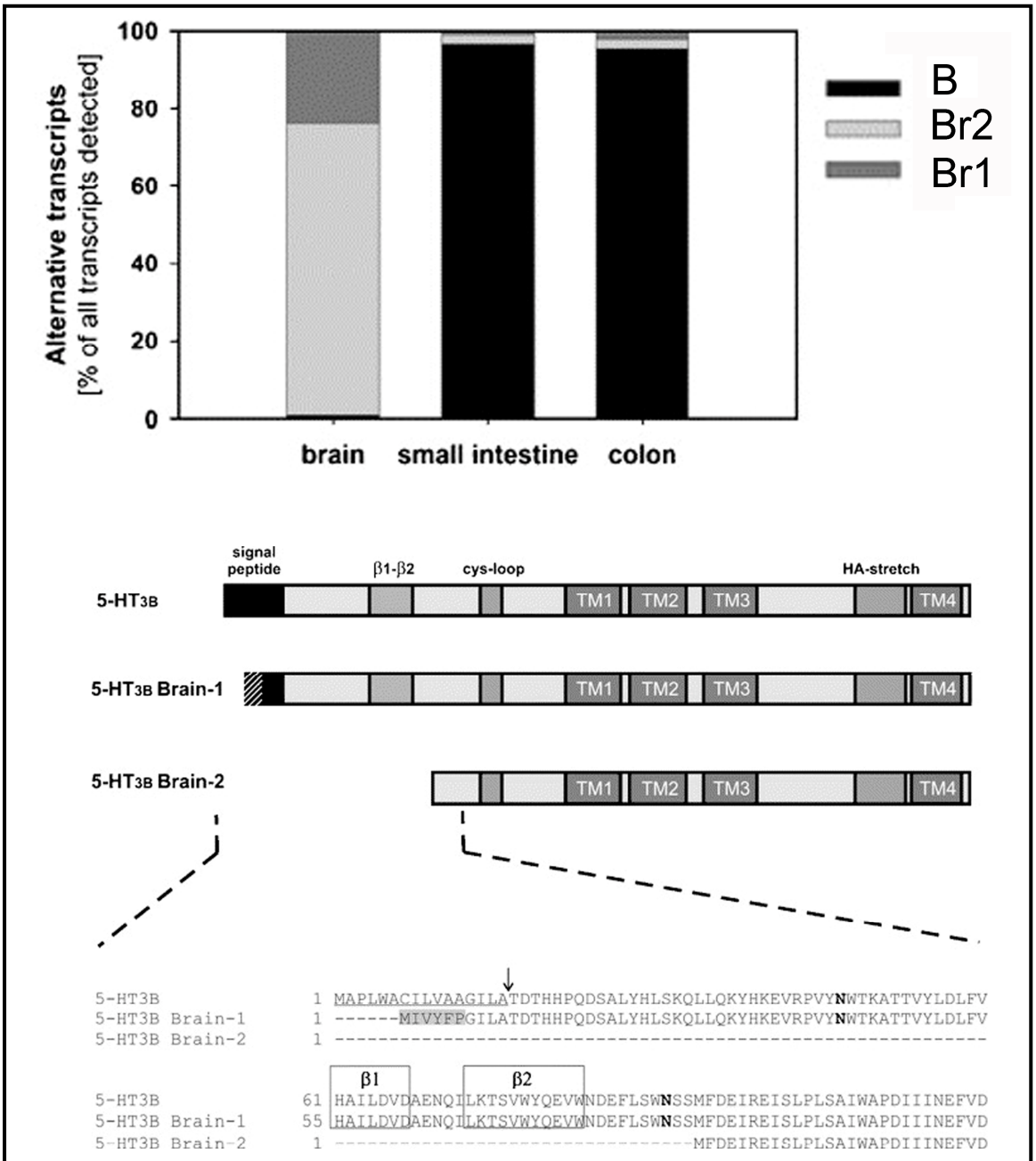

Figure 7.1 5-HT$_3$R alternative transcripts. Above: Relative abundance of B, brain-1 (Br1) and brain-2 (Br2) transcripts in brain and gut. **Below:** Br1 and Br2 secondary structure. The part of the localization signal that differs between the intestinal and Brain-1 form is marked by hatching. Potential glycosylation sites are shown in bold. Figure taken from Tzvetkov *et al.*, 2007, with copyright permission from *Gene*.

Unpublished data from our lab suggests that Br1 and Br2 can each co-assemble with the A subunit, forming functional receptors in *Xenopus* oocytes with distinct agonist sensitivities and desensitisation kinetics. When A and Br1 cRNA is injected; and when A and Br2 cRNA is injected, receptor responses

show distinct EC_{50} values (with EC_{50} A<ABr2<ABr1<AB) and Hill coefficients (n_H A>ABr2>ABr1>AB), suggesting that both Br1 and Br2 subunits can be incorporated into receptors with the A subunit.

A previous study has reported that A-homomers have a conductance of 0.4 pS whilst A-B heteromers have a much higher conductance of 16 pS (Davies *et al.*, 1999), highlighting the functional significance of the B subunit. This difference is due to the presence of four intracellular arginine residues, which if mutated in the A subunit to the B subunit equivalent residues, increases the conductance close to that of A-B heteromers (Davies *et al.*, 1999) (Fig. 7.2).

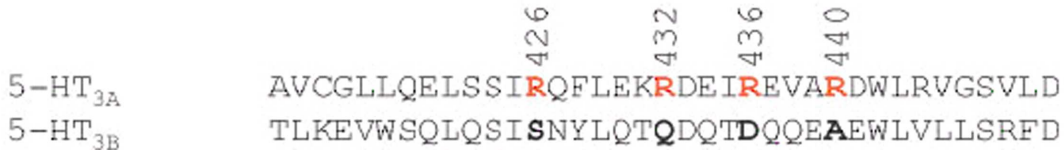

Figure 7.2 Four intracellular arginine mutations located in the M2-M3 intracellular loop confer high conductance to the B subunit. Taken from Davies *et al.*, 1999 with copyright permission from *Nature*.

Since the conductance of A homomers is too low to detect using single-channel electrophysiology, identifying A-B heteromers is facilitated by the fact that only A-B heteromers have a conductance high enough to be detected. The aim of this study was to determine whether Br1 and Br2 subunits form functional receptors in HEK293 cells and to determine the conductance of these different receptor channels.

7.2 Results

7.2.1 Single-channel recordings

Channels detected from whole-cell attached patches of HEK293 cells expressing human 5-HT_3AB receptors opened in bursts interrupted by brief sojourns in the closed state. Bursts were typically 20-200 ms in duration although brief single openings were also observed (Fig. 7.3). Several hundred events were recorded and current voltage relationships were plotted using the mean amplitude for channels at each voltage. Conductance was calculated using the Nernst equation and was found to be 30 ± 1.2 pS (Fig. 7.4).

ABr1 channels were measured using the same method. Channel events were similar to AB receptors with typical bursts of ~100 ms and with similar kinetic behaviour (i.e. brief open-closed time and burst frequency) (Fig. 7.3). Conductance was 33 ± 1.1 pS (Fig. 7.4).

No channels could be detected from ABr2 transfected cells. Transfection parameters were varied, including varying the ratio of A to Br2 DNA, varying the total DNA concentration used and also using different DNA samples. Nonetheless, no Br2 currents could be detected. Whole-cell macroscopic currents of cells confirmed the expression of 5-HT_3 receptors (data not shown) but no single-channel events could be detected.

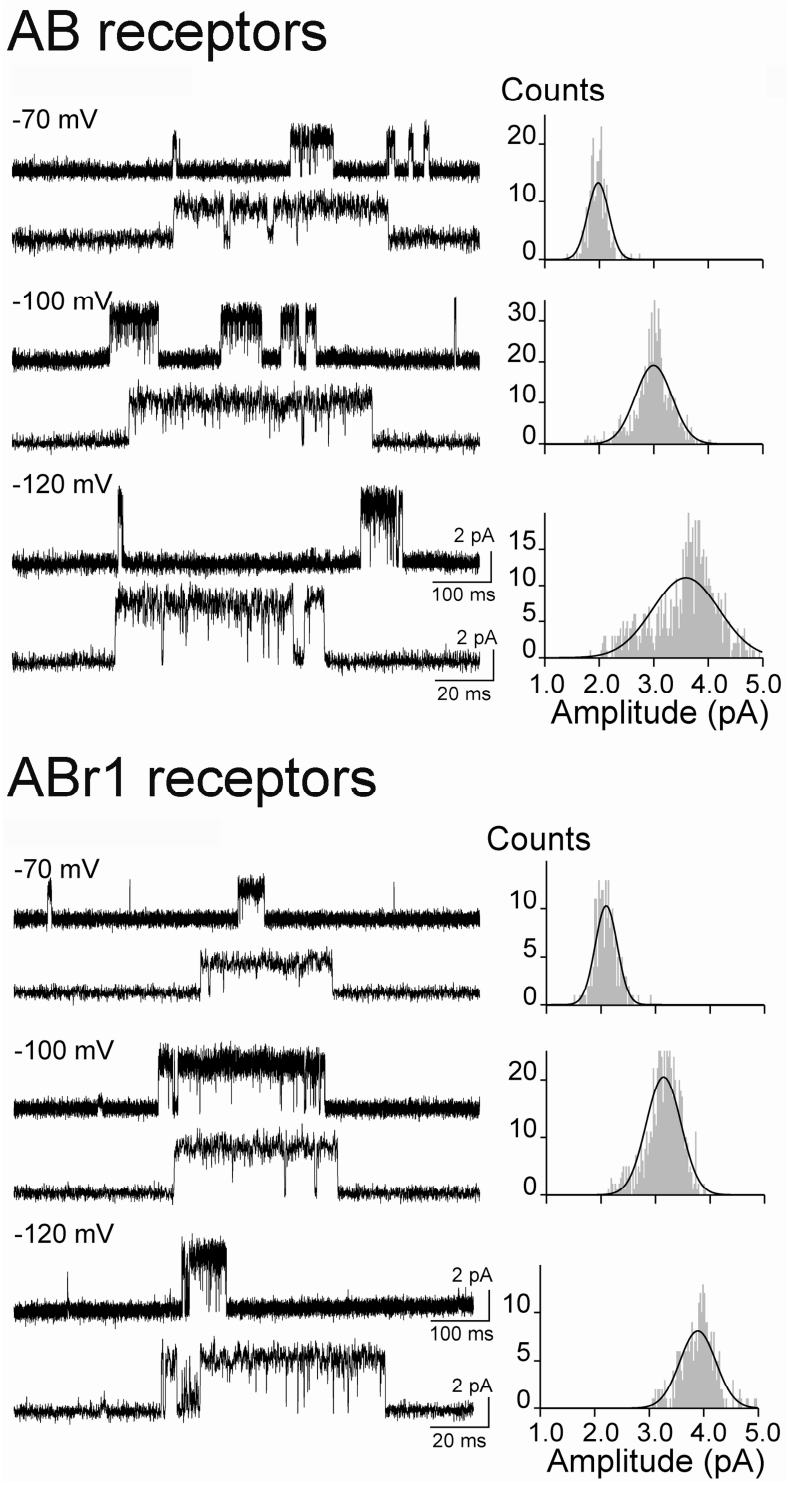

Figure 7.3 Sample traces and amplitude histograms for single-channel 5-HT$_3$ AB and ABr1 receptors expressed in HEK293 cells. Each histogram represents data from at least three patched cells.

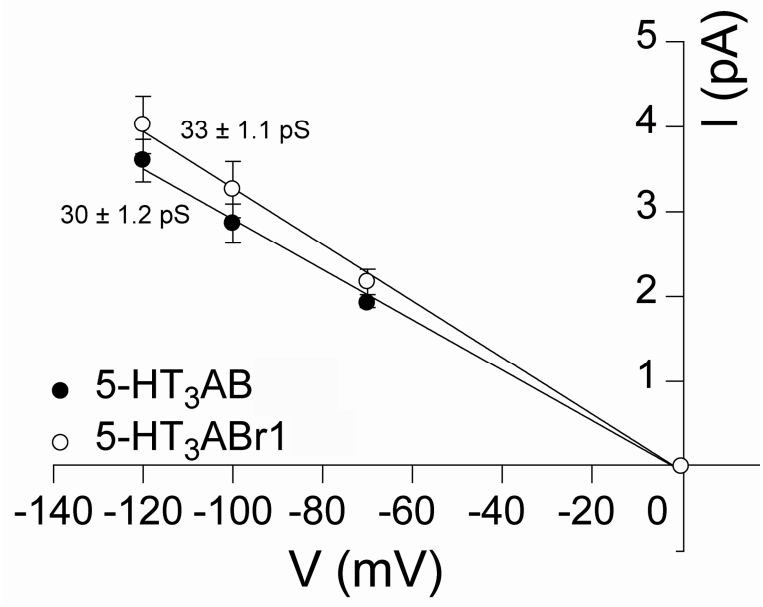

Figure 7.4 Current-voltage (IV) relationships for AB and ABr1 channels expressed in HEK293 cells. Receptors show identical conductance. Data is mean ± SEM for at least three cells. Data are not significantly different ($p>0.05$, unpaired t-test).

7.2.2 Flexstation analysis of heteromeric 5-HT$_3$ receptors expressed in HEK293 cells

HEK293 cells stably expressing 5-HT$_3$A receptors were transfected with B, Br1 and Br2 receptor subunit DNA using the microporator system (DigitalBio). Concentration-response data were prepared for each receptor type (A, AB, ABr1 and ABr2) and relative fluorescence was plotted, yielding concentration-response curves (Fig. 7.5). Data for each receptor type was collected from at least five separate transfections. Maximum fluorescence was decreased for heteromeric receptors compared to control (A homomeric) receptors (Fig. 7.5). EC_{50} values were 0.36 µM, 0.26 µM, 0.53 µM and 0.46 µM for A, AB, ABr1 and ABr2 receptors respectively, not significantly different ($p>0.05$, t-test) and Hill coefficients were 0.49, 1, 1 and 0.9 for A, AB, ABr1 and ABr2 receptors respectively (Figure 7.5; Table 7.1).

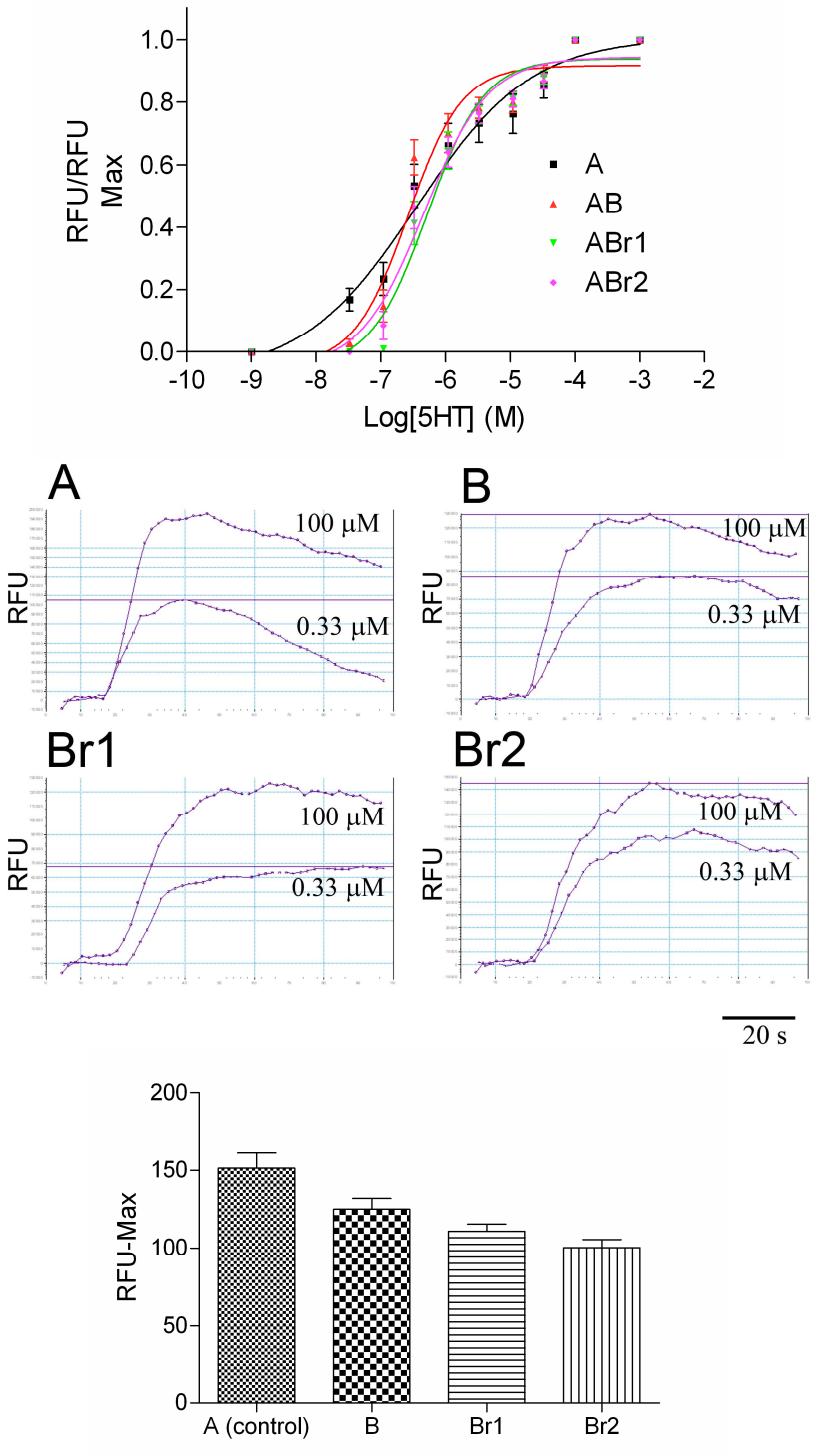

Figure 7.5 Concentration-response curves for homomeric and heteromeric 5-HT$_3$ receptors expressed in HEK293 cells stably expressing 5-HT$_3$A homomers. Above: Concentration-response curves. **Middle:** Sample traces from Flexstation (0.33 µM and 100 µM 5-HT). **Below:** Maximum relative fluorescence (RFU) for 5-HT-evoked responses in homomeric A (control) and heteromeric AB, ABr1 and ABr2 receptors.

Table 7.1 Parameters derived from concentration-response curves.

Subunit Composition	pEC_{50} (μM) mean ± SEM	EC_{50} (μM)	n_H mean ± SEM	RFU Max mean ± SEM	n
A	6.447 ± 0.17	0.36	0.5 ± 0.1	151.5 ± 9.6	15
AB	6.580 ± 0.07	0.26	1.0 ± 0.1*	125.1 ± 6.8*	15
ABr1	6.280 ± 0.06	0.53	1.0 ± 0.1*	110.9 ± 4.5*	15
ABr2	6.336 ± 0.07	0.46	0.9 ± 0.1*	110.5 ± 5.1*	15

n_H is the Hill coefficient, n indicates number of replicates. pEC_{50} values are not significantly different. * denotes significance from A homomers (where $p<0.05$, unpaired t-test).

7.3 Discussion

5-HT_3 receptor antagonists are currently used for the treatment of post-operative, radiotherapy- and chemotherapy-induced nausea and vomiting as well as irritable bowel syndrome. It is expected that 5-HT_3 antagonists will have wider therapeutic applications in the future, thus it is important to understand the consequences of subunit composition on the pharmacology and physiology of these receptors (Thompson and Lummis, 2007; Thompson *et al.*, 2007). With the higher conductance conferred by the addition of the B subunit and with its abundant expression levels (Tzvetkov *et al.*, 2007), B subunits are critical to brain 5-HT_3 signalling. Single-channel currents from AB heteromers were previously reported to be 16 pS (Davies *et al.*, 1999; Kelley *et al.*, 2003). My findings here of 30 pS are higher than these finding and may be due to different experimental conditions. More importantly, however, ABr1 channels showed similar behaviour and identical conductance to AB channels, confirming that they can be expressed in HEK293 cells and form functional channels with similar properties to AB receptors. This is an important finding, confirming the functionality of this abundantly expressed brain 5-HT_3 subunit.

Since the Br2 is missing such a large amount of sequence, it is unsurprising that functional channels were not observed with single-channel electrophysiology. This finding would suggest that either Br2 subunits can be expressed in oocytes but not HEK293 cells or that our previous findings are in fact an experimental artefact. Attempts to further validate these findings using the Flexstation yielded ambiguous results. The EC_{50} value arrived at for A homomers (0.36 µM) is close to a previously published value of 0.2 µM (Price and Lummis, 2005), where the same fluorometric assay was used. Other studies using electrophysiological methods have published EC_{50} values of 2.1 µM and 1.4 µM for the same receptors expressed in HEK293 cells and *Xenopus* oocytes respectively (Reeves *et al.*, 2001; Spier *et al.*, 2000). Whilst there was found to be no change in EC_{50} for stable A cells transfected with the different B

subunits, there was a significant increase in Hill coefficient and a decrease in the maximum response (RFU-Max). This is in contrast to that reported when these receptors are expressed in *Xenopus* oocytes where the opposite is observed - a decrease in Hill coefficient from 2.2 to 1.1 when the B subunit is incorporated into receptors (Lochner and Lummis, 2010). Additionally, since the B subunit has a higher conductance than the A subunit (Kelley *et al.*, 2003), an increase in RFU-Max may be expected for heteromeric receptors, although we cannot be sure if this is the case. Therefore this observed decrease in RFU-Max may be either an experimental artefact or a consequence of decreased open probability in heteromeric channels. Of course, transfections may not have been successful, but the significantly different Hill coefficients would suggest otherwise. As our preliminary work on Br2 receptors (in oocytes) yielded an A-like concentration-response profile (i.e. similar Hill coefficient and EC_{50}), it seems likely that this is indeed an experimental artefact and that the Br2 subunit does not form functional channels. Furthermore, since this subunit is missing extracellular loops D and A as well as the β1-β2 loop, which is essential for gating (Reeves *et al.*, 2005), it is unlikely to be involved in the formation of a functional 5-HT binding site. Despite this finding, the high abundance of Br2 transcripts detected in the brain warrant further investigation of the role of Br2. Perhaps this transcript plays an intracellular role in regulating receptor transcription and/or surface expression. Such an explanation could account for our previous results in oocytes, where a change in EC_{50} was observed for ABr2 receptors. Br2 cRNA may have altered the formation and/or regulation of homomeric A receptors. On the other hand, expressed Br2 subunits may have been incorporated into receptors with a stoichiometry too low to increase channel conductance (perhaps one Br2 subunit per receptor), but enough to affect the concentration-response profile. Further studies could determine if Br2 subunits reach the cell surface using immuno-staining or with conjugated fluorescent tags.

7.4 Conclusions

The 5-HT_3 Br1 subunit can form functional heteromeric channels with the A subunit and these heteromeric channels have a conductance of 30 pS, identical to AB receptors. The Br1 subunit is therefore an important component in brain 5-HT_3 signalling. The Br2 subunit does not form functional channels with the A subunit in HEK293 cells and is unlikely to form functional 5-HT_3 receptors. However, the high abundance of the Br2 transcript suggests that it may play an intracellular role in receptor regulation and/or surface expression and further experiments on Br2 should focus on these aspects.

Chapter 8

Future directions and final remarks

Future directions

The aim of this thesis was to investigate the structure and function of Cys-loop receptors and to generate a greater understanding of these receptors in general. I began by assessing the biophysical properties of RDL receptors. I followed on from this by assessing the efficacy of a range of agonists on RDL receptors, thereby identifying the critical determinants of agonist binding. Following on from this work, I identified several residues in loops B, C and D that are involved in ligand binding. I have also identified the binding location of ginkgolides and bilobalide in the channel pore. Finally, during a visit to Cecilia Bouzat's lab in Bahía Blanca, Argentina, I made single-channel recordings of heteromeric 5-HT_3 receptors, confirming the functionality of brain variant subunit Br1.

The work on biophysical properties of RDL receptors has confirmed that these receptors express quickly (within 24 h) in *Xenopus* oocytes and that they are chloride selective channels. Further work on this property could include mutagenesis of the -1' residue (alanine) to a glutamate - the equivalent residue in the cation-selective nAChR and 5-HT_3R - to determine if the ion selectivity filter is in the same location in RDL receptors.

RDL receptors showed resistance to changes in pH. This insensitivity to changes in pH distinguishes these receptors from their vertebrate orthologues, the $GABA_A$ receptors, and this difference may be due to the absence of charged residues involved in receptor gating. Future work could involve mutagenesis of charged residues in the pre-M1 and β1-β2 loop regions, since these regions contain many key gating residues (Bartos *et al.*, 2009a). This may lead to a greater general understanding of pH sensitivity in Cys-loop receptors.

In Chapter 4 I identified the critical features of agonists that bind to and activate RDL receptors; a charged amine and an anionic centre are required for agonists to bind. Additionally, there is a size requirement for agonists, with the

most potent agonists being ~5 Å in length. This work provides a set of structure activity relationship (SAR) data which could be used to generate potential antagonists. Further work could include the generation of a large set of GABA analogues, which may lead to the identification of an RDL specific antagonist. This may be useful for insecticide development as well as a tool for further studies in invertebrate neuroscience.

In Chapter 5 I identified several residues that are involved in ligand binding in RDL receptors. Loop B residues E204 and F206 and loop C residue Y254 seem the most likely candidates for interactions with the ammonium end of GABA. Loop D residues R111 and Y109 seem the most likely candidates for interactions with the carboxylate of GABA. Homology modelling and docking experiments support these binding interactions. Further studies could involve unnatural amino acid mutagenesis of these residues: fluorination of aromatic residues would determine whether there is a role for π electron density on the face of aromatic rings in ligand binding. Charged residues should be substituted with unnatural amino acids with similar side chains structure but with varying charge. These studies would clarify beyond doubt the role of these candidate 'binding' residues.

In Chapter 6 I identified *Ginkgo biloba* extracts, ginkgolides and bilobalide, as antagonists of RDL receptors with IC_{50} values similar to picrotoxin. Ginkgolides wash out more slowly than picrotoxin, making these compounds more potent blockers of RDL channels. Mutagenesis, modelling and mutant cycle analysis identified the 2' and 6' M2 channel-lining residues as being part of the ginkgolide binding site. Whole insect bioassays confirmed the insecticidal potency of these compounds, leading to the hypothesis that these compounds exert their insecticidal properties through RDL-like receptors. Further work could involve screening these compounds on a range of insect species, identifying susceptible and resistant species. Resistant species should be genetically catalogued with special attention to Cys-loop receptor structure, and particularly, the M2 2' and 6' residues.

In Chapter 7 I confirmed that the brain 5-HT_3R B subunit variant Br1 co-expresses with the A subunit, forming functional heteromeric receptor channels with a conductance similar to heteromeric AB receptors. Br2 containing channels however could not be detected in this study, leading to the hypothesis that this transcript (Br2) may play a role in other cellular processes such as receptor trafficking and/or regulation of expression. It is also quite possible that this transcript is not translated at all. Further studies on these subunits could involve mutagenesis studies and molecular modelling, as has led to the further understanding of the arrangement of A and B subunits in heteromeric 5-HT_3 receptors (Lochner and Lummis, 2010). Immunocytochemistry studies, using antibodies or fluorescent tags, could complement such work to determine whether Br2 subunits reach the cell surface.

Final remarks

In this thesis I have identified the critical determinants of RDL receptor function: pH sensitivity, ionic selectivity, agonist requirements and binding site residues. I have also identified natural compounds (ginkgolides) which block RDL receptors and which are potent insecticides. Together these findings provide potential for the development of RDL-targeting insecticides as well as pharmacological probes which may be useful in further studies on insect GABA receptors. I have also confirmed that 5-HT_3 receptor brain subunit Br1 forms functional receptor channels. Overall this work has lead to a greater understanding of Cys-loop receptor function and the findings presented here may benefit further biomedical and neuroscience research.

References

Ahlemeyer, B, Krieglstein, J (2003) Neuroprotective effects of *Ginkgo biloba* extract. *Cell Mol Life Sci* **60**(9)**:** 1779-1792.

Ahn, YJ (1997) Potent Insecticidal Activity of *Ginkgo biloba* Derived Trilactone Terpenes Against *Nilaparvata lugens*. *ACS Symposium series* **658:** 90-105.

Akabas, MH (2004) $GABA_A$ receptor structure-function studies: a reexamination in light of new acetylcholine receptor structures. *Int Rev Neurobiol* **62:** 1-43.

Amin, J, Weiss, DS (1993) $GABA_A$ receptor needs two homologous domains of the β-subunit for activation by GABA but not by pentobarbital. *Nature* **366**(6455)**:** 565-569.

Amin, J, Weiss, DS (1994) Homomeric ρ1 GABA channels: activation properties and domains. *Receptors Channels* **2**(3)**:** 227-236.

Aronstein, K, ffrench-Constant, R (1995) Immunocytochemistry of a novel GABA receptor subunit Rdl in *Drosophila melanogaster*. *Invert Neurosci* **1**(1)**:** 25-31.

Auerbach, A (2010) The gating isomerization of neuromuscular acetylcholine receptors. *J Physiol* **588**(4): 573-586.

Bafna, PA, Purohit, PG, Auerbach, A (2008) Gating at the mouth of the acetylcholine receptor channel: energetic consequences of mutations in the αM2-cap. *PLoS One* **3**(6)**:** e2515.

Bali, M, Akabas, MH (2007) The location of a closed channel gate in the $GABA_A$ receptor channel. *J Gen Physiol* **129**(2)**:** 145-159.

Bargmann, CI (1998) Neurobiology of the *Caenorhabditis elegans* genome. *Science* **282**(5396)**:** 2028-2033.

Barnard, EA (1992) Receptor classes and the transmitter-gated ion channels. *Trends Biochem Sci* **17**(10)**:** 368-374.

Barnard, EA, Skolnick, P, Olsen, RW, Mohler, H, Sieghart, W, Biggio, G, Braestrup, C, Bateson, AN, Langer, SZ (1998) International Union of Pharmacology. XV. Subtypes of γ-aminobutyric acidA receptors: classification on the basis of subunit structure and receptor function. *Pharmacol Rev* **50**(2)**:** 291-313.

Bartos, M, Corradi, J, Bouzat, C (2009a) Structural Basis of Activation of Cys-Loop Receptors: the Extracellular-Transmembrane Interface as a Coupling Region. *Mol Neurobiol* **40**(3): 236-252

Bartos, M, Price, KL, Lummis, SC, Bouzat, C (2009b) Glutamine 57 at the complementary binding site face is a key determinant of morantel selectivity for α7 nicotinic receptors. *J Biol Chem* **284**(32)**:** 21478-21487.

Beene, DL, Brandt, GS, Zhong, W, Zacharias, NM, Lester, HA, Dougherty, DA (2002) Cation-π interactions in ligand recognition by serotonergic (5-HT_3A) and nicotinic acetylcholine receptors: the anomalous binding properties of nicotine. *Biochemistry* **41**(32)**:** 10262-10269.

Beene, DL, Price, KL, Lester, HA, Dougherty, DA, Lummis, SC (2004) Tyrosine residues that control binding and gating in the 5-HT_3 receptor revealed by unnatural amino acid mutagenesis. *J Neurosci* **24**(41)**:** 9097-9104.

Beg, AA, Jorgensen, EM (2003) EXP-1 is an excitatory GABA-gated cation channel. *Nat Neurosci* **6**(11)**:** 1145-1152.

Belelli, D, Callachan, H, Hill-Venning, C, Peters, JA, Lambert, JJ (1996) Interaction of positive allosteric modulators with human and *Drosophila* recombinant GABA receptors expressed in *Xenopus laevis* oocytes. *Br J Pharmacol* **118**(3)**:** 563-576.

Bocquet, N, Nury, H, Baaden, M, Le Poupon, C, Changeux, JP, Delarue, M, Corringer, PJ (2009) X-ray structure of a pentameric ligand-gated ion channel in an apparently open conformation. *Nature* **457**(7225)**:** 111-114.

Boileau, AJ, Newell, JG, Czajkowski, C (2002) $GABA_A$ receptor β_2Tyr97 and Leu99 line the GABA-binding site. Insights into mechanisms of agonist and antagonist actions. *J Biol Chem* **277**(4)**:** 2931-2937.

Bouzat, C, Bartos, M, Corradi, J, Sine, SM (2008) The interface between extracellular and transmembrane domains of homomeric Cys-loop receptors governs open-channel lifetime and rate of desensitization. *J Neurosci* **28**(31)**:** 7808-7819.

Brejc, K, van Dijk, WJ, Klaassen, RV, Schuurmans, M, van Der Oost, J, Smit, AB, Sixma, TK (2001) Crystal structure of an ACh-binding protein reveals the ligand-binding domain of nicotinic receptors. *Nature* **411**(6835)**:** 269-276.

Bruss, M, Barann, M, Hayer-Zillgen, M, Eucker, T, Gothert, M, Bonisch, H (2000a) Modified 5-HT_3A receptor function by co-expression of alternatively spliced human 5-HT_3A receptor isoforms. *Naunyn Schmiedebergs Arch Pharmacol* **362**(4-5)**:** 392-401.

Bruss, M, Eucker, T, Gothert, M, Bonisch, H (2000b) Exon-intron organization of the human 5-HT_3A receptor gene. *Neuropharmacology* **39**(2)**:** 308-315.

Buckingham, SD, Biggin, PC, Sattelle, BM, Brown, LA, Sattelle, DB (2005) Insect GABA receptors: splicing, editing, and targeting by antiparasitics and insecticides. *Mol Pharmacol* **68**(4)**:** 942-951.

Buckingham, SD, Hosie, AM, Roush, RL, Sattelle, DB (1994) Actions of agonists and convulsant antagonists on a *Drosophila melanogaster* GABA receptor (Rdl) homo-oligomer expressed in *Xenopus* oocytes. *Neurosci Lett* **181**(1-2)**:** 137-140.

Burzomato, V, Beato, M, Groot-Kormelink, PJ, Colquhoun, D, Sivilotti, LG (2004) Single-channel behavior of heteromeric α1β glycine receptors: an attempt to detect a conformational change before the channel opens. *J Neurosci* **24**(48)**:** 10924-10940.

Casida, JE (1993) Insecticide action at the GABA-gated chloride channel: recognition, progress, and prospects. *Arch Insect Biochem Physiol* **22**(1-2)**:** 13-23.

Casida, JE (2009) Pest toxicology: the primary mechanisms of pesticide action. *Chem Res Toxicol* **22**(4)**:** 609-619.

Chakrapani, S, Bailey, TD, Auerbach, A (2004) Gating dynamics of the acetylcholine receptor extracellular domain. *J Gen Physiol* **123**(4)**:** 341-356.

Chen, JC, Chesler, M (1992) Modulation of extracellular pH by glutamate and GABA in rat hippocampal slices. *J Neurophysiol* **67**(1)**:** 29-36.

Chen, L, Durkin, KA, Casida, JE (2006) Structural model for γ-aminobutyric acid receptor noncompetitive antagonist binding: widely diverse structures fit the same site. *Proc Natl Acad Sci U S A* **103**(13)**:** 5185-5190.

Cheng, X, Wang, H, Grant, B, Sine, SM, McCammon, JA (2006) Targeted molecular dynamics study of C-loop closure and channel gating in nicotinic receptors. *PLoS Comput Biol* **2**(9)**:** e134.

Chesler, M (1990) The regulation and modulation of pH in the nervous system. *Prog Neurobiol* **34**(5)**:** 401-427.

Corradi, J, Gumilar, F, Bouzat, C (2009) Single-channel kinetic analysis for activation and desensitization of homomeric 5-HT_3A receptors. *Biophys J* **97**(5)**:** 1335-1345.

Corry, B (2006) An energy-efficient gating mechanism in the acetylcholine receptor channel suggested by molecular and Brownian dynamics. *Biophys J* **90**(3)**:** 799-810.

Costa, PF, Emilio, MG, Fernandes, PL, Ferreira, HG, Ferreira, KG (1989) Determination of ionic permeability coefficients of the plasma membrane of *Xenopus laevis* oocytes under voltage clamp. *J Physiol* **413:** 199-211.

Curtis, DR, Johnston, GA (1974) Amino acid transmitters in the mammalian central nervous system. *Ergeb Physiol* **69**(0)**:** 97-188.

Cutting, GR, Curristin, S, Zoghbi, H, O'Hara, B, Seldin, MF, Uhl, GR (1992) Identification of a putative γ-aminobutyric acid (GABA) receptor subunit ρ2 cDNA and colocalization of the genes encoding ρ2 (GABRR2) and ρ1 (GABRR1) to human chromosome 6q14-q21 and mouse chromosome 4. *Genomics* **12**(4)**:** 801-806.

Cutting, GR, Lu, L, O'Hara, BF, Kasch, LM, Montrose-Rafizadeh, C, Donovan, DM, Shimada, S, Antonarakis, SE, Guggino, WB, Uhl, GR, et al. (1991) Cloning of the γ-aminobutyric acid (GABA) ρ1 cDNA: a GABA receptor subunit highly expressed in the retina. *Proc Natl Acad Sci U S A* **88**(7)**:** 2673-2677.

Cymes, GD, Grosman, C (2008) Pore-opening mechanism of the nicotinic acetylcholine receptor evinced by proton transfer. *Nat Struct Mol Biol* **15**(4)**:** 389-396.

Dahan, DS, Dibas, MI, Petersson, EJ, Auyeung, VC, Chanda, B, Bezanilla, F, Dougherty, DA, Lester, HA (2004) A fluorophore attached to nicotinic acetylcholine receptor β M2 detects productive binding of agonist to the αδ site. *Proc Natl Acad Sci U S A* **101**(27)**:** 10195-10200.

Das, P, Bell-Horner, CL, Machu, TK, Dillon, GH (2003) The $GABA_A$ receptor antagonist picrotoxin inhibits 5-hydroxytryptamine type 3A receptors. *Neuropharmacology* **44**(4)**:** 431-438.

Das, P, Dillon, GH (2005) Molecular determinants of picrotoxin inhibition of 5-hydroxytryptamine type 3 receptors. *J Pharmacol Exp Ther* **314**(1)**:** 320-328.

Davies, PA, Pistis, M, Hanna, MC, Peters, JA, Lambert, JJ, Hales, TG, Kirkness, EF (1999) The 5-HT3B subunit is a major determinant of serotonin-receptor function. *Nature* **397**(6717)**:** 359-363.

Davies, PA, Wang, W, Hales, TG, Kirkness, EF (2003) A novel class of ligand-gated ion channel is activated by Zn^{2+}. *J Biol Chem* **278**(2)**:** 712-717.

DeFeudis, FV, Drieu, K (2000) *Ginkgo biloba* extract (EGb 761) and CNS functions: basic studies and clinical applications. *Curr Drug Targets* **1**(1)**:** 25-58.

Del Castillo, J, Katz, B (1957) Interaction at end-plate receptors between different choline derivatives. *Proc R Soc Lond B Biol Sci* **146**(924)**:** 369-381.

Del Castillo, J, Morales, T., and Sanchez, V. (1963) Action of piperazine on the neurotransmitter system of *Ascaris lumbricoides*. *Nature* **200:** 706-707.

Dellisanti, CD, Yao, Y, Stroud, JC, Wang, ZZ, Chen, L (2007) Crystal structure of the extracellular domain of nAChR α1 bound to α-bungarotoxin at 1.94 Å resolution. *Nat Neurosci* **10**(8)**:** 953-962.

Dougherty, DA (1996) Cation-π interactions in chemistry and biology: a new view of benzene, Phe, Tyr, and Trp. *Science* **271**(5246)**:** 163-168.

Dougherty, DA (2007) Cation-π interactions involving aromatic amino acids. *J Nutr* **137**(6 Suppl 1)**:** 1504S-1508S; discussion 1516S-1517S.

Dougherty, DA (2008) Cys-loop neuroreceptors: structure to the rescue? *Chem Rev* **108**(5)**:** 1642-1653.

Drieu, K, Vranckx, R, Benassayad, C, Haourigi, M, Hassid, J, Yoa, RG, Rapin, JR, Nunez, EA (2000) Effect of the extract of *Ginkgo biloba* (EGb 761) on the circulating and cellular profiles of polyunsaturated fatty acids: correlation with the anti-oxidant properties of the extract. *Prostaglandins Leukot Essent Fatty Acids* **63**(5)**:** 293-300.

Du, W, Awolola, TS, Howell, P, Koekemoer, LL, Brooke, BD, Benedict, MQ, Coetzee, M, Zheng, L (2005) Independent mutations in the Rdl locus confer dieldrin resistance to *Anopheles gambiae* and *An. arabiensis*. *Insect Mol Biol* **14**(2):179-183.

Duan, S, Cooke, IM (2000) Glutamate and GABA activate different receptors and Cl(-) conductances in crab peptide-secretory neurons. *J Neurophysiol* **83**(1)**:** 31-37.

Dupuis**,** JP, Bazelot**,** M, Barbara**,** GS, Paute**,** S, Gauthier**,** M, Raymond-Delpech**,** V. (2010) Homomeric RDL and heteromeric RDL/LCCH3

GABA receptors in the honeybee antennal lobes: two candidates for inhibitory transmission in olfactory processing. *J Neurophysiol* **103**(1): 458-468.

Eguchi, Y, Ihara, M, Ochi, E, Shibata, Y, Matsuda, K, Fushiki, S, Sugama, H, Hamasaki, Y, Niwa, H, Wada, M, Ozoe, F, Ozoe, Y (2006) Functional characterization of *Musca* glutamate- and GABA-gated chloride channels expressed independently and coexpressed in *Xenopus* oocytes. *Insect Mol Biol* **15**(6)**:** 773-783.

Enz, R, Cutting, GR (1999) GABAC receptor ρ subunits are heterogeneously expressed in the human CNS and form homo- and heterooligomers with distinct physical properties. *Eur J Neurosci* **11**(1)**:** 41-50.

Erkkila, BE, Weiss, DS, Wotring, VE (2004) Picrotoxin-mediated antagonism of α3β4 and α7 acetylcholine receptors. *Neuroreport* **15**(12)**:** 1969-1973.

Etter, A, Cully, DF, Liu, KK, Reiss, B, Vassilatis, DK, Schaeffer, JM, Arena, JP (1999) Picrotoxin blockade of invertebrate glutamate-gated chloride channels: subunit dependence and evidence for binding within the pore. *J Neurochem* **72**(1)**:** 318-326.

ffrench-Constant, RH, Mortlock, DP, Shaffer, CD, MacIntyre, RJ, Roush, RT (1991) Molecular cloning and transformation of cyclodiene resistance in *Drosophila*: an invertebrate γ-aminobutyric acid subtype A receptor locus. *Proc Natl Acad Sci U S A* **88**(16)**:** 7209-7213.

ffrench-Constant, RH, Rocheleau, TA, Steichen, JC, Chalmers, AE (1993a) A point mutation in a *Drosophila* GABA receptor confers insecticide resistance. *Nature* **363**(6428)**:** 449-451.

ffrench-Constant, RH, Steichen, JC, Rocheleau, TA, Aronstein, K, Roush, RT (1993b) A single-amino acid substitution in a γ-aminobutyric acid subtype A receptor locus is associated with cyclodiene insecticide resistance in *Drosophila* populations. *Proc Natl Acad Sci U S A* **90**(5)**:** 1957-1961.

Galzi, JL, Devillers-Thiery, A, Hussy, N, Bertrand, S, Changeux, JP, Bertrand, D (1992) Mutations in the channel domain of a neuronal nicotinic receptor convert ion selectivity from cationic to anionic. *Nature* **359**(6395)**:** 500-505.

Gisselmann, G, Plonka, J, Pusch, H, Hatt, H (2004) *Drosophila melanogaster* GRD and LCCH3 subunits form heteromultimeric GABA-gated cation channels. *Br J Pharmacol* **142**(3)**:** 409-413.

Gisselmann, G, Pusch, H, Hovemann, BT, Hatt, H (2002) Two cDNAs coding for histamine-gated ion channels in *D. melanogaster*. *Nat Neurosci* **5**(1)**:** 11-12.

Grosman, C, Zhou, M, Auerbach, A (2000) Mapping the conformational wave of acetylcholine receptor channel gating. *Nature* **403**(6771)**:** 773-776.

Grutter, T, de Carvalho, LP, Dufresne, V, Taly, A, Edelstein, SJ, Changeux, JP (2005) Molecular tuning of fast gating in pentameric ligand-gated ion channels. *Proc Natl Acad Sci U S A* **102**(50)**:** 18207-18212.

Gunthorpe, MJ, Lummis, SC (2001) Conversion of the ion selectivity of the 5-HT_3A receptor from cationic to anionic reveals a conserved feature of the ligand-gated ion channel superfamily. *J Biol Chem* **276**(24)**:** 10977-10983.

Hamill, OP, Marty, A, Neher, E, Sakmann, B, Sigworth, FJ (1981) Improved patch-clamp techniques for high-resolution current recording from cells and cell-free membrane patches. *Pflugers Arch* **391**(2)**:** 85-100.

Hansen, SB, Sulzenbacher, G, Huxford, T, Marchot, P, Taylor, P, Bourne, Y (2005) Structures of *Aplysia* AChBP complexes with nicotinic agonists and antagonists reveal distinctive binding interfaces and conformations. *EMBO J* **24**(20)**:** 3635-3646.

Hargreaves, AC, Gunthorpe, MJ, Taylor, CW, Lummis, SC (1996) Direct inhibition of 5-HT_3 receptors by antagonists of L-type $Ca2^+$ channels. *Mol Pharmacol* **50**(5): 1284-1294.

Harrison, JB, Chen, HH, Sattelle, E, Barker, PJ, Huskisson, NS, Rauh, JJ, Bai, D, Sattelle, DB (1996) Immunocytochemical mapping of a C-terminus anti-peptide antibody to the GABA receptor subunit, RDL in the nervous system in *Drosophila melanogaster*. *Cell Tissue Res* **284**(2)**:** 269-278.

Harrison, NJ, Lummis, SC (2006) Locating the carboxylate group of GABA in the homomeric ρ $GABA_A$ receptor ligand-binding pocket. *J Biol Chem* **281**(34)**:** 24455-24461.

Hawthorne, R, Cromer, BA, Ng, HL, Parker, MW, Lynch, JW (2006) Molecular determinants of ginkgolide binding in the glycine receptor pore. *J Neurochem* **98**(2)**:** 395-407.

Heads, JA, Hawthorne, RL, Lynagh, T, Lynch, JW (2008) Structure-activity analysis of ginkgolide binding in the glycine receptor pore. *J Neurochem* **105**(4)**:** 1418-1427.

Hidalgo, P, MacKinnon, R (1995) Revealing the architecture of a K^+ channel pore through mutant cycles with a peptide inhibitor. *Science* **268**(5208)**:** 307-310.

Hilf, RJ, Dutzler, R (2009) Structure of a potentially open state of a proton-activated pentameric ligand-gated ion channel. *Nature* **457**(7225)**:** 115-118.

Hilf, RJ, Dutzler, R (2008) X-ray structure of a prokaryotic pentameric ligand-gated ion channel. *Nature* **452**(7185)**:** 375-379.

Hogg, RC, Buisson, B, Bertrand, D (2005) Allosteric modulation of ligand-gated ion channels. *Biochem Pharmacol* **70**(9)**:** 1267-1276.

Hosie, AM, Aronstein, K, Sattelle, DB, ffrench-Constant, RH (1997) Molecular biology of insect neuronal GABA receptors. *Trends Neurosci* **20**(12)**:** 578-583.

Hosie, AM, Baylis, HA, Buckingham, SD, Sattelle, DB (1995) Actions of the insecticide fipronil, on dieldrin-sensitive and- resistant GABA receptors of *Drosophila melanogaster*. *Br J Pharmacol* **115**(6)**:** 909-912.

Hosie, AM, Buckingham, SD, Presnail, JK, Sattelle, DB (2001) Alternative splicing of a *Drosophila* GABA receptor subunit gene identifies determinants of agonist potency. *Neuroscience* **102**(3)**:** 709-714.

Hosie, AM, Ozoe, Y, Koike, K, Ohmoto, T, Nikaido, T, Sattelle, DB (1996) Actions of picrodendrin antagonists on dieldrin-sensitive and -resistant *Drosophila* GABA receptors. *Br J Pharmacol* **119**(8)**:** 1569-1576.

Hosie, AM, Sattelle, DB (1996a) Agonist pharmacology of two *Drosophila* GABA receptor splice variants. *Br J Pharmacol* **119**(8)**:** 1577-1585.

Hosie, AM, Sattelle, DB (1996b) Allosteric modulation of an expressed homo-oligomeric GABA-gated chloride channel of *Drosophila melanogaster*. *Br J Pharmacol* **117**(6)**:** 1229-1237.

Huang, RQ, Dillon, GH (1999) Effect of extracellular pH on GABA-activated current in rat recombinant receptors and thin hypothalamic slices. *J Neurophysiol* **82**(3)**:** 1233-1243.

Huang, SH, Duke, RK, Chebib, M, Sasaki, K, Wada, K, Johnston, GA (2004) Ginkgolides, diterpene trilactones of *Ginkgo biloba*, as antagonists at recombinant $\alpha1\beta2\gamma2$ $GABA_A$ receptors. *Eur J Pharmacol* **494**(2-3)**:** 131-138.

Huxtable, R, Franconi, F, Giotti, A (1987) The biology of taurine. Methods and mechanisms. *Adv Exp Med Biol* **217:** 1-404.

Itil, TM, Eralp, E, Tsambis, E, Itil, KZ, Stein, U (1996) Central Nervous System Effects of *Ginkgo Biloba*, a Plant Extract. *Am J Ther* **3**(1)**:** 63-73.

Ivic, L, Sands, TT, Fishkin, N, Nakanishi, K, Kriegstein, AR, Stromgaard, K (2003) Terpene trilactones from *Ginkgo biloba* are antagonists of cortical glycine and $GABA_A$ receptors. *J Biol Chem* **278**(49)**:** 49279-49285.

Jensen, AA, Bergmann, ML, Sander, T, Balle, T (2010) Ginkgolide X is a potent antagonist of anionic Cys-loop receptors with a unique selectivity profile at glycine receptors. *J Biol Chem* **285**(13)**:** 10141-10153.

Jensen, ML, Timmermann, DB, Johansen, TH, Schousboe, A, Varming, T, Ahring, PK (2002) The β subunit determines the ion selectivity of the $GABA_A$ receptor. *J Biol Chem* **277**(44)**:** 41438-41447.

Jones, AK, Sattelle, DB (2008) The Cys-loop ligand-gated ion channel gene superfamily of the nematode, *Caenorhabditis elegans*. *Invert Neurosci* **8**(1)**:** 41-47.

Jones, AK, Sattelle, DB (2007) The Cys-loop ligand-gated ion channel gene superfamily of the red flour beetle, *Tribolium castaneum*. *BMC Genomics* **8:** 327.

Jones, AK, Sattelle, DB (2006) The Cys-loop ligand-gated ion channel superfamily of the honeybee, *Apis mellifera*. *Invert Neurosci* **6**(3)**:** 123-132.

Jones, MV, Sahara, Y, Dzubay, JA, Westbrook, GL (1998) Defining affinity with the $GABA_A$ receptor. *J Neurosci* **18**(21)**:** 8590-8604.

Kaku, K, Matsumura, F (1994) Identification of the site of mutation within the M2 region of the GABA receptor of the cyclodiene-resistant German cockroach. *Comp Biochem Physiol C Pharmacol Toxicol Endocrinol* **108**(3): 367-376.

Kaila, K (1994) Ionic basis of $GABA_A$ receptor channel function in the nervous system. *Prog Neurobiol* **42**(4)**:** 489-537.

Kaila, K, Voipio, J (1987) Postsynaptic fall in intracellular pH induced by GABA-activated bicarbonate conductance. *Nature* **330**(6144)**:** 163-165.

Kash, TL, Jenkins, A, Kelley, JC, Trudell, JR, Harrison, NL (2003) Coupling of agonist binding to channel gating in the $GABA_A$ receptor. *Nature* **421**(6920)**:** 272-275.

Kelley, SP, Dunlop, JI, Kirkness, EF, Lambert, JJ, Peters, JA (2003) A cytoplasmic region determines single-channel conductance in 5-HT_3 receptors. *Nature* **424**(6946)**:** 321-324.

Keramidas, A, Moorhouse, AJ, French, CR, Schofield, PR, Barry, PH (2000) M2 pore mutations convert the glycine receptor channel from being anion- to cation-selective. *Biophys J* **79**(1)**:** 247-259.

Kondratskaya, EL, Fisyunov, AI, Chatterjee, SS, Krishtal, OA (2004) Ginkgolide B preferentially blocks chloride channels formed by heteromeric glycine receptors in hippocampal pyramidal neurons of rat. *Brain Res Bull* **63**(4)**:** 309-314.

Kraig, RP, Ferreira-Filho, CR, Nicholson, C (1983) Alkaline and acid transients in cerebellar microenvironment. *J Neurophysiol* **49**(3)**:** 831-850.

Krishek, BJ, Amato, A, Connolly, CN, Moss, SJ, Smart, TG (1996a) Proton sensitivity of the $GABA_A$ receptor is associated with the receptor subunit composition. *J Physiol* **492 (Pt 2):** 431-443.

Krishek, BJ, Moss, SJ, Smart, TG (1996b) A functional comparison of the antagonists bicuculline and picrotoxin at recombinant $GABA_A$ receptors. *Neuropharmacology* **35**(9-10)**:** 1289-1298.

Kumar, S, Nussinov, R (2002) Close-range electrostatic interactions in proteins. *Chembiochem* **3**(7)**:** 604-617.

Lape, R, Colquhoun, D, Sivilotti, LG (2008) On the nature of partial agonism in the nicotinic receptor superfamily. *Nature* **454**(7205)**:** 722-727.

Lee, WY, Sine, SM (2005) Principal pathway coupling agonist binding to channel gating in nicotinic receptors. *Nature* **438**(7065)**:** 243-247.

Lee, HJ, Rocheleau, T, Zhang, HG, Jackson, MB, ffrench-Constant, RH (1993) Expression of a *Drosophila* GABA receptor in a baculovirus insect cell system. Functional expression of insecticide susceptible and resistant GABA receptors from the cyclodiene resistance gene *Rdl*. *FEBS Lett* **335**(3): 315-318.

Leisgen, C, Kuester, M, Methfessel, C (2007) The roboocyte: automated electrophysiology based on *Xenopus* oocytes. *Methods Mol Biol* **403**: 87-109.

Li, P, Slaughter, M (2007) Glycine receptor subunit composition alters the action of GABA antagonists. *Vis Neurosci* **24**(4)**:** 513-521.

Liman, ER, Tytgat J, and Hess P. (1992) Subunit stoichiometry of a mammalian K^+ channel determined by construction of multimeric cDNAs. *Neuron* **9**(5): 861-871.

Littleton, JT, Ganetzky, B (2000) Ion channels and synaptic organization: analysis of the *Drosophila* genome. *Neuron* **26**(1)**:** 35-43.

Liu, X, Buchanan, ME, Han, KA, Davis, RL (2009) The $GABA_A$ receptor RDL suppresses the conditioned stimulus pathway for olfactory learning. *J Neurosci* **29**(5)**:** 1573-1579.

Liu, X, Davis, RL (2009) The GABAergic anterior paired lateral neuron suppresses and is suppressed by olfactory learning. *Nat Neurosci* **12**(1)**:** 53-59.

Liu, X, Krause, WC, Davis, RL (2007) $GABA_A$ Receptor RDL Inhibits *Drosophila* Olfactory Associative Learning. *Neuron* **56**(6)**:** 1090-1102.

Lochner, M, Lummis, SC (2010) Agonists and antagonists bind to an A-A interface in the heteromeric 5-HT_3AB receptor. *Biophys J* **98**(8)**:** 1494-1502.

Lovell, SC, Davis, IW, Arendall, WB, 3rd, de Bakker, PI, Word, JM, Prisant, MG, Richardson, JS, Richardson, DC (2003) Structure validation by Cα geometry: φ, ψ and Cβ deviation. *Proteins* **50**(3)**:** 437-450.

Ludmerer, SW, Warren, VA, Williams, BS, Zheng, Y, Hunt, DC, Ayer, MB, Wallace, MA, Chaudhary, AG, Egan, MA, Meinke, PT, Dean, DC, Garcia, ML, Cully, DF, Smith, MM (2002) Ivermectin and nodulisporic acid receptors in *Drosophila melanogaster* contain both γ-aminobutyric acid-gated Rdl and glutamate-gated GluCl α chloride channel subunits. *Biochemistry* **41**(20)**:** 6548-6560.

Lummis, SC (2009) Locating GABA in GABA receptor binding sites. *Biochem Soc Trans* **37**(Pt 6)**:** 1343-1346.

Lummis, SC, Beene, DL, Lee, LW, Lester, HA, Broadhurst, RW, Dougherty, DA (2005a) Cis-trans isomerization at a proline opens the pore of a neurotransmitter-gated ion channel. *Nature* **438**(7065)**:** 248-252.

Lummis, SC, D, LB, Harrison, NJ, Lester, HA, Dougherty, DA (2005b) A cation-π binding interaction with a tyrosine in the binding site of the $GABA_C$ receptor. *Chem Biol* **12**(9)**:** 993-997.

Luque, JM, Malherbe, P, Richards, JG (1994) Localization of $GABA_A$ receptor subunit mRNAs in the rat locus coeruleus. *Brain Res Mol Brain Res* **24**(1-4)**:** 219-226.

Lynch, JW, Rajendra, S, Barry, PH, Schofield, PR (1995) Mutations affecting the glycine receptor agonist transduction mechanism convert the competitive antagonist, picrotoxin, into an allosteric potentiator. *J Biol Chem* **270**(23)**:** 13799-13806.

McGonigle, I, Lummis, SC (2010) Molecular Characterization of Agonists That Bind to an Insect GABA Receptor. *Biochemistry* **49**(13): 2897-2902

McGonigle, I, Lummis, SC (2009) RDL receptors. *Biochem Soc Trans* **37**(6)**:** 1404-1406.

McGurk, KA, Pistis, M, Belelli, D, Hope, AG, Lambert, JJ (1998) The effect of a transmembrane amino acid on etomidate sensitivity of an invertebrate GABA receptor. *Br J Pharmacol* **124**(1)**:** 13-20.

Mdzinarishvili, A, Kiewert, C, Kumar, V, Hillert, M, Klein, J (2007) Bilobalide prevents ischemia-induced edema formation *in vitro* and *in vivo*. *Neuroscience* **144**(1)**:** 217-222.

Mecozzi, S, West, AP, Jr., Dougherty, DA (1996) Cation-π interactions in aromatics of biological and medicinal interest: electrostatic potential surfaces as a useful qualitative guide. *Proc Natl Acad Sci U S A* **93**(20)**:** 10566-10571.

Melis, C, Lummis, SC, Molteni, C (2008) Molecular dynamics simulations of GABA binding to the $GABA_C$ receptor: the role of Arg104. *Biophys J* **95**(9)**:** 4115-4123.

Millar, NS, Buckingham, SD, Sattelle, DB (1994) Stable expression of a functional homo-oligomeric *Drosophila* GABA receptor in a *Drosophila* cell line. *Proc Biol Sci* **258**(1353): 307-314.

Miller, C (1989) Genetic manipulation of ion channels: a new approach to structure and mechanism. *Neuron* **2**(3): 1195-1205.

Miller, PS, Smart, TG (2010) Binding, activation and modulation of Cys-loop receptors. *Trends Pharmacol Sci* **31**(4)**:** 161-174.

Miyazawa, A, Fujiyoshi, Y, Unwin, N (2003) Structure and gating mechanism of the acetylcholine receptor pore. *Nature* **423**(6943)**:** 949-955.

Mu, TW, Lester, HA, Dougherty, DA (2003) Different binding orientations for the same agonist at homologous receptors: a lock and key or a simple wedge? *J Am Chem Soc* **125**(23)**:** 6850-6851.

Mukhtasimova, N, Lee, WY, Wang, HL, Sine, SM (2009) Detection and trapping of intermediate states priming nicotinic receptor channel opening. *Nature* **459**(7245)**:** 451-454.

Muroi, Y, Czajkowski, C, Jackson, MB (2006) Local and global ligand-induced changes in the structure of the $GABA_A$ receptor. *Biochemistry* **45**(23)**:** 7013-7022.

Muroi, Y, Theusch, CM, Czajkowski, C, Jackson, MB (2009) Distinct structural changes in the $GABA_A$ receptor elicited by pentobarbital and GABA. *Biophys J* **96**(2)**:** 499-509.

Narusuye, K, Nakao, T, Abe, R, Nagatomi, Y, Hirase, K, Ozoe, Y (2007) Molecular cloning of a GABA receptor subunit from *Laodelphax striatella* (Fallén) and patch clamp analysis of the homo-oligomeric receptors expressed in a *Drosophila* cell line. *Insect Mol Biol* **16**(6): 723-733.

Newell, JG, Czajkowski, C (2003) The $GABA_A$ receptor α1 subunit Pro174-Asp191 segment is involved in GABA binding and channel gating. *J Biol Chem* **278**(15)**:** 13166-13172.

Niesler, B, Frank, B, Kapeller, J, Rappold, GA (2003) Cloning, physical mapping and expression analysis of the human 5-HT_3 serotonin receptor-like genes HTR3C, HTR3D and HTR3E. *Gene* **310:** 101-111.

Niesler, B, Walstab, J, Combrink, S, Moller, D, Kapeller, J, Rietdorf, J, Bonisch, H, Gothert, M, Rappold, G, Bruss, M (2007) Characterization of the novel human serotonin receptor subunits 5-HT3C,5-HT3D, and 5-HT3E. *Mol Pharmacol* **72**(1)**:** 8-17.

Olsen, RW (2006) Picrotoxin-like channel blockers of $GABA_A$ receptors. *Proc Natl Acad Sci U S A* **103**(16)**:** 6081-6082.

Ong, J, Kerr, DI (2000) Recent advances in GABAB receptors: from pharmacology to molecular biology. *Acta Pharmacol Sin* **21**(2)**:** 111-123.

Padgett, CL, Hanek, AP, Lester, HA, Dougherty, DA, Lummis, SC (2007) Unnatural amino acid mutagenesis of the $GABA_A$ receptor binding site residues reveals a novel cation-π interaction between GABA and β_2Tyr97. *J Neurosci* **27**(4)**:** 886-892.

Panicker, S, Cruz, H, Arrabit, C, Slesinger, PA (2002) Evidence for a centrally located gate in the pore of a serotonin-gated ion channel. *J Neurosci* **22**(5)**:** 1629-1639.

Persohn, E, Malherbe, P, Richards, JG (1991) *In situ* hybridization histochemistry reveals a diversity of $GABA_A$ receptor subunit mRNAs in neurons of the rat spinal cord and dorsal root ganglia. *Neuroscience* **42**(2)**:** 497-507.

Pless, SA, Dibas, MI, Lester, HA, Lynch, JW (2007) Conformational variability of the glycine receptor M2 domain in response to activation by different agonists. *J Biol Chem* **282**(49)**:** 36057-36067.

Pless, SA, Lynch, JW (2009a) Distinct conformational changes in activated agonist-bound and agonist-free glycine receptor subunits. *J Neurochem* **108**(6)**:** 1585-1594.

Pless, SA, Lynch, JW (2009b) Ligand-specific conformational changes in the α1 glycine receptor ligand-binding domain. *J Biol Chem* **284**(23)**:** 15847-15856.

Pless, SA, Lynch, JW (2009c) Magnitude of a conformational change in the glycine receptor β1-β2 loop is correlated with agonist efficacy. *J Biol Chem* **284**(40)**:** 27370-27376.

Pless, SA, Millen, KS, Hanek, AP, Lynch, JW, Lester, HA, Lummis, SC, Dougherty, DA (2008) A cation-π interaction in the binding site of the glycine receptor is mediated by a phenylalanine residue. *J Neurosci* **28**(43)**:** 10937-10942.

Price, KL, Lummis, SC (2005) FlexStation examination of 5-HT_3 receptor function using $Ca2^+$ - and membrane potential-sensitive dyes: advantages and potential problems. *J Neurosci Methods* **149**(2)**:** 172-177.

Price, KL, Millen, KS, Lummis, SC (2007) Transducing agonist binding to channel gating involves different interactions in 5-HT_3 and $GABA_C$ receptors. *J Biol Chem* **282**(35)**:** 25623-25630.

Purohit, P, Auerbach, A (2007) Acetylcholine receptor gating at extracellular transmembrane domain interface: the "pre-M1" linker. *J Gen Physiol* **130**(6)**:** 559-568.

Qian, H, Pan, Y, Zhu, Y, Khalili, P (2005) Picrotoxin accelerates relaxation of $GABA_C$ receptors. *Mol Pharmacol* **67**(2)**:** 470-479.

Ranganathan, R, Cannon, SC, Horvitz, HR (2000) MOD-1 is a serotonin-gated chloride channel that modulates locomotory behaviour in *C. elegans*. *Nature* **408**(6811)**:** 470-475.

Rayes, D, De Rosa, MJ, Sine, SM, Bouzat, C (2009) Number and locations of agonist binding sites required to activate homomeric Cys-loop receptors. *J Neurosci* **29**(18)**:** 6022-6032.

Raymond-Delpech, V, Matsuda, K, Sattelle, BM, Rauh, JJ, Sattelle, DB (2005) Ion channels: molecular targets of neuroactive insecticides. *Invert Neurosci* **5**(3-4)**:** 119-133.

Reeves, DC, Goren, EN, Akabas, MH, Lummis, SC (2001) Structural and electrostatic properties of the 5-HT_3 receptor pore revealed by substituted cysteine accessibility mutagenesis. *J Biol Chem* **276**(45)**:** 42035-42042.

Reeves, DC, Jansen, M, Bali, M, Lemster, T, Akabas, MH (2005) A role for the β1-β2 loop in the gating of 5-HT_3 receptors. *J Neurosci* **25**(41)**:** 9358-9366.

Roberts, E, Frankel, S (1950) γ-Aminobutyric acid in brain: its formation from glutamic acid. *J Biol Chem* **187**(1)**:** 55-63.

Sali, A, Blundell, TL (1993) Comparative protein modelling by satisfaction of spatial restraints. *J Mol Biol* **234**(3)**:** 779-815.

Sammelson, RE, Caboni, P, Durkin, KA, Casida, JE (2004) GABA receptor antagonists and insecticides: common structural features of 4-alkyl-1-phenylpyrazoles and 4-alkyl-1-phenyltrioxabicyclooctanes. *Bioorg Med Chem* **12**(12)**:** 3345-3355.

Sattelle, DB, Harrison, JB, Chen, HH, Bai, D, Takeda, M (2000) Immunocytochemical localization of putative γ-aminobutyric acid receptor subunits in the head ganglia of *Periplaneta americana* using an anti-RDL C-terminal antibody. *Neurosci Lett* **289**(3)**:** 197-200.

Sattelle, DB, Jones, AK, Sattelle, BM, Matsuda, K, Reenan, R, Biggin, PC (2005) Edit, cut and paste in the nicotinic acetylcholine receptor gene family of *Drosophila melanogaster*. *Bioessays* **27**(4)**:** 366-376.

Sattelle, DB, Pinnock, RD, Wafford, KA, David, JA (1988) GABA receptors on the cell-body membrane of an identified insect motor neuron. *Proc R Soc Lond B Biol Sci* **232**(1269)**:** 443-456.

Schmieden, V, Grenningloh, G, Schofield, PR, Betz, H (1989) Functional expression in *Xenopus* oocytes of the strychnine binding 48 kd subunit of the glycine receptor. *EMBO J* **8**(3)**:** 695-700.

Schnee, M, Rauh, J, Buckingham, SD, Sattelle, DB (1997) Pharmacology of skeletal muscle GABA-gated chloride channels in the cockroach *Periplaneta americana*. *J Exp Biol* **200**(Pt 23)**:** 2947-2955.

Schofield, PR, Darlison, MG, Fujita, N, Burt, DR, Stephenson, FA, Rodriguez, H, Rhee, LM, Ramachandran, J, Reale, V, Glencorse, TA, et al. (1987) Sequence and functional expression of the $GABA_A$ receptor shows a ligand-gated receptor super-family. *Nature* **328**(6127)**:** 221-227.

Schreiber, G, Fersht, AR (1995) Energetics of protein-protein interactions: analysis of the barnase-barstar interface by single mutations and double mutant cycles. *J Mol Biol* **248**(2)**:** 478-486.

Shi, J, Blundell, TL, Mizuguchi, K (2001) FUGUE: sequence-structure homology recognition using environment-specific substitution tables and structure-dependent gap penalties. *J Mol Biol* **310**(1)**:** 243-257.

Shirai, Y, Hosie, AM, Buckingham, SD, Holyoke, CW, Jr., Baylis, HA, Sattelle, DB (1995) Actions of picrotoxinin analogues on an expressed, homo-oligomeric GABA receptor of *Drosophila melanogaster*. *Neurosci Lett* **189**(1)**:** 1-4.

Shotkoski, F, Lee, HJ, Zhang, HG, Jackson, MB, ffrench-Constant, RH (1994) Functional expression of insecticide-resistant GABA receptors from the mosquito *Aedes aegypti*. *Insect Mol Biol* **3**(4): 283-287.

Shotkoski, F, Zhang, HG, Jackson, MB, ffrench-Constant, RH (1996) Stable expression of insect GABA receptors in insect cell lines. Promoters for efficient expression of *Drosophila* and mosquito Rdl GABA receptors in stably transformed mosquito cell lines. *FEBS Lett* **380**(3): 257-262.

Sieghart, W (1995) Structure and pharmacology of γ-aminobutyric acid A receptor subtypes. *Pharmacol Rev* **47**(2)**:** 181-234.

Sigel, E, Baur, R, Kellenberger, S, Malherbe, P (1992) Point mutations affecting antagonist affinity and agonist dependent gating of $GABA_A$ receptor channels. *EMBO J* **11**(6)**:** 2017-2023.

Sine, SM, Engel, AG (2006) Recent advances in Cys-loop receptor structure and function. *Nature* **440**(7083)**:** 448-455.

Sixma, TK, Smit, AB (2003) Acetylcholine binding protein (AChBP): a secreted glial protein that provides a high-resolution model for the extracellular domain of pentameric ligand-gated ion channels. *Annu Rev Biophys Biomol Struct* **32:** 311-334.

Smit, AB, Syed, NI, Schaap, D, van Minnen, J, Klumperman, J, Kits, KS, Lodder, H, van der Schors, RC, van Elk, R, Sorgedrager, B, Brejc, K, Sixma, TK, Geraerts, WP (2001) A glia-derived acetylcholine-binding protein that modulates synaptic transmission. *Nature* **411**(6835)**:** 261-268.

Somogyi, P, Fritschy, JM, Benke, D, Roberts, JD, Sieghart, W (1996) The γ2 subunit of the $GABA_A$ receptor is concentrated in synaptic junctions containing the α1 and β2/3 subunits in hippocampus, cerebellum and globus pallidus. *Neuropharmacology* **35**(9-10)**:** 1425-1444.

Spier, AD, Lummis, SC (2000) The role of tryptophan residues in the 5-HT_3 receptor ligand binding domain. *J Biol Chem* **275**(8)**:** 5620-5625.

Staley, KJ, Soldo, BL, Proctor, WR (1995) Ionic mechanisms of neuronal excitation by inhibitory $GABA_A$ receptors. *Science* **269**(5226)**:** 977-981.

Stein, LD, Bao, Z, Blasiar, D, Blumenthal, T, Brent, MR, Chen, N, Chinwalla, A, Clarke, L, Clee, C, Coghlan, A, Coulson, A, D'Eustachio, P, Fitch, DH, Fulton, LA, Fulton, RE, Griffiths-Jones, S, Harris, TW, Hillier, LW, Kamath, R, Kuwabara, PE, Mardis, ER, Marra, MA, Miner, TL, Minx, P, Mullikin, JC, Plumb, RW, Rogers, J, Schein, JE, Sohrmann, M, Spieth, J, Stajich, JE, Wei, C, Willey, D, Wilson, RK, Durbin, R, Waterston, RH (2003) The genome sequence of *Caenorhabditis briggsae*: a platform for comparative genomics. *PLoS Biol* **1**(2)**:** E45.

Strambi, C, Cayre, M, Sattelle, DB, Augier, R, Charpin, P, Strambi, A (1998) Immunocytochemical mapping of an RDL-like GABA receptor subunit and of GABA in brain structures related to learning and memory in the cricket *Acheta domesticus*. *Learn Mem* **5**(1-2)**:** 78-89.

Sun, L, Dong, H, Guo, C, Qian, J, Sun, J, Ma, L, Zhu, C (2006) Larvicidal activity of extracts of *Ginkgo biloba* exocarp for three different strains of *Culex pipiens pallens*. *J Med Entomol* **43**(2)**:** 258-261.

Swensen, AM, Golowasch, J, Christie, AE, Coleman, MJ, Nusbaum, MP, Marder, E (2000) GABA and responses to GABA in the stomatogastric ganglion of the crab *Cancer borealis*. *J Exp Biol* **203**(Pt 14)**:** 2075-2092.

Taylor, CW, Laude, AJ (2002) IP_3 receptors and their regulation by calmodulin and cytosolic $Ca2^+$. *Cell Calcium* **32**(5-6)**:** 321-334.

Thompson, AJ, Lochner, M, Lummis, SC (2007) The antimalarial drugs quinine, chloroquine and mefloquine are antagonists at 5-HT_3 receptors. *Br J Pharmacol* **151**(5)**:** 666-677.

Thompson, AJ, Lochner, M, Lummis, SC (2008) Loop B is a major structural component of the 5-HT_3 receptor. *Biophys J* **95**(12)**:** 5728-5736.

Thompson, AJ, Lummis, SC (2007) The 5-HT_3 receptor as a therapeutic target. *Expert Opin Ther Targets* **11**(4)**:** 527-540.

Thompson, AJ, Lummis, SC (2003) A single ring of charged amino acids at one end of the pore can control ion selectivity in the 5-HT_3 receptor. *Br J Pharmacol* **140**(2)**:** 359-365.

Tzvetkov, MV, Meineke, C, Oetjen, E, Hirsch-Ernst, K, Brockmoller, J (2007) Tissue-specific alternative promoters of the serotonin receptor gene HTR3B in human brain and intestine. *Gene* **386**(1-2)**:** 52-62.

Ulens, C, Akdemir, A, Jongejan, A, van Elk, R, Bertrand, S, Perrakis, A, Leurs, R, Smit, AB, Sixma, TK, Bertrand, D, de Esch, IJ (2009) Use of acetylcholine binding protein in the search for novel α7 nicotinic receptor ligands. *In silico* docking, pharmacological screening, and X-ray analysis. *J Med Chem* **52**(8)**:** 2372-2383.

Unwin, N (1995) Acetylcholine receptor channel imaged in the open state. *Nature* **373**(6509)**:** 37-43.

Unwin, N, Miyazawa, A, Li, J, Fujiyoshi, Y (2002) Activation of the nicotinic acetylcholine receptor involves a switch in conformation of the α subunits. *J Mol Biol* **319**(5)**:** 1165-1176.

Urbanics, R, Leniger-Follert, E, Lubbers, DW (1978) Time course of changes of extracellular H^+ and K^+ activities during and after direct electrical stimulation of the brain cortex. *Pflugers Arch* **378**(1)**:** 47-53.

Verdonk, ML, Cole, JC, Hartshorn, MJ, Murray, CW, Taylor, RD (2003) Improved protein-ligand docking using GOLD. *Proteins* **52**(4)**:** 609-623.

Wagner, DA, Czajkowski, C, Jones, MV (2004) An arginine involved in GABA binding and unbinding but not gating of the $GABA_A$ receptor. *J Neurosci* **24**(11)**:** 2733-2741.

Wang, J, Lester, HA, Dougherty, DA (2007) Establishing an ion pair interaction in the homomeric ρ1 γ-aminobutyric acid type A receptor that contributes to the gating pathway. *J Biol Chem* **282**(36)**:** 26210-26216.

Westh-Hansen, SE, Rasmussen, PB, Hastrup, S, Nabekura, J, Noguchi, K, Akaike, N, Witt, MR, Nielsen, M (1997) Decreased agonist sensitivity of human $GABA_A$ receptors by an amino acid variant, isoleucine to valine, in the α1 subunit. *Eur J Pharmacol* **329**(2-3)**:** 253-257.

Westh-Hansen, SE, Witt, MR, Dekermendjian, K, Liljefors, T, Rasmussen, PB, Nielsen, M (1999) Arginine residue 120 of the human $GABA_A$ receptor α1, subunit is essential for GABA binding and chloride ion current gating. *Neuroreport* **10**(11)**:** 2417-2421.

Wilkins, ME, Hosie, AM, Smart, TG (2002) Identification of a β subunit TM2 residue mediating proton modulation of GABA type A receptors. *J Neurosci* **22**(13)**:** 5328-5333.

Wilkins, ME, Hosie, AM, Smart, TG (2005) Proton modulation of recombinant $GABA_A$ receptors: influence of GABA concentration and the β subunit TM2-TM3 domain. *J Physiol* **567**(Pt 2)**:** 365-377.

Wilson, G, Karlin, A (2001) Acetylcholine receptor channel structure in the resting, open, and desensitized states probed with the substituted-cysteine-accessibility method. *Proc Natl Acad Sci U S A* **98**(3)**:** 1241-1248.

Wilson, GG, Karlin, A (1998) The location of the gate in the acetylcholine receptor channel. *Neuron* **20**(6)**:** 1269-1281.

Woodward, RM, Polenzani, L, Miledi, R (1993) Characterization of bicuculline/baclofen-insensitive (ρ-like) γ-aminobutyric acid receptors expressed in *Xenopus* oocytes. II. Pharmacology of γ-aminobutyric acid A and γ-aminobutyric acid B receptor agonists and antagonists. *Mol Pharmacol* **43**(4)**:** 609-625.

Xiu, X, Puskar, NL, Shanata, JA, Lester, HA, Dougherty, DA (2009) Nicotine binding to brain receptors requires a strong cation-π interaction. *Nature* **458**(7237)**:** 534-537.

Zhang, D, Pan, ZH, Zhang, X, Brideau, AD, Lipton, SA (1995a) Cloning of a γ-aminobutyric acid type C receptor subunit in rat retina with a methionine residue critical for picrotoxinin channel block. *Proc Natl Acad Sci U S A* **92**(25)**:** 11756-11760.

Zhang, HG, ffrench-Constant, RH, Jackson, MB (1994) A unique amino acid of the *Drosophila* GABA receptor with influence on drug sensitivity by two mechanisms. *J Physiol* **479 (Pt 1):** 65-75.

Zhang, HG, Lee, HJ, Rocheleau, T, ffrench-Constant, RH, Jackson, MB (1995b) Subunit composition determines picrotoxin and bicuculline sensitivity of *Drosophila* γ-aminobutyric acid receptors. *Mol Pharmacol* **48**(5)**:** 835-840.

Zhang, J, Xue, F, Chang, Y (2008) Structural determinants for antagonist pharmacology that distinguish the ρ1 $GABA_C$ receptor from $GABA_A$ receptors. *Mol Pharmacol* **74**(4)**:** 941-951.

Zheng, Y, Hirschberg, B, Yuan, J, Wang, AP, Hunt, DC, Ludmerer, SW, Schmatz, DM, Cully, DF (2002) Identification of two novel *Drosophila melanogaster* histamine-gated chloride channel subunits expressed in the eye. *J Biol Chem* **277**(3)**:** 2000-2005.

Zhong, W, Gallivan, JP, Zhang, Y, Li, L, Lester, HA, Dougherty, DA (1998) From *ab initio* quantum mechanics to molecular neurobiology: a cation-π binding site in the nicotinic receptor. *Proc Natl Acad Sci U S A* **95**(21)**:** 12088-12093.

Zhu, XZ, Li, XY, Liu, J (2004) Recent pharmacological studies on natural products in China. *Eur J Pharmacol* **500**(1-3)**:** 221-230.

Zouridakis, M, Zisimopoulou, P, Poulas, K, Tzartos, SJ (2009) Recent advances in understanding the structure of nicotinic acetylcholine receptors. *IUBMB Life* **61**(4)**:** 407-423.